



Establishment of photosynthetic complexes in the chloroplast

Dissertation

Zur Erlangung des Doktorgrades der Naturwissenschaften

Fakultät für Biologie

Ludwig-Maximilians-Universität München

vorgelegt von

Salar Abu-Torab Torabi

aus Berlin

München, August 2014

Erstgutachter:

PD Dr. Jörg Meurer

Zweitgutachter:

Prof. Dr. Wolfgang Frank

Tag der mündlichen Prüfung:

18.11.2014

Content

1. Introduction	6
1.1 Evolution of oxygenic photosynthesis	6
1.2 Oxygenic photosynthesis in the thylakoid membrane of plants	7
1.3 The RNA metabolism of the chloroplast	8
1.4 The <i>psbB</i> gene cluster	10
1.5 Photosystem II, the water splitting enzyme	12
1.6 Assembly and repair mechanisms of PSII	13
1.7 Aim of this dissertation	16
2. Materials and Methods	18
2.1 Database analysis	18
2.2 Vectors	19
2.3 Oligonucleotides	19
2.4 Bacterial strains.....	19
2.5 Antibodies	19
2.6 Plant materials and growth conditions	19
2.7 Complementation of <i>hcf145-1</i> and <i>hcf145-2</i>	20
2.8 Generation of <i>HCF145</i> RNAi-lines in tobacco.....	21
2.9 Complementation of $\Delta psbN$ mutants	21
2.10 <i>Agrobacterium tumefaciens</i> mediated transformation of tobacco	21
2.11 Rapid DNA isolation for PCR analysis.....	22
2.12 RNA isolation and gel blot analysis.....	22
2.13 Spectroscopic analysis	23
2.14 Fluorescence imaging.....	23
2.15 Measurements of PSII photoinhibition and recovery.....	23
2.16 77K fluorescence measurement	23
2.17 Protein analysis and immunoprecipitation	24
2.18 Separation of thylakoid membrane complexes by BN-PAGE.....	24
2.19 Topology studies on PsbN	25
2.20 In vivo labeling of chloroplast proteins	25
3. Results.....	26
3.1 HCF145 stabilizes <i>psaA-psaB-rps14</i> transcripts.....	26
3.1.1 Comparison of two allelic mutations in the AT5G08720 locus.....	27
3.1.2 HCF145 is localized to the chloroplast	31
3.1.3 HCF145 consists of two duplicated and conserved domains	31
3.1.4 The function of HCF145 is conserved among <i>Embryophyta</i>	33
3.1.5 Light-induced accumulation of HCF145.....	36
3.1.6 Light- and stress-dependent expression of <i>HCF145</i>	36

3.1.7	HCF145 is a rate limiting factor of PSI accumulation	38
3.1.8	HCF145 is associated to the 5' UTR of <i>psaA</i> transcripts.....	40
3.2	PsbN is required for the assembly of the PSII RC	41
3.2.1	Localization and topology of PsbN	41
3.2.2	Light-induced expression of PsbN	42
3.2.3	Targeted inactivation of the <i>PsbN</i> gene	42
3.2.4	Transcript profile of the <i>psbB</i> operon in $\Delta psbN-F$ and $\Delta psbN-R$	43
3.2.5	Establishment of a semi-sterile culture technique.....	45
3.2.6	Growth phenotype of the $\Delta psbN$ plants.....	46
3.2.7	PSII activity is reduced in the $\Delta psbN$ mutants	47
3.2.8	Levels of PSII proteins were reduced in $\Delta psbN-F$ and $\Delta psbN-R$	49
3.2.9	Translation of chloroplast encoded proteins in $\Delta psbN$ mutants	50
3.2.10	PSII complex formation is affected in $\Delta psbN$ mutants	52
3.2.11	Time-resolved assembly studies in $\Delta psbN$ mutants	55
3.2.12	Low temperature chlorophyll fluorescence analysis	59
3.2.13	The thylakoid ultrastructure is changed in $\Delta psbN$ mutants.....	60
3.2.14	Photosensitivity of $\Delta psbN$ mutants	60
3.2.15	Phosphorylation of the PSII antennae is altered in $\Delta psbN$ mutants	63
3.2.16	Allotopic complementation of $\Delta psbN$ mutants	64
4.	Discussion	66
4.1	HCF145 is a nuclear-encoded factor affecting <i>psaA</i> -5' UTR stability	66
4.1.1	SRPBCC superfamily domains have diverse functions	66
4.1.2	The TMR motifs confer RNA binding specificity to HCF145	67
4.1.3	Phylogenetic conservation of HCF145	67
4.1.4	The low abundant HCF145 accumulates already in eoplasts.....	69
4.1.5	HCF145 protects the <i>psaA-psaB-rps14</i> transcripts at the 5' UTR.....	70
4.1.6	PSI biogenesis highly depends on HCF145	70
4.1.7	HCF145 might be linked to a metabolic pathway.....	71
4.1.8	HCF145 might be integrated into a signal transduction pathway	72
4.1.9	Outlook of the HCF145 project.....	73
4.2	PsbN is required for the assembly of PSII	73
4.2.1	PsbN is not a constituent subunit of PSII.....	73
4.2.2	PsbN is specifically required for PSII RC formation.....	75
4.2.3	PsbN shares functional characteristics with HCF136	76
4.2.4	The $\Delta psbN$ mutants are extremely light sensitive	78
4.2.5	Outlook of the PsbN project.....	79
4.2.6	Establishment of a semi-sterile culture system	79
	Summary	81

Zusammenfassung	83
Abbreviations	85
Literature	89
Appendix	100
Acknowledgements	107
Publications	108
Curriculum vitae	109
Eidesstattliche Versicherung	110
Erklärung	110

1. Introduction

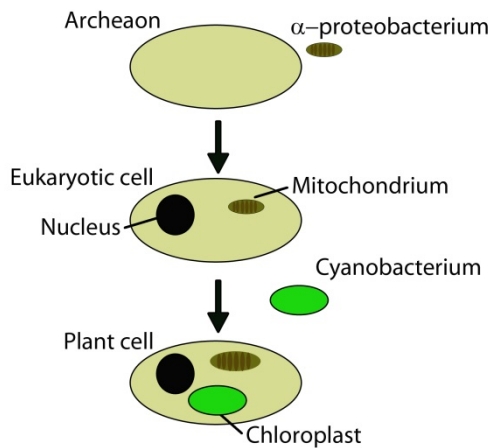
1.1 Evolution of oxygenic photosynthesis

The assimilation of organic compounds driven by the exhaustless energy of the sun is essential for nearly all organisms on the planet. These processes called photosynthesis span the capture of light with pigments, the conversion of the sunlight's energy into chemical energy by oxidizing inorganic compounds and the synthesis of energy rich organic compounds, which are the building blocks of life. According to the by-products of these different energy conversion reactions, that occur mainly in photosynthetic bacteria, they are referred to anoxygenic or oxygenic photosynthesis. Among these reactions the oxygenic photosynthesis is unique and the most important, as it implies the oxidation of water followed by a release of oxygen and moreover reaches the highest yields in the fixation of carbon dioxide (Raven 2009; Raven et al. 2013).

At least 500 million years after the onset of oxygenic photosynthesis the atmosphere of the earth changed dramatically (Planavsky et al., 2014). This big step of oxygen evolution is called the great oxygen event and it is coincident with the proliferation of cyanobacterium-like organisms able to perform oxygenic photosynthesis about 2,4 to 2,1 billion years ago (Holland, 2002; Tomitani et al., 2006; Rasmussen et al., 2008). Beside the cyanobacteria, today the eukaryotic organisms algae and land plants produce most of the oxygen in our world.

Chloroplasts are organelles of plants which allow them to perform oxygenic photosynthesis. The chloroplasts of the plant cells and the mitochondria of all eukaryotic cells are believed to derive out of a process called endosymbiosis about 1,5 billion years ago (Martin and Müller, 1998; Heckman et al., 2001). First, a heterotrophic eukaryotic cell arose after an archaeobacterium-like cell engulfed an α -proteobacterium, which became the mitochondrion. Later, a plant cell originated by the incorporation of a cyanobacterial ancestor into a eukaryotic cell (Figure 1). During evolution the bacteria became part of the host cell and genetic information was exchanged. Accordingly, a massive gene transfer from the endosymbionts to the host cell nucleus occurred, which is still an ongoing process (Millen et al., 2001; Stegemann and Bock, 2006).

The genome size of a plant chloroplast was reduced to about 100 genes compared to the about 3000 genes of a cyanobacterium. Mainly proteins of high demand like the core subunits of the photosynthetic complexes and ribosomal proteins are still encoded in the



chloroplast, while most of the chloroplast proteins are nucleus encoded and are imported from the cytosol. Therefore most nucleus encoded chloroplast proteins have an N-terminal extension which serves as a transit signal for chloroplast import. After correct targeting of the protein the transit peptide is cleaved off (von Heijne et al., 1989; Bruce, 2000).

Figure 1. Endosymbiotic theory. Eukaryotic cells with two genetic compartments, the nucleus and the mitochondria, arose in an endosymbiosis between an archaeon and an α -proteobacterium. Subsequently, the chloroplasts of plant cells evolved after a cyanobacterium was engulfed by a eukaryotic cell.

1.2 Oxygenic photosynthesis in the thylakoid membrane of plants

Thylakoids are a formation of flatten membrane vesicles and protein complexes, at which the light reaction of oxygenic photosynthesis takes place in cyanobacteria and plants. In the chloroplasts of land plants the thylakoid membrane systems form a network of densely packed thylakoid stacks called grana lamellae, which are connected by unstacked membrane regions, the stroma lamellae (Adam et al., 2011). Four major photosynthetic protein complexes are embedded in the thylakoid membranes which are connected in a series forming the electron transport chain or produce adenosine triphosphate (ATP) (Figure 2).

The Photosystem II (PSII), which is mainly found in the grana stacks, converts the captured light energy into chemical energy (Rochaix, 2011). By splitting water, electrons are gained while protons and oxygen are released into the thylakoid lumen. The electrons are transferred via the plastoquinone pool (Q) to the cytochrome b_6f complex (Cyt b_6f), which leads to a further release of protons into the thylakoid lumen by the Q-cycle (Joliot and Joliot, 2006). This generates a proton gradient across the membrane which is used as a motive force to produce ATP by the ATP synthase complex, which is mainly localized in the unstacked thylakoid region (Figure 2).

Photosystem I (PSI), acts as a light driven oxido-reductase and is also enriched in the stroma lamellae. By oxidizing plastocyanin (PC), a soluble luminal protein, electrons are transferred from Cyt b_6f to PSI and ferredoxin is reduced at the stromal side of the membrane. Ultimately the ferredoxin nicotinamide adenine dinucleotide phosphate (NADP⁺) reductase (FNR) produces NADPH, which together with the generated ATP drives the Calvin-Benson cycle for carbon fixation (Rochaix, 2011). Beside the linear electron flow, the generation of the reduction equivalent ATP is supported by a cyclic electron transport between PSI and Cyt b_6f (Allen, 2003; Joliot and Joliot, 2006; Figure 2).

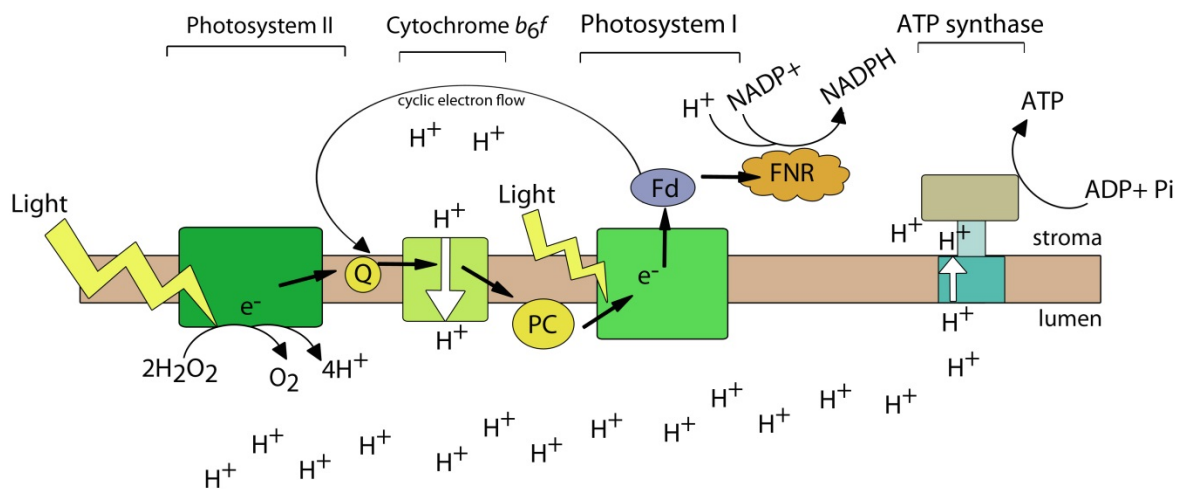


Figure 2. The photosynthetic electron transport chain in the thylakoid membrane. Illustration of thylakoid membrane complexes converting light energy into electrochemical energy. The electron transport chain generates a proton (H⁺) gradient between the two compartments (stroma/lumen) and to reduce NADP⁺. The reflux of protons into the stroma drives the ATP synthase complex. For more details, see text.

1.3 The RNA metabolism of the chloroplast

Although the genome, the transcription and translation apparatus of chloroplasts are of eubacterial origin, during the evolution their organization changed and it gained eukaryotic features. The gene expression of bacteria is mainly regulated at the transcriptional level. Bacterial genes of the same metabolic pathway are often organized in operons. The transcription is initiated and regulated at a single promoter region upstream of the 5' untranslated region (UTR) and terminated at the terminator region in the 3' UTR region of the gene cluster. Genes of one operon are translated from a polycistronic transcript and a

ribosomal binding site in front of each single gene avoids the release of the ribosome after reaching the stop codon of the prior gene (Lawrence, 2002; Levin-Karp et al., 2013).

The plastid genes are also often organized in gene clusters with a single eubacterial-like promoter region in the 5' UTR as in cyanobacteria (Bock, 2007). But beside the plastid encoded RNA polymerase (PEP), the transcription of plastid genes is also performed by a nucleus encoded RNA polymerase (NEP). Different than in bacteria most polycistronic transcripts of plastid gene clusters are processed to smaller RNAs in order to produce translational competent mRNA (Stoppel and Meurer, 2012).

Processing of precursor transcripts and formation of 5'- and 3'-ends is achieved by endo- and exonucleases homologous to the RNases found in bacteria (Drager et al., 1999; Hicks et al., 2002; Mathy et al., 2007; Li de la Sierra-Gallay et al., 2008; Schein et al., 2008; Newman et al., 2011; Stoppel et al., 2012). Plastid genes have acquired a divergence of sequences in their intergenic regions, the 5'- and 3'-UTRs, introns and editing sites. The presence of only few RNases with little sequence specificity in chloroplasts requires a gene specific action of newly evolved nucleus encoded factors (Stoppel and Meurer, 2012; Manvaski et al., 2012).

Most of these factors identified so far belong to the helical repeat protein superfamily, including tetratricopeptide repeat (TPR) proteins, pentatricopeptide repeat (PPR) proteins and octotricopeptide repeat (OPR) proteins (Stern et al., 2010; Barkan, 2011). The PPR proteins, which are not found in bacteria, are thought to act exclusively in organellar gene expression. This family consists of over 400 members in angiosperms, about half of which are predicted to be localized in the chloroplast and half in the mitochondria. They are defined by degenerate 35-amino acid repeats, which most probably bind single stranded RNA in a sequence specific manner (Schmitz-Linneweber and Small, 2008; Williams-Carrier et al., 2008; Prikryl et al., 2011). The other plant specific RNA binding domain protein families identified in the chloroplast have only few members (Amann et al., 2004; Barkan et al., 2007; Kroeger et al., 2009; Watkins et al., 2011). In addition to the nuclear factors which are highly specific for individual processing events, a family of nucleus encoded chloroplast ribonucleoproteins (cpRNPs) are proposed to regulate larger sets of chloroplast transcripts (Nakamura et al., 2004; Kupsch et al., 2012).

1.4 The *psbB* gene cluster

The *psbB* gene cluster is a good example for the high complexity and divergence of transcriptional and posttranscriptional processes in the chloroplast. In land plants the inner core antenna of PSII, CP47 (PsbB), two low molecular weight subunits of PSII, PsbTc and PsbH, and the subunits of the cytochrome *b₆f* complex, cytochrome *b₆* (PetB) and subunit IV (PetD) are transcribed from a single PEP promotor region. Additionally *PsbN* is located on the opposite strand in the intercistronic region between *PsbTc* and *PsbH* (Figure 3).

PsbN encodes a low molecular weight protein of 4.7 kDa and was originally named open reading frame (ORF) 43 (Kohchi et al., 1988). Because it was identified by N-terminal sequencing in PSII fraction, it was given the name PsbN (Ikeuchi et al., 1989). Later on it turned out that PsbN was mistaken for PsbTc, as they share some weak homology in the N-terminal part (Kashino et al., 2002). The PEP mediated expression of *psbN* was found to be regulated by the sigma-like transcription factor SIG3. The read-through transcripts of *psbN* are thought to function as a natural occurring antisense RNA to the *psbB-psbT* mRNA. It was suggested that the formation of RNA double strand hybrids under oxidative stress protects the *psbTc* mRNA from nucleolytic degradation by single-strand specific nucleases (Zghidi et al., 2007; Zghidi-Abouzid et al., 2011). Recently, PsbN was proposed to be involved in the formation of both photosystems (Krech et al., 2013), although its precise molecular function remained unclear.

Intergenic processing of the pentacistronic *psbB-psbT-psbH-petB-petD* transcripts and splicing of the group two introns in the *petB* and *petD* genes generates about 20 different mono, di-, and oligocistronic transcripts (Barkan, 1988; Westhoff and Herrmann, 1988; Stoppel et al., 2011). A nucleus encoded peptide chain release factor 2-like protein (PrfB), which specifically terminates UGA stop codons in the chloroplasts, affects the stabilization and translation of *psbB* transcripts (Meurer et al., 1996; Meurer et al., 2002; Figure 3).

The TPR-like protein HCF107 was found to influence the stability and translation efficiency of the *psbH* mRNA by specific binding to its 5' end (Felder et al., 2001; Sane et al., 2005; Hammani et al., 2012). In addition, the intercistronic region of *psbH-petB* is bound by the PPR protein HCF152, which is thought to define and protect the respective 5' or 3' RNA termini (Meierhoff et al., 2003a; Nakamura et al., 2003; Pfalz et al., 2009). The processed 3' end of *petB* was shown to be stabilized by PrfB3, which is a vascular plant specific RNA

binding factor that shows high homology to a bacterial peptide chain release factors (Stoppel et al., 2011). The translation and processing of monocistronic *petD* transcripts seem to be dependent on the PPR protein CRP1, although it could be only proven that this protein is associated with *petA* and *psaC* transcripts, which accumulations were also affected in *crp1* mutants (Barkan et al., 1994; Fisk et al., 1999; Williams-Carrier et al., 2008; Figure 3).

Furthermore, six proteins were found to be required for the splicing of *petB* and *petD* genes. Among these the APO domain family proteins APO1 and APO2 and the CRM domain family proteins CAF1 and CAF2 are specific for *petB* or *petD*, respectively. The other CRM domain family proteins CFM3 and CRS2 and the proteins WTF1 and RNC1 are involved in the splicing of both introns (Figure 3). Except CRS2, of which homologues are found in *Chlorophyta*, all of these factors are specific for *Embryophyta*. This agrees with the sole presence of both introns in land plants.

Additionally, editing sites are found within the *psbB* gene cluster of some members of the *Embryophyta*. Recently, 116 C-to-U editing sites were identified in the *psbB* gene cluster of the moss *Takakia lepidozoides*. In contrast, tobacco and maize have only one of these editing sites in the coding region of *petB* (Figure 3) and none is present in *Arabidopsis* (Stoppel and Meurer, 2013).

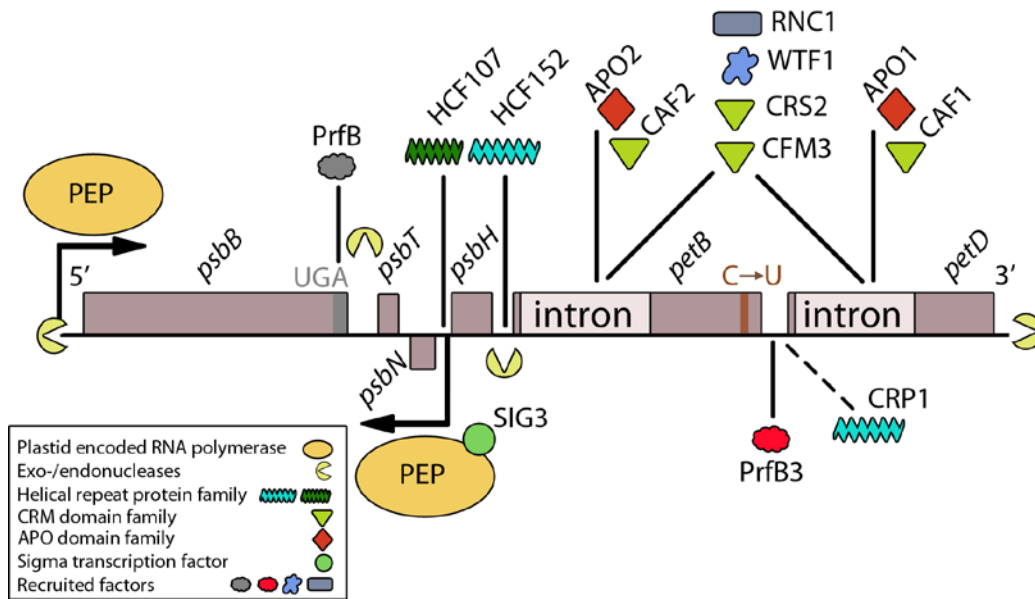


Figure 3. Scheme of the tobacco *psbB* gene cluster and of trans-acting factors involved in transcriptional and posttranscriptional processes. For further details, see text.

1.5 Photosystem II, the water splitting enzyme

Photosystem II is a multiprotein pigment-containing complex, which consists at least of two dozen subunits as well as antenna proteins (Shi and Schröder, 2004; Komenda et al., 2012). The crystal structure of the phylogenetic highly conserved PSII complex was resolved in *Thermosynechococcus vulcanus* at a resolution of 1.9 Å (Umena et al., 2011). The PSII core consists of the two similar plastid encoded transmembrane subunits D1 (PsbA) and D2 (PsbB), which form a heterodimer inside the membrane and bind all redox active co-factors needed for the photochemical charge separation, quinone reduction and water splitting. On the luminal side the manganese cluster and the extrinsic oxygen evolving complex (OEC), consisting of the nucleus encoded subunits PsbO, PsbP and PsbQ, are attached.

The PSII core is flanked by the plastid encoded inner antenna proteins CP43 (PsbC) and CP47 (PsbB) which bind 14 and 16 chlorophyll-*a* molecules, respectively (Nelson and Ben-Shem, 2004). The core antenna passes the excitation energy to the pigments bound to the PSII core, which consist of 4 chlorophyll-*a* and 2 pheophytin-*a* molecules and absorb light around 680 nm (P680) (Saito et al., 2013). The heme cofactor binding cytochrome *b*₅₉₉ complex (cyt *b*₅₉₉) is a heterodimer composed of PsbE and PsbF and is part of PSII core.

Although it seems not to be involved in the primary electron transport of PSII, as it shows very slow responding redox kinetics, it is essential for the PSII assembly. Furthermore, several low molecular weight subunits, that are involved in PSII assembly, stabilization, dimerization and photo-protection, are attached to Photosystem II (Shi and Schöder, 2004; Shi et al. 2011).

1.6 Assembly and repair mechanisms of PSII

The PSII de novo assembly as well as the insertion of newly synthesized D1 are assumed to take place in the unstacked thylakoid regions of chloroplasts, while the functional PSII complex is found mainly in the stacked grana regions. The association of polysomes to the exposed region of the thylakoids, the localization of the PSII assembly factor HCF136, the co-translational assembly of the D1 protein and the existence of smaller PSII subcomplexes in the stroma lamellae corroborate this hypothesis (Yamamoto et al., 1981; Meurer et al., 1998b; Zhang et al., 1999). The PSII complex is thought to be assembled from independently formed modules. The assembly process is believed to occur in a stepwise manner and through a number of intermediate steps, which are to some extent translationally regulated (Nickelsen and Rengstl, 2013).

First, the small precomplexes pre-D1 containing the precursor form of D1 (pD1) and most likely PsbI, and pre-D2 consisting of D2 bound to PsbE and PsbF are assembled to the heterodimeric reaction center of PSII (RC) (Figure 4). Subsequently pre-CP47 represented by the inner core antenna protein CP47 and probably together or accompanied with the low molecular weight subunits PsbH, PsbL, PsbM, PsbX and PsbTc bind to the RC forming the RC-47 (Figure 4).

After the binding of the pre-CP43, consisting of the PSII core antenna CP43 and the small subunits PsbK and PsbZ, the PSII monomer (PSII-M) is formed (Figure 4). This is followed by the attachment of the oxygen-evolving complex on the luminal side of the PSII-M. Now the PSII dimer (PSII-D) is formed and finally the outer antenna proteins CP29, CP26 and CP24 and the trimeric light harvesting complex (LHCII) attach, thereby forming the PSII supercomplexes (PSII-SC) (Figure 4). This supramolecular organization of PSII was recently shown to be influenced by the small PSII subunit PsbW (Garcia-Cerdan et al., 2011).

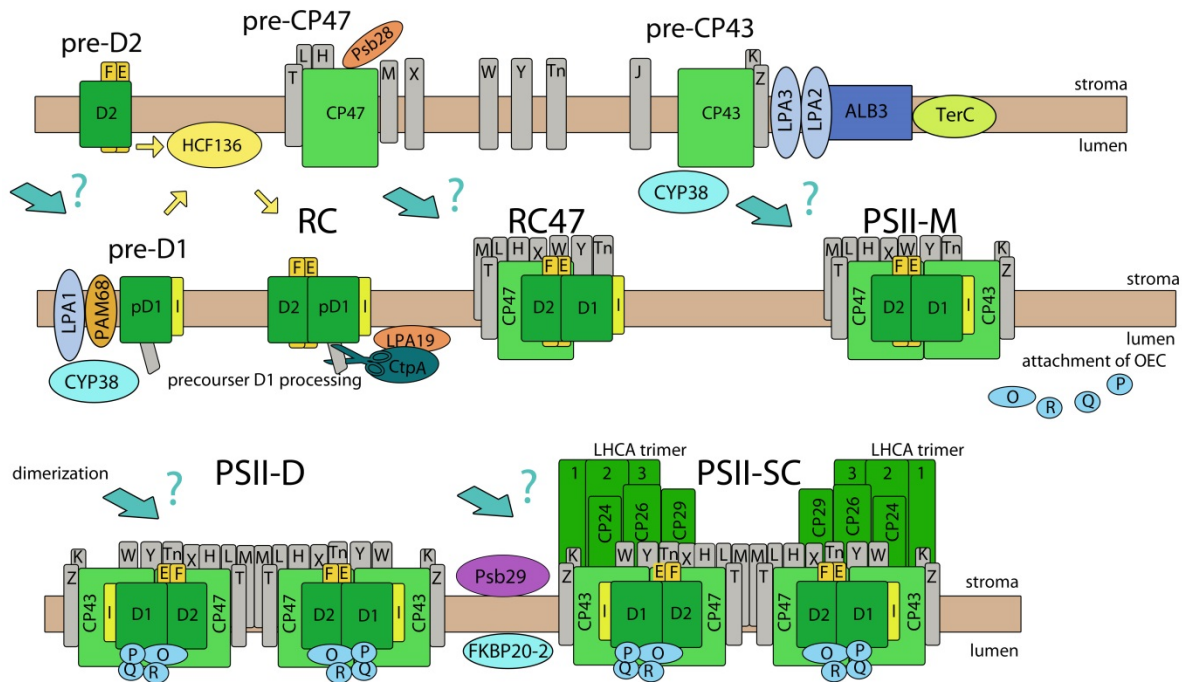


Figure 4. Assembly of the PSII complex in higher plants. Proposed scheme for the sequential assembly of PSII complexes mediated by various nucleus encoded assembly factors. The question marks indicate that the attachment site and function of most nucleus encoded factors as well as of the small subunits to PSII-precomplexes and PSII-complexes is largely unclear. For details, see text.

Most of these highly complex steps, which are only poorly understood, are mediated by chaperones and assembly factors. The first factor identified, HCF136, resides mainly in the stroma lamellae and is required for an efficient formation of the PSII RC (Meurer et al., 1998b; Plücker et al., 2002; Figure 4).

After the formation of the PSII RC the C-terminal extension of pD1 is processed by the specific luminal protease CtpA. This event is mediated by LPA19, also called Psb27-H2, which shares about 30% sequence identity to Psb27-H1 another homolog to Psb27 of cyanobacteria (Wei et al., 2010; Chi et al., 2012; Mabbitt et al., 2014). The D1 synthesis as well as further PSII assembly steps are influenced by LPA1 (Peng et al., 2006). A similar function was suggested for PAM68 which probably interacts with LPA1 and D1 (Armbruster et al., 2010). The folding and insertion of D1 and supposedly also of CP43 is assisted by the immunophilin CYP38, which is presumably necessary for the correct assembly of the OEC (Sirpio et al., 2008; Figure 4).

The synthesis and stable insertion of CP43 depends on the cooperation of LPA2 and LPA3 and their interaction with the membrane insertase ALB3. Furthermore, TerC, which is required for efficient insertion of thylakoid membrane proteins, was recently shown to interact with ALB3 (Ossenbühl et al., 2004; Cai et al., 2010; Schneider et al., 2014; Figure 4). The biogenesis of CP47 is influenced by Psb28, which might be important for the synthesis of chlorophylls and/or apoproteins of the inner core antenna (Dobakova et al., 2009). The formation of PSII-SC was shown to be dependent on Psb29 and the immunophilin FKBP20-2 (Keren et al., 2005; Lima et al., 2006; Fu et al., 2007; Figure 4). Due to the highly conserved structure and function of PSII most of the assembly factors were already present in cyanobacteria and preserved a similar function.

The best-studied and probably most important protection mechanism against excess of light is the D1 repair cycle. Due to an increased charge separation and formation of reactive oxygen species (ROS) the D1 protein gets damaged and replaced. This mechanism is thought to protect the remaining PSII and the other components of the electron transport chain (Ohad et al., 1990). Most probably, many of the assembly factors involved in the *de novo* biogenesis of PSII are also involved in the D1 repair cycle. For this purpose PSII migrates to the stroma lamellae where the damaged D1 is exchanged (Mulo et al., 2008).

The broken D1 is excised and degraded by Deg and FtsH proteases. This repair process is thought to be regulated by phosphorylation of the PSII RC proteins leading to conformational changes in the thylakoid membrane. Thereby, the access of the proteases and the migration of PSII to the stroma exposed membranes are facilitated (Haussuhl et al., 2001; Fristedt et al., 2009; Nixon et al., 2010; Komenda et al., 2012; Tikkanen and Aro, 2012).

1.7 Aim of this dissertation

Among the plastid genomes of different algae and land plant species gene rearrangements, losses, gains and duplications can be observed (Wicke et al., 2011). Forward genetic approaches often identified novel plant-specific genes involved in the RNA metabolism of the chloroplast (Meurer et al., 1998a; Baginsky et al., 2007; Stoppel et al., 2011; Stoppel et al., 2012). This suggests that beside the known RNA binding protein families, a large number of novel nuclear encoded proteins involved in the chloroplasts RNA metabolism remains elusive.

The first part of this thesis is a continued approach of a forward genetic screen, which identified several mutants affected in photosynthesis due to their high chlorophyll fluorescence phenotype (*hcf*) (Meurer et al., 1996). The *hcf145* mutant was proven to be affected in the accumulation of the *psaA-psaB-rps14* transcripts, suggesting that the corresponding protein is involved in the stabilization of the *psaA* mRNA (Lezhneva and Meurer, 2004). Within this work further attempts were made to verify the assumed function and to get insights into the phylogenetic origin, conservation and regulation of this newly evolved factor.

In contrast to the fast evolving RNA metabolism, most proteins directly involved in photosynthesis remained highly conserved. Reverse genetic approaches by plastid transformation in tobacco helped to study the function of many chloroplast encoded proteins in land plants in the past decades (Ruf et al., 1997; Kofer et al., 1998; Hager et al., 1999; Schwenkert et al., 2006; Umate et al., 2008). The second part of the thesis is part of a transplastomic approach, that addresses the function of low molecular weight proteins encoded in the chloroplast.

A spectinomycin resistance marker (*aadA*) was inserted into the corresponding coding region to generate the plastid gene knockouts. To consider site effects onto adjacent genes, due to the extraordinary localization of *PsbN* on the opposite strand to the *psbB* gene cluster, the *aadA* cassette was inserted in both directions resulting in two lines $\Delta psbN-F$ and $\Delta psbN-R$.

Within this thesis the expression, localization, topology and association to photosynthetic complexes of *PsbN* was addressed. By minimizing the secondary effects due to light stress, the primary defect in the $\Delta psbN-F$ and $\Delta psbN-R$ mutants was investigated intensively using various spectroscopic, immunological and native PAGE analyses. To

reassure the revealed function of PsbN in PSII assembly, the $\Delta psbN-F$ and $\Delta psbN-R$ lines were complemented by a nuclear encoded version of PsbN fused to a transit peptide for chloroplast import. Furthermore, the $\Delta psbN-F$ and $\Delta psbN-R$ lines were preliminary compared to the $\Delta psbN$ lines described by Krech et al. (2013). Additionally, a semi-sterile culture technique was established for a rapid growth of the mutants on sucrose supplemented medium and flower development.

2. Materials and Methods

General molecular methods were performed according to standard protocols (Sambrook and Russell, 2001) or using commercial kits.

2.1 Database analysis

Analyses of gene models and coverage by full-length mRNAs or expressed sequence tags (ESTs)

NCBI www.ncbi.nlm.nih.gov

TAIR www.arabidopsis.org

DNA and amino acid sequence alignments

NCBI Blast 2 sequences <http://blast.ncbi.nlm.nih.gov/Blast.cgi>

MultAlin (Corpet, 1988)

CLUSTAL-W2 <http://www.ebi.ac.uk/Tools/msa/clustalw2/>

Prediction of protein structure

I-Tasser <http://zhang.bioinformatic.ku.edu/I-TASSER/output.html>

Prediction of transit peptides for organellar import

BaCelLo <http://gpcr.biocomp.unibo.it/bacello>

ChloroP <http://www.cbs.dtu.dk/services/ChloroP>

MitoProt <http://ihg.gsf.de/ihg/mitoprot.html>

Predotar <http://urgi.versailles.inra.fr/predotar/predotar.html>

PSORT <http://psort.ims.u-tokyo.ac.jp/form.html>

TargetP <http://www.cbs.dtu.dk/services/TargetP>

Wolf Psort <http://wolfpsort.org/>

2.2 Vectors

pENTR/D-TOPO	(Invitrogen)
pB7FWG2	(Plant System Biology)
pB7GWIWG2(I)	(Plant System Biology)

2.3 Oligonucleotides

Oligonucleotides used for amplification of DNA regions and as hybridization probes in RNA gel blot analysis were purchased through MWG Biotech AG or Metabion international AG. A list of all primers used in this work can be found in the appendix.

2.4 Bacterial strains

Agrobacterium tumefaciens:

GV3101 (pMP90RK) (Koncz et al., 1994)

Escherichia coli:

DH5 α Bethesda Research Laboratory

2.5 Antibodies

Antisera against PsbN were generated against the synthetic peptide QPSQQLRDPFEEHGD (Agrisera). Antisera against the HCF145 were generated against the synthetic peptide RQLNSRKDNGNTILRT (Pineda). Other antisera CP43, PsbH, and PsaA (Agrisera), anti-phosphothreonine (Cell Signaling) and secondary antibodies (Sigma-Aldrich) were purchased, or described elsewhere (Umate et al., 2008; Qi et al., 2012).

2.6 Plant materials and growth conditions

The *Arabidopsis hcf145-1* line, accession Wassilewskija originated from a T-DNA collection (Feldmann, 1991) as previously described (Lezhneva and Meurer, 2004). The T-DNA

insertion line *hcf145-2* (SALK_011411), accession Columbia was obtained from SALK collection (<http://signal.salk.edu>). Unless stated otherwise selection, propagation and growth of the *Arabidopsis* wild-type and mutant plants was facilitated as previously described (Lezhneva and Meurer, 2004).

For regulation experiments, *Arabidopsis* wild-type plants were grown on soil in a 17 h light (20°C)/8 h dark (18°C) cycle with a photon flux density (PFD) of 50 $\mu\text{mol photons m}^{-2} \text{s}^{-1}$ for three weeks. For the treatments, the plants were carefully transferred to reaction tubes, with the roots into liquid medium and subjected to growth light (GL 24 h), dark (24 h), red light (660 nm; 20 $\mu\text{mol photons m}^{-2} \text{s}^{-1}$; 24 h), far red light (720 nm; 1 $\mu\text{mol photons m}^{-2} \text{s}^{-1}$; 24 h), cold (4°C; GL; 24 h), heat (40°C; GL; 1 h), DCMU (50 μM ; GL; 24 h), Paraquat (MV) (50 μM ; GL; 24 h).

For co-immunoprecipitation analyses wild-type plants and complemented lines were grown on soil in a 17 h light (20°C) 8 h dark (18°C) cycle for one week and another 3-4 weeks in a 8 h light 17 h dark cycle with a PFD of 100 $\mu\text{mol photons m}^{-2} \text{s}^{-1}$. *Nicotiana tabacum* L. cv. Petit Havana (Wild type) and *HCF145RNAi* lines and ΔpsbN tobacco plants were grown on sucrose supplemented medium in continuous light with a PFD of 6-10 $\mu\text{mol photons m}^{-2} \text{s}^{-1}$ at 25°C as described (Torabi et al., 2014). Growth under preferential state I condition was achieved by covering the light source (HE 21W/60, Osram) with a dark-red filter (027 Medium Red, Lee Filters).

2.7 Complementation of *hcf145-1* and *hcf145-2*

The cDNA of At5g08720 was obtained from the RIKEN BioResource Center (Seki et al., 2002). For complementation of *hcf145-1* the cDNA was amplified using *Pfu* polymerase (Fermentas) and the primers 720-ATG-f-P and 720-3UTR-r-P. The purified PCR product was blunt-end ligated into the *SmaI* linearized pSEX001-VS (Reiss et al., 2000). For complementation of *hcf145-2* the cDNA was amplified using the PhusionTM High-Fidelity DNA Polymerase (New England Biolabs) and the primers Cacc-145-for and 145-rev. The resulting PCR product was cloned into pENTR/D-TOPO (Invitrogen) followed by insertion into the binary Gateway vector pB7FWG2 (Plant System Biology) in frame with the GFP coding region using LR Clonase II (Invitrogen). Both vectors were introduced into *Agrobacterium tumefaciens* GV3101 (pMP90RK) and subsequently transformed into the corresponding heterozygous *hcf145* mutants using the floral dip method (Clough and Bent,

1998). Transformed seedlings were selected with BASTA and the complemented homozygous mutants were identified by PCR analyses.

2.8 Generation of *HCF145* RNAi-lines in tobacco

A 255 bp fragment of the *Nicotiana tabacum* EST (Accession, FG168642), which is highly homologous to the cDNA of *AtHCF145*, was reverse transcribed from total tobacco RNA using Titan One Tube RT-PCR Kit (Roche) with the primers A1-for and A1-rev. The resulting PCR product was cloned into pENTR/D-TOPO (Invitrogen) followed by insertion into the binary Gateway vector pB7GWIWG2(I) (Plant System Biology). Subsequently *Agrobacterium tumefaciens* mediated transformation of wild-type tobacco was performed.

2.9 Complementation of $\Delta psbN$ mutants

The cDNA of *PsbN* (ATCG00700) was amplified with the primer psbN-for and psbN-rev and the cDNA of the N-terminal transit peptide of *PsbS* (AT1G44575) was amplified with the primers psbS-for and psbS-rev. Both fragments were digested with *HindIII* and ligated using T4-Ligase (Fermentas). The ligation was purified using spin columns (Quiagen) and amplified by PCR with the primers psbS-for and psbN-rev. The resulting fragment of the right size was extracted from an agarose gel using spin columns (Quiagen). The fragment was cloned into pENTR/D-TOPO (Invitrogen) followed by insertion into pB7FWG2 (Plant System Biology) using LR Clonase II (Invitrogen). Subsequently *Agrobacterium tumefaciens* mediated transformation of wild type and $\Delta psbN$ mutants was performed.

2.10 *Agrobacterium tumefaciens* mediated transformation of tobacco

Leaves of 3-week-old in vitro cultured tobacco plants were cut into squares of about 0.5x0.5 cm and placed on a petri dish with regeneration medium (RMOP) (Svab et al., 1990). Transformed agrobacteria were pre cultured in 4 ml LB Medium with 50 µg/ml of the antibiotics rifampicin (rif), gentamycin (gent) and spectinomycin (spec) (LB-RGS) for 15 h. 25 ml of LB-RGS were inoculated with 1 ml of the pre-culture and grown until an optical density (OD) of 0.6-0.8. The bacteria were collected (4000 g; 20 min) and resuspended in 25 ml agro-transformations media (MS medium or sterile ddH₂O; 0.02% silvet). The explants

were vacuum infiltrated and incubated for 10 min in the bacteria suspension. The leaf pieces were dapped on sterile filter paper to remove residual liquid and placed on RMOP. After co-cultivation of 2 days the leaf pieces were washed two times (sterile ddH₂O; 250 µg/ml carbenicillin [carb] and cefotaxime [cef]) and placed on selection medium (RMOP, 2.5 µg/ml phosphinotricine [ppt], 250 µg/ml carb and cef). The selection medium was refreshed weekly and the callus was cut to provide good contact with the medium. After 4-6 weeks resistant shoots were cut and placed on MS medium (5 µg/ml ppt; 250 µg/ml carb and cef). When the shoots developed roots they were transferred to soil or to semi sterile culture for seed production.

2.11 Rapid DNA isolation for PCR analysis

A small leaf piece (area $\leq 10 \text{ mm}^2$) was homogenized in 400 µl extraction buffer (200 mM Tris/HCL; pH 7.5; 250 mM NaCl; 25 mM EDTA; 0,5% w/v SDS) using two stainless steel bearing balls ($\text{\O} = 4 \text{ mm}$), a 2 ml reaction tube (Eppendorf) and a bead-beater (MM300, Retsch) for 2 min at a frequency of 30 Hz. The homogenate was centrifuged (16,000 g; 4°C) for 10 min and 300 µl of the supernatant was mixed with 300 µl isopropanol in a new reaction tube. After 2 min incubation at room temperature the solution was spun (16,000 g; 4°C) for 15 min, the supernatant was discarded and the pellet was air-dried. To dissolve the DNA from the dried pellet, 100 µl ddH₂O was added without mixing and incubated at 4°C over-night. For one PCR reaction 1 µl of the DNA solution was used. The solution could be stored at minus 20°C.

2.12 RNA isolation and gel blot analysis

Total leaf RNA and immunoprecipitated RNA was isolated with TriPure Isolation Reagent (Roche) as recommended by the provider. For gel blot analyses glyoxylated RNA was electrophoresed as described (Westhoff and Herrmann, 1988) and transferred to a nylon membrane (Biodyne A® 0,45 µM, PALL) with a set up capillary blot using 20x saline sodium citrate (SSC) transfer buffer. After the transfer the membrane was washed in 2x SSC and UV-crosslinked (Stratagene UV 1800). Hybridization probes were generated by T4 polynucleotide kinase (New England Biolabs) mediated end labeling of oligonucleotides with [³²P] γ-ATP (Hartmann Analytic) or by random labeling of PCR products using Klenow fragment polymerase (Fermentas) with [³²P] dCTP (Hartmann Analytic). Hybridization was

performed with ExpressHyb™ hybridisation solution (BD Biosciences; USA) according to the user's manual.

2.13 Spectroscopic analysis

Chlorophyll *a* fluorescence induction kinetics were measured using pulse modulated fluorometers (Imaging-PAM; Dual-PAM-100; PAM101, Walz). For the measurement of P700 absorbance changes PAM101 was used. All spectroscopic analyses were performed as described (Meurer et al., 1996). The quantum yield of photochemical energy conservation (Φ_{PSI}) and the quantum yield of non-photochemical energy dissipation due to donor side limitation ($\Phi_{\text{PSI ND}}$) were calculated as described (Klughammer and Schreiber, 1994).

2.14 Fluorescence imaging

The stable expressed HCF145-GFP fusion in the *hcf145-2com_{gfp}* was visualized in guard cells using a fluorescence microscope (Axio Imager, Zeiss).

2.15 Measurements of PSII photoinhibition and recovery

Small leaves or leaf discs (\varnothing 8-10 mm) were pre-treated for 20 min in ddH₂O or in lincomycin (200 mg/l) for 20 min in the darkness. The leaves were placed on wet filter paper (Whatman®) in a petri dish and were covered with wet lens tissue paper (Macherey-Nagel). The maximum quantum yield of PSII was measured after each hour of application of photoinhibitory light by the Imaging PAM (Walz). The recovery from photoinhibition was measured by application of low light ($5 \mu\text{mol photons m}^{-2} \text{s}^{-1}$) from an external light source and the effective quantum yield of PSII was measured each hour by the Imaging PAM (Walz).

2.16 77K fluorescence measurement

Thylakoids set to a concentration of 10 μg chlorophyll/ml were transferred into a glass capillary (0.7-mm internal diameter) and were carefully frozen in liquid nitrogen. Fluorescence was excited at 430 nm and the slits used were in the range of 1 to 2 nm. The

emission was recorded between 670 and 770 nm using a Jobin Yvon Spex Fluorolog spectrofluorometer (Hamamtsu R 374).

2.17 Protein analysis and immunoprecipitation

Thylakoid membrane proteins and soluble chloroplast proteins were isolated as described (Stoppel et al., 2011). For total protein isolation fresh or frozen plant material was homogenized in isolation buffer (10 mM EDTA; 2 mM EGTA; 50 mM Tris-HCl; pH 8,0; 10 mM DTT; proteinase inhibitor cocktail, Roche). Soluble and membrane proteins were separated in 10% and 15% SDS-PAGE (Laemmli, 1970) and transferred to polyvinylidenfluorid (PVDF) membrane (Immobilon™ 0,45µm, Millipore). For the detection of small proteins (≤ 10 kda) Tricine-SDS-PAGE ($\geq 15\%$), shorter transfer times and membranes with a smaller pore size were used (0,2 µm PVDF; 0,1 µm nitrocellulose membrane). Co-immunoprecipitation experiments were performed with soluble chloroplast proteins of wild type and *hcf145-2com_{gfp}* using magnetic beads (GFP-Trap®, Chromotek) as recommended by the provider.

2.18 Separation of thylakoid membrane complexes by BN-PAGE

Thylakoid membranes were dissolved in ice-cold ACA Puffer (750 mM aminocaproic acid; 50 mM Bis-Tris pH 7; 5 mM EDTA-Na₂) to a concentration of 0,375 µg chlorophyll/µl. Subsequently, the thylakoids were solubilized on ice for 10 min by the addition of 10% β-dodecyl-maltoside to a final concentration of 1%. After centrifugation (20 min; 14000 g; 4°C) the supernatant was mixed with BN-loading puffer (750 mM aminocaproic acid; 5% Serva-G 250). Per lane solubilized thylakoid membrane complexes appropriate to 10-50 µg of chlorophyll were separated in a 4–12% BN-PAGE as described (Schwenkert et al., 2006). The gel was used for western blot of the first dimension or the lanes were cut and stored at -20°C. To perform a second dimension SDS-PAGE, the lanes were incubated 20 min at room temperature in denaturing buffer (2% SDS; 66,7 mM Na₂CO₃; 100 mM DTT). The separated proteins were transferred to PVDF or nitrocellulose membrane for western blot or the gels were stained with silver or colloidal coomassie.

2.19 Topology studies on PsbN

Topology studies were basically performed as described (Karnauchov et al., 1997).

Salt treatment of thylakoid membranes

Freshly isolated thylakoid membranes were resuspended at 0.5 mg chlorophyll/ml in HS buffer (0.1 M sucrose; 10 mM HEPES-NaOH pH 8.0) or in HS buffer containing 2 M NaBr, 2 M NaSCN, 0.1 M Na₂CO₃, and 0.1 mM NaOH, respectively. After 1 h incubation on ice, the samples were diluted with two volumes of HS buffer and separated into pellet and soluble fraction by centrifugation (20.000 g; 4°C; 10 min)

Protease treatment of thylakoid membranes

Freshly isolated thylakoids were resuspended at 0.5 mg chlorophyll/ml in HS buffer and sonified 20 times for 3 sec on ice, to form about 50% inside-out vesicles. Thylakoids and inside-out vesicle thylakoids were treated with the protease thermolysin (200 µg/ml) on ice. The proteolysis was stopped by supplementation of 20 mM EDTA. Thylakoids were washed with HS buffer containing EDTA (20 mM) and separated by SDS-PAGE.

2.20 In vivo labeling of chloroplast proteins

Leaf discs (Ø 4 mm) were incubated with labeling buffer (1 mM KH₂PO₄ pH 6.3; 0.1% Tween-20; cycloheximide 20 µg/ml) for 30 min to suppress protein synthesis in the cytosol. After addition of [³⁵S]-methionine (Hartmann Analytics) at a final concentration of 0.7 mCi/ml the leaf discs were vacuum infiltrated and incubated in the light. Before protein isolation the leaf discs were washed two times with 20 mM Na₂CO₃.

3. Results

3.1 HCF145 stabilizes *psaA-psaB-rps14* transcripts

The previously described *hcf145-1* mutant accumulates less than 10% of the tricistronic *psaA-psaB-rps14* mRNA as compared to the WT (Lezhneva and Meurer, 2004). This precursor RNA is produced by the plastid-encoded polymerase (PEP). Run on analysis revealed that the nucleus-encoded factor HCF145 is involved primarily in *psaA-psaB-rps14* mRNA stabilization rather than in transcription of the tricistronic *psaA* gene cluster in *Arabidopsis* (Lezhneva and Meurer, 2004). Other deficiencies on the transcript and translational level were not observed at that time using RNA gel blot, array and in vivo labeling analyses (Lezhneva and Meurer, 2004; Cho et al., 2009).

The tetracistronic *ycf3-psaA-psaB-rps14* precursor which is generated by the NEP accumulates at slightly higher rates. Both precursors have the same 3' end indicating that the determinant for RNA stabilization is located at the 5' end of the tricistronic transcript (Lezhneva and Meurer, 2004). The monocistronic *rps14*, which results from cleavage of the precursor RNAs, accumulates at almost WT-comparable levels. According to reduced *psaA-psaB-rps14* mRNA levels, amounts of PSI were reduced to a similar degree. In order to identify the nuclear *HCF145* gene the *hcf145-1* mutant has been mapped roughly on the upper arm of chromosome 5 in-between the molecular SSLP markers *nga158* and *nga151* (<http://www.arabidopsis.org>) located at positions 1.69 and 4.67 Mbp, respectively (Lezhneva and Meurer, 2004).

Further mapping using 1281 F2 mutant plants derived from backcrosses to the *Arabidopsis* accession *Landsberg erecta* localized the mutation at the map position of about 2.8 Mbp with zero recombinants in the region covered by the two bacterial artificial chromosomes T2K12 and T5E8. A dozen T-DNA insertion lines around this region were ordered and analyzed preliminary by chlorophyll fluorescence imaging. One Salk_01411 line of the AT5G08720 locus (*hcf145-2*) showed all characteristics of a seedling lethal photosystem I mutant, which all resembled the *hcf145-1* phenotype (Lezhneva and Meurer, 2004). Sequencing of the AT5G08720 locus in *hcf145-1* identified a deletion of 39 nucleotides including the guanine residue of the 3' junction of intron eight.

3.1.1 Comparison of two allelic mutations in the AT5G08720 locus

3.1.1.1 Genotyping analysis

To confirm the 39 nucleotide deletion in intron 8 of the AT5G08720 locus in the previously described *hcf145-1* line (Lezhneva and Meurer, 2004), a polymerase chain reaction (PCR) analysis using the oligonucleotides ex8-for and ex10-rev2 was performed (Figure 5A/B). The reaction amplified a fragment of 409 bp for the wild type and a fragment of 372 bp for *hcf145-1* mutants. In the heterozygous mutants the PCR amplified as expected both fragments. Furthermore a third band migrating at higher molecular weight appeared which is likely to represent mismatching annealing products of the larger wild-type and smaller mutant allele fragments (Figure 5B).

To approve the presence of the T-DNA insertion in exon 8 of the *hcf145-2* mutant, two separate PCR reactions were carried out. The first reaction with the oligonucleotides ex7-for and ex10-rev1 amplified a fragment of 850 bp in the wild type and heterozygous mutants, while no fragment was obtained from T-DNA insertion line *hcf145-2*. In the second reaction with the oligonucleotides ex10-rev1 and LBb1, a fragment of 582 bp was only obtained from the heterozygous and homozygous *hcf145-2* mutants, confirming a T-DNA insertion in the exon 8 of the AT5G08720 locus (Figure 5C).

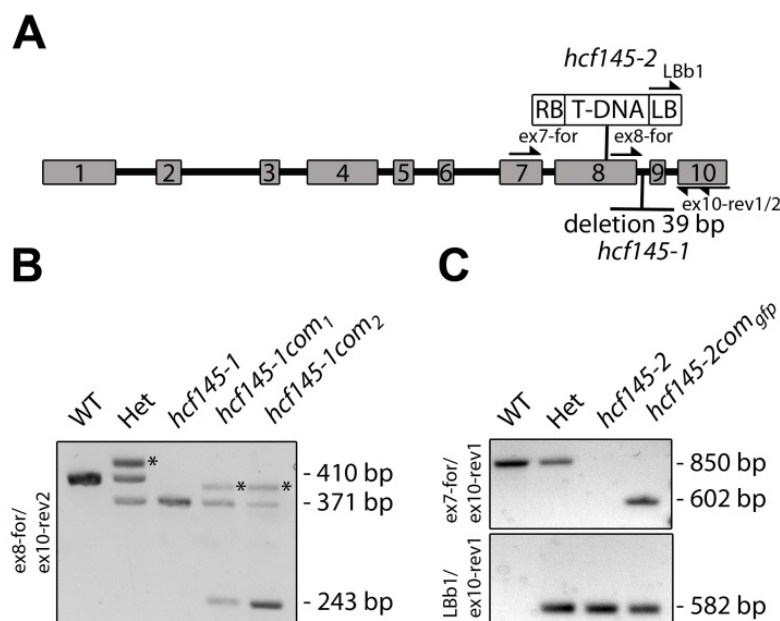


Figure 5. Genotyping of two allelic mutants in the *AT5G08720* locus. (A) Scheme of the *HCF145* gene, consisting of ten exons (1-10). The positions of the 39 base pair (bp) deletion mutation in *hcf145-1* and the T-DNA insertion in *hcf145-2* as well as the binding sites of oligonucleotides used for PCR analysis are indicated. RB, right boarder of the T-DNA. LB, left boarder of the T-DNA. (B) and (C) PCR analysis to identify wild type (WT), heterozygous mutants (Het), *hcf145* mutants and complemented (com) lines using the oligonucleotides indicated on the left. Fragment sizes are indicated on the right. Asterisks mark mismatching annealing products of wild-type and mutant allele fragments. For details, see text.

3.1.1.2 Spectroscopic analysis

The *hcf145-1* and *hcf145-2* mutant plants displayed a comparable phenotype. Both lines appeared pale and were only able to survive on sucrose-supplemented medium (Figure 6A). Also the photosynthetic performance was comparable as revealed by chlorophyll *a* fluorescence measurements and P700 absorbance kinetics. The singlet-excited states of chlorophyll could hardly be quenched upon application of actinic light in both *hcf145* mutant lines resulting in a strong *hcf* phenotype (Figure 6A/B). The maximum and the effective quantum yield of PSII was 0.54 ± 0.05 and 0.11 ± 0.04 as compared to 0.81 ± 0.01 and 0.76 ± 0.03 in the WT, respectively.

The P700 absorbance kinetics was below the limit of detection as shown before in *hcf145-1* and other PSI mutants (Meurer et al., 1996; Lezhneva and Meurer, 2004; Figure 6C).

3.1.1.3 Complementation analysis

The generation of *hcf145-1com* mutants was performed by Dr. Lina Lezhneva. The full-length *hcf145* cDNA was used for complementation test in heterozygous *hcf145-1* plants, while the cDNA fused to *GFP* was used in heterozygous *hcf145-2* plants. The transgenes were expressed under the control of the cauliflower mosaic virus 35S promoter. Transformed plants were selected after the treatment with “BASTA” and homozygous mutants were identified by PCR analysis (Figure 5A).

In the PCR analysis of the *hcf145-1com* lines a fragment of the same size as in the *hcf145-1* line and a fragment from the transformed cDNA of 243 bp were amplified. Similar to the heterozygous *hcf145-1* lines a third mismatching annealing product of larger size appeared in the *hcf145-1com* lines (Figure 5B). The first PCR reaction of the complemented line *hcf145-2com_{gfp}* amplified only a fragment corresponding to the size expected from the *hcf145* cDNA. In the second PCR analyses a fragment with the same size as in the mutant and heterozygous lines was obtained (Figure 5C). The constitutive expression of the introduced cDNA restored the wild-type growth and *hcf* phenotype in both *hcf145* lines (Figure 6A). This proved that the observed defects of the mutants are solely caused by the lack of HCF145.

3.1.1.4 Immunological analysis

Previously, the impaired accumulation of PSI proteins in the *hcf145-1* line was extensively studied (Lezhneva and Meurer, 2004). To confirm a similar PSI deficiency in both allelic *hcf145* lines, immunological analyses with total protein extracts were performed (Figure 6D). In the extracts of both mutant lines PsaA was hardly detectable, while in both complemented lines a signal with higher intensity than 50% of wild-type levels was observed. The PSII subunit PsbH accumulated in both mutant lines to amounts comparable to those in the wild type and complemented lines. This again shows that both allelic mutations cause a primary defect in the accumulation of PSI and that the overexpression of the *hcf145* cDNA could nearly fully restore this defect in both mutants.

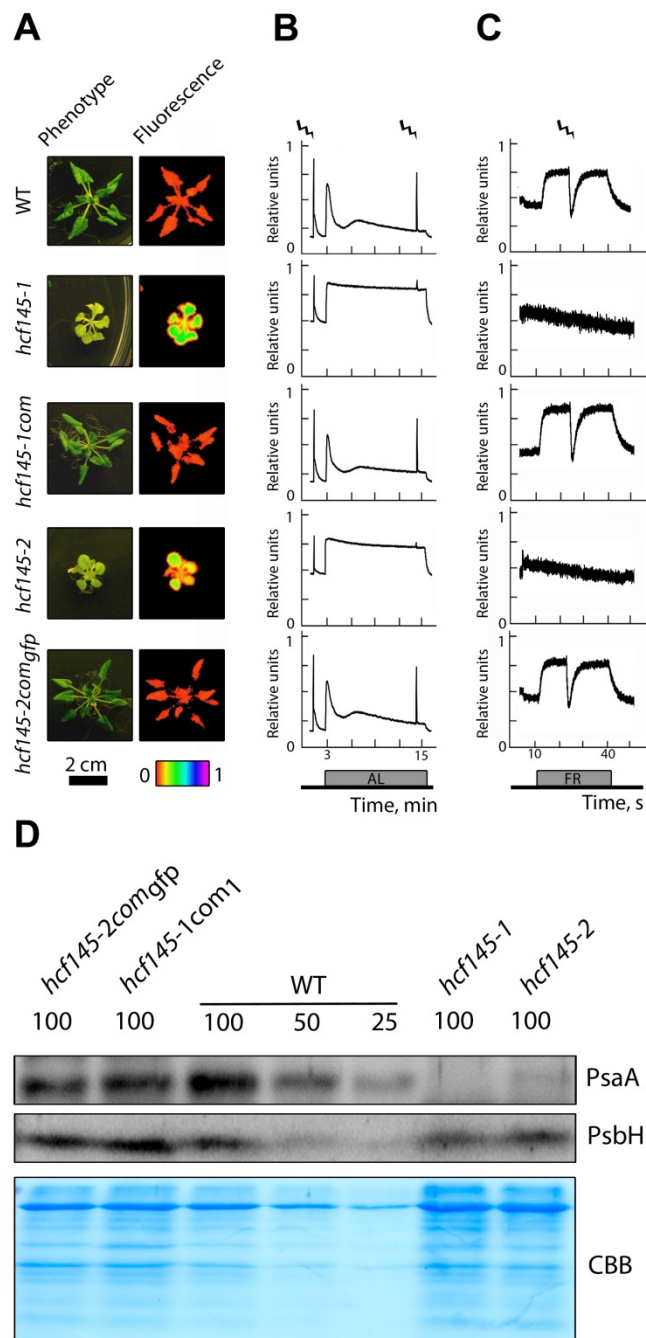


Figure 6. Spectroscopic and immunological analyses of *Arabidopsis hcf145* mutants. (A) Photographs and chlorophyll *a* fluorescence image of dark adapted 3-week-old plants grown on sucrose supplemented medium at $10 \mu\text{mol photons m}^{-2} \text{s}^{-1}$. The color gradient bar scales the relative fluorescence values. (B) Chlorophyll *a* fluorescence kinetic and (C) P700 redox kinetics. (B) and (C) Strokes indicate saturating light pulses and the grey bars indicate the duration of actinic light (AL) or far red light (FR) application. (D) Immunoblot analyses using the antisera for the PSI core subunit PsaA and the PSII subunit PsbH. Protein loading correspond to 4, 2 and $1\mu\text{g}$ of chlorophyll (100, 50 and 25 respectively). CBB, Coomassie blue

3.1.2 HCF145 is localized to the chloroplast

Although many public available prediction programs proposed a chloroplast localization of HCF145, in the Arabidopsis Information Resource (TAIR) and the Universal Protein Resource (UniProt) it is also predicted to be localized in mitochondria. This is because peptides of HCF145 were found in a proteome analysis in the mitochondria (Heazlewood et al., 2004). Expression of the HCF145-GFP fusion in the *hcf145-2* lines showed a spotted GFP fluorescence exclusively in chloroplasts of stomata cells, confirming the subcellular localization within this organelle (Figure 7A).

3.1.3 HCF145 consists of two duplicated and conserved domains

HCF145 has a modular organization and consists of an N-terminal transit peptide for chloroplast import (TP) followed by two highly conserved motifs (145motif-1 and 145motif-2/Figure 7B/Appendix), which belong to the SRPBCC (START/RHO alpha C/PITP/Bet v1/CoxG/CalC) ligand-binding domain superfamily (Radauer et al., 2008). Furthermore two additional unknown repeated motifs (TMR1 and TMR2) with the consensus sequence MP4xL3xGRxDLxxAI2-3xHGG3xVAxL5-27xGYW were identified at the C-terminus (Figure 7B/Appendix). In *Arabidopsis* 37 proteins, most of them with unknown function, belong to the SRPBCC superfamily. Notably, this annotation is rather based on proposed structural than on sequence similarities. Among these structurally related SRPBCC superfamily proteins found in *Arabidopsis* only one protein 145motif-like (145motif-L) shows some sequence similarities to HCF145 (Figure 7B). 145motif-L also contains an N-terminal extension but otherwise consists of only one SRPBCC domain with about 60% similarity to both 145-motifs. A homologous protein of 145motif-L could also be found in some cyanobacteria (Figure 7B).

The two additional repeated motifs at the C-terminus of HCF145 consist of 68 and 69 amino acid residues and are separated by only one amino acid residue (Figure 7B). Remarkably, similar C-terminal motifs are found as multiple repeats in quite diverse proteins of some algae and one protein with three repeated TMR motifs in the cyanobacteria *Microcoleus sp.* PCC 7113. Homologues of HCF145 found in some members of the green algae have a modular organization like HCF145 with two truncated forms of the SRPBCC domains and two TMR motifs (Figure 7B). But except these, none of the TMR proteins found in algae and cyanobacteria contain sequences with similarities to the SRPBCC domain.

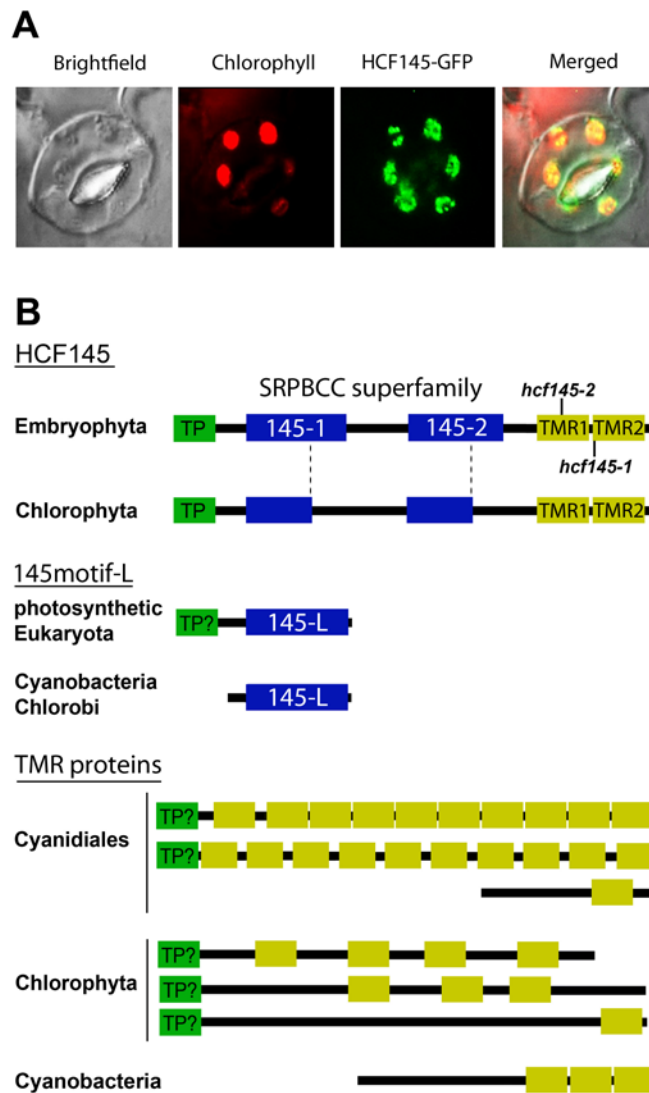


Figure 7. Subcellular localization and structure of HCF145. (A) Fluorescence microscope pictures of the HCF145-GFP fusion in the chloroplasts of *hcf145-2com_{gfp}* guard cells **(B)** In *Embryophyta* HCF145 proteins have a N-terminal chloroplast transit peptide (TP), two duplicated ligand-binding domain superfamily motifs (SRPBCC) called 145motif-1 and 145motif-2 (145-1 and 145-2), and two duplicated transcript binding motif repeat (TMR) domains. The mutations found in the *hcf145-1* and *hcf145-2* lines are localized in the TMR motifs. HCF145 proteins of *Chlorophyta* have truncated versions of the 145motifs. One related plant protein 145motif-like (145motif-L) has a predicted transit peptide and a homologous SRPBCC motif (145-L). A homologue of 145motif-L is present in cyanobacteria. TMR proteins with TMR motifs of diverse compositions are found in cyanidiales, chlorophyta and cyanobacteria.

3.1.4 The function of HCF145 is conserved among *Embryophyta*

To prove conservation of function *HCF145* knockouts were investigated in an early member of land plants, the moos *Physcomitrella patens* (Figure 8 and Figure 9, collaboration with Prof. W. Frank, LMU, Biocenter). The *pphcf145* mutants were less green and grew slower than the wild type, and showed a *hcf* phenotype (Figure 8A/B). In strong contrast to *Arabidopsis hcf145* and other PSI mutants, the maximum quantum yield of PSII was unchanged in *Physcomitrella hcf145* knockouts (0.70 ± 0.00 and 0.69 ± 0.01 , respectively) as compared to the WT (0.69 ± 0.02) demonstrating a functional PSII activity. Upon application of actinic light the fluorescence could hardly be quenched in the mutants, indicating disturbances in the photosynthetic electron transport rate (Figure 8C).

PSI activity was estimated by measuring light-induced P700 absorbance changes. The detected signal in the WT was comparable to that obtained in *Arabidopsis* (Lezhneva and Meurer, 2004). Under growth light conditions PSI was about 18% oxidized and short saturating light pulses of 600 ms were sufficient to induce a complete reduction of PSI in far red background light. In the mutants the signal was below the limit of detection, even when using a higher sensitivity for measurements, demonstrating a severe loss of PSI activity (Figure 8C). A specific PSI deficiency could also be confirmed by immunological analysis of three independent *pphcf145* mutants. All mutants accumulated only about 25% of PsaA, while levels of the PSII core subunit D2 (PsbD) were unchanged, as compared to the WT (Figure 9A).

The organization of the plastid *ycf3-psaA-psaB-rps14* gene cluster, the localization of the two *ycf3* introns, and the *psaA* 5' UTR are conserved in land plants including mosses (Figure 9B/ Appendix). Hybridization with specific probes of the *ycf3* and *psaA* genes yielded two lower and two higher abundant transcripts in RNA gel blot analysis of the WT, respectively (Figure 9C). According to their sizes, the higher abundant transcripts are most likely produced by the PEP.

A marked difference to higher plants is the presence of two instead of one abundant transcript which is generated by the PEP (Lezhneva and Meurer, 2004; Cho et al., 2009). Therefore, it is likely that endonucleolytic processing in the *psaB-rps14* intergenic region results in the accumulation of a second abundant transcript generated by the PEP in *Physcomitrella patens*. This was tested by using a specific probe of the *rps14* gene, which resulted in only one tetracistronic and one abundant tricistronic transcript (Figure 9C).

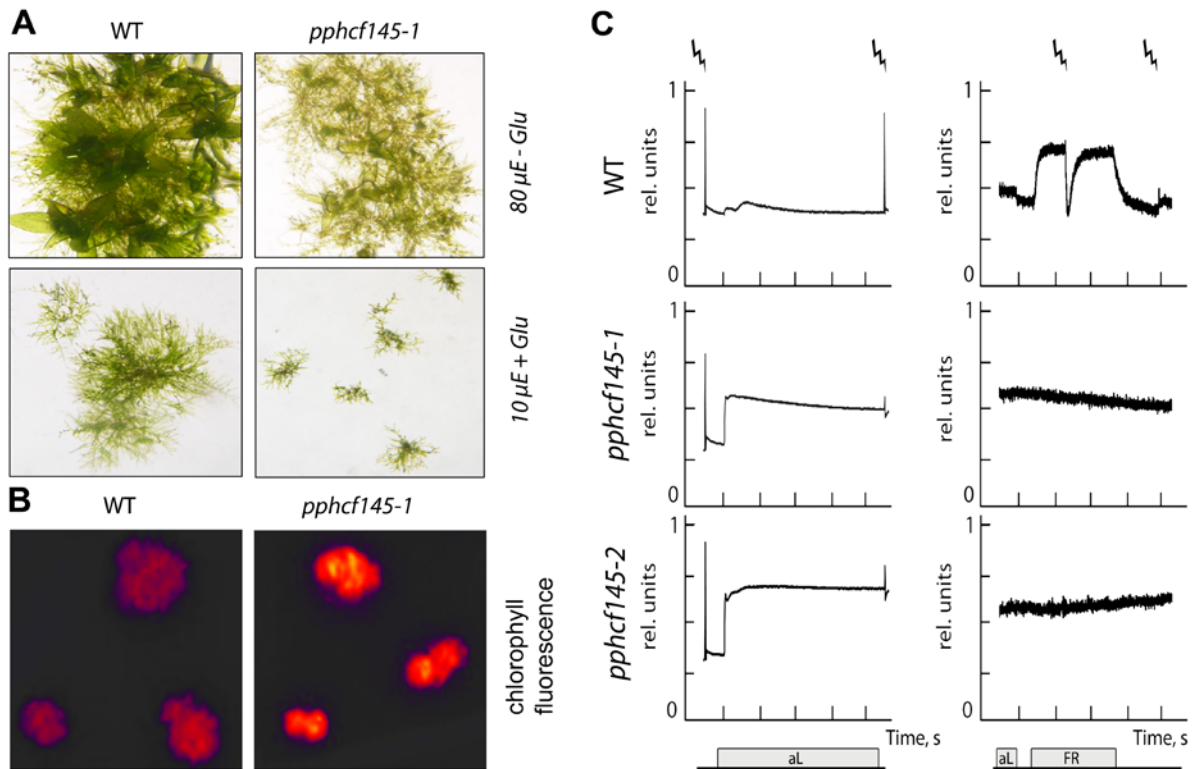


Figure 8. Growth and spectroscopic phenotype of *pphcf145*. (A) Wild type (WT) and *pphcf145-1* grown with and without glucose (Glu) at 80 and 10 $\mu\text{mol photons m}^{-2}\text{s}^{-1}$. (B) Chlorophyll fluorescence of WT and the *pphcf145-1*. (C) Chlorophyll *a* fluorescence and P700 redox kinetics in WT, *pphcf145-1* and *pphcf145-2*. Strokes indicate saturating light pulses and the bars indicate the duration of actinic light (AL) or far red light (FR) application. The *pphcf145* mutants were generated and photographed by Dr. Muhammad Asif Arif.

Accordingly, processing of both precursor transcripts produces tricistronic *ycf3-psaA-psaB* and dicistronic *psaA-psaB* transcripts. The three mutants were unable to accumulate the two abundant *psaA-psaB-rps14* and *psaA-psaB* transcripts both generated by the PEP, while the larger low abundant transcripts of the NEP appeared at normal levels (Figure 9C). As observed in the *Arabidopsis hcf145* mutant (Lezhneva and Meurer, 2004), precursors generated by the NEP are stable and only transcripts starting with the *psaA* 5' UTR are unstable in the corresponding *Physcomitrella* mutants.

The specificity of this phenotype was tested using a *psbA* specific probe. As expected, *psbA* transcripts were unchanged in the *pphcf145* mutants (Figure 9C). This illustrates that the function of HCF145 is conserved among *Embryophyta* and that the target of HCF145 is very likely located in the *psaA* 5' UTR. Inspection of this region in *Embryophyta* demonstrates a high conservation directly downstream of the *psaA* transcription start (Appendix).

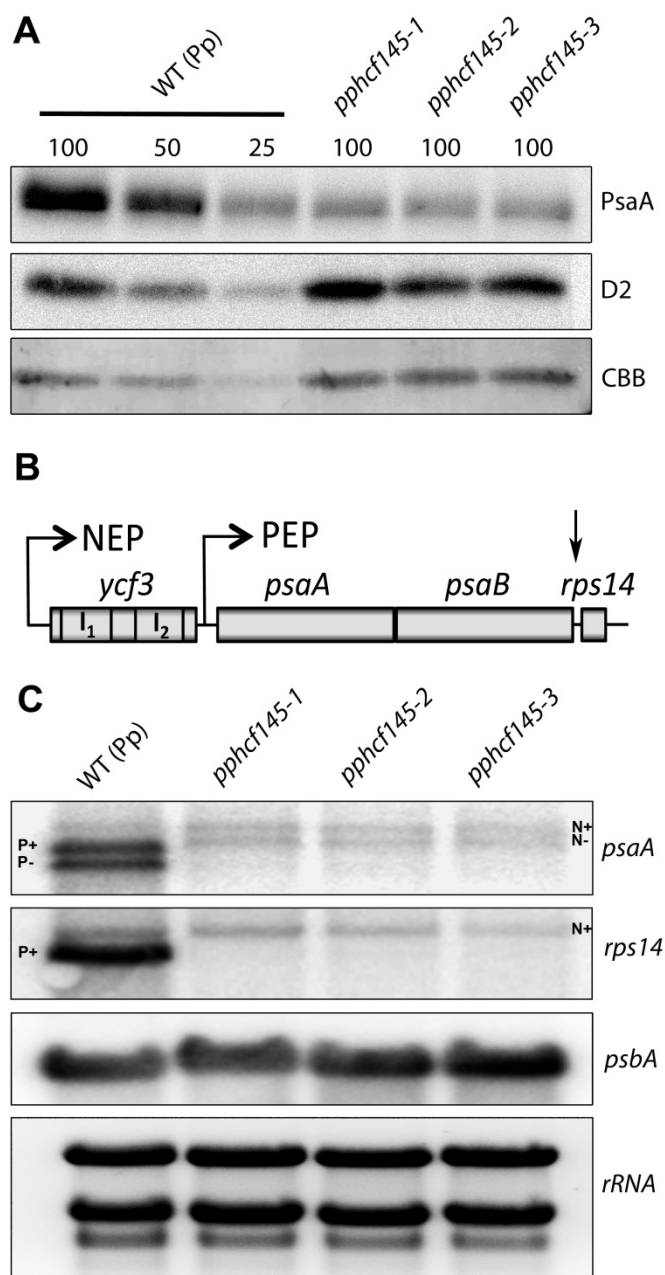


Figure 9. Immunological and RNA gel blot analyses of *pphcf145*. (A) Immunoblot analysis with specific antibodies for PsaA and D2. CBB, Coomassie blue. (B) Gene model of the NEP generated tetracistronic *ycf3-psaA-psaB-rps14* transcripts and the PEP generated tricistronic *psaA-psaB-rps14* transcripts. The *ycf3* introns (I₁ and I₂) and the *rps14* processing site (arrow) are indicated. (C) RNA gel blot analysis using 10 µg total RNA of wild type and *pphcf145* lines and hybridization probes specific for *psaA*, *rps14* and *psbA*. rRNA, ribosomal RNA. Unprocessed NEP (N⁺) and PEP (P⁺) generated transcripts and processed NEP (N⁻) and PEP (P⁻) transcript are indicated next to the corresponding band. RNA gel blot analyses were performed by Dr. Muhammad Asif Arif.

3.1.5 Light-induced accumulation of HCF145

Antibodies were raised against an epitope of the C-terminus of HCF145 partially covering the second TMR domain. The limit of detection of HCF145 lay in the range of about 20 fmol as revealed by titration analysis indicating an exceedingly satisfactory sensitivity of the antibodies. Since the endogenous HCF145 could not be detected in *Arabidopsis* wild-type plants using various growth conditions and isolation methods, the light induced expression of HCF145 was investigated.

For that purpose, total protein extracts of seedlings germinated for 8 days in the light, for 8 days in darkness and after exposure to 4, 8, 24 and 96 hours of light, were analyzed immunologically. Most chloroplast proteins usually accumulate after several hours of light induction of dark-grown seedlings (Meurer et al., 1998; Torabi et al. 2014). In contrast, HCF145 accumulated in dark grown seedlings and the signal disappeared during light induction, whereas the nucleus encoded subunit of the water splitting complex PsbP and the PSII core antenna CP47 could not be detected in the dark samples but accumulated upon light induction (Figure 10A).

To address the question whether HCF145 is a soluble or a membrane associated protein, the protein extracts of 8 hour illuminated seedlings were fractionated into soluble and membrane proteins. The immunological analysis revealed that HCF145, migrating at about 75 kDa, is mainly found in the soluble protein fraction (Appendix). The specificity of the antibody was tested by the comparison with complemented lines expressing various tagged versions of HCF145. All three recombinant forms could be identified by their size, whereas the WT version was lacking in all complemented lines (Appendix).

3.1.6 Light- and stress-dependent expression of *HCF145*

To investigate the regulation of *hcf145* and *psaA* transcript levels under different environmental conditions, 3-week-old *Arabidopsis* plants were subjected to various light and stress conditions (Figure 10B). After 24 h of dark, far red light (FR) and red light (RL) the *hcf145* transcript levels decreased notably, while the *psaA* transcript levels significantly increased in the dark and were unchanged in FR and RL. Cold incubation at 4°C for 24 h did not show any effect whereas 40°C heat stress for 1 h induced a significant down regulation of *hcf145*, while the *psaA* transcript levels remained stable.

Upon treatment with the PSII inhibitor DCMU (Hsu et al., 1986), *hcf145* and *psaA* transcript levels increased substantially. The stressor paraquat, which induces oxidative stress by H₂O₂ production (Laloi et al., 2007), led to a significant decrease of both transcript levels (Figure 10B).

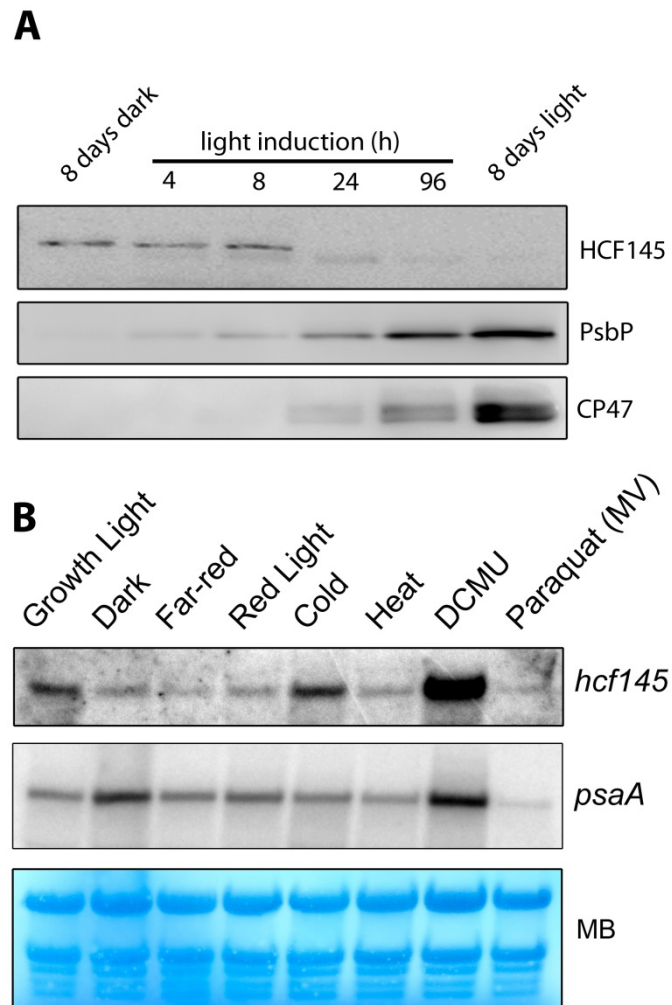


Figure 10. Changes in the expression level of *HCF145* under various conditions. (A) Immunological analysis of HCF145, PsbP and CP47 accumulation during deetiolation. 8-day-old etiolated *Arabidopsis* seedlings were illuminated with 50 $\mu\text{mol photons m}^{-2}\text{s}^{-1}$ for 4, 8, 24 and 96 hours. Seedlings grown for 8 days in the light were used for comparison. (B) *HCF145* and *PsaA* transcript accumulation in 3-week-old *Arabidopsis* plants grown at 50 $\mu\text{mol photons m}^{-2}\text{s}^{-1}$ and after 24 h incubation in the dark, in far red light (720 nm, 1 $\mu\text{mol photons m}^{-2}\text{s}^{-1}$), in red light (660 nm, 20 $\mu\text{mol photons m}^{-2}\text{s}^{-1}$), at 4°C (cold), in 50 μM DCMU and Paraquat, and after 1 h incubation at 40°C (heat). MB, Methylene blue. The RNA gel blot analyses were performed by Dr. Nikolay Manavski.

3.1.7 HCF145 is a rate limiting factor of PSI accumulation

RNAi lines in tobacco were generated to compare different suppression levels of HCF145. Most of the lines had a paler appearance than the wild type and displayed a *hcf* phenotype. For further analyses, four different lines were selected according to their growth rate and paleness.

Fluorescence analysis clearly showed that all these RNAi lines (*nthcf145i1-nthcf145i4*), were unable to fully quench singlet-excited states of chlorophyll upon application of actinic light. The P700 redox kinetic measurements of PSI approved that all lines exhibited a significantly reduced PSI activity (Figure 11 A/B). In *nthcf145i-1* and *nthcf145i-2* P700 activity was reduced to about 40% and 8% as compared to the WT, respectively. In *nthcf145i-3* and *nthcf145i-4* the signal was at the limit of detection even when using a higher sensitivity for measurements (Figure 11B).

To test if the reduced PSI activity measured in the RNAi lines is linked to a loss in PSI accumulation, immunological analyses using antisera specific for PsaA were performed. In the lines *nthcf145i-1* and *nthcf145i-2* PsaA accumulated to about 50% and less than 25% as compared to the WT levels, respectively. In *nthcf145i-3* and *nthcf145i-4* the PsaA signal was barely detectable (Figure 11D). Thus the reduced PSI activity corresponds to reduced PSI levels in the RNAi lines.

RNA gel blot analyses were then performed to investigate *psaA/B* transcript levels in transgenic knock down lines. In all four lines amounts of *psbB* RNAs were not changed but those of *psaA* transcripts were considerably reduced with the lowest reductions in *nthcf145i-1* (~75%) and the strongest in *nthcf145i-4* (<25%) (Figure 11C). This demonstrates that even slight reduction of *psaA* RNA levels induces a considerable loss of PsaA and PsaB proteins and that the function of HCF145 in regulating *psaA-psaB-rps14* transcript levels is likely to be rate limiting for the amounts of PSI.

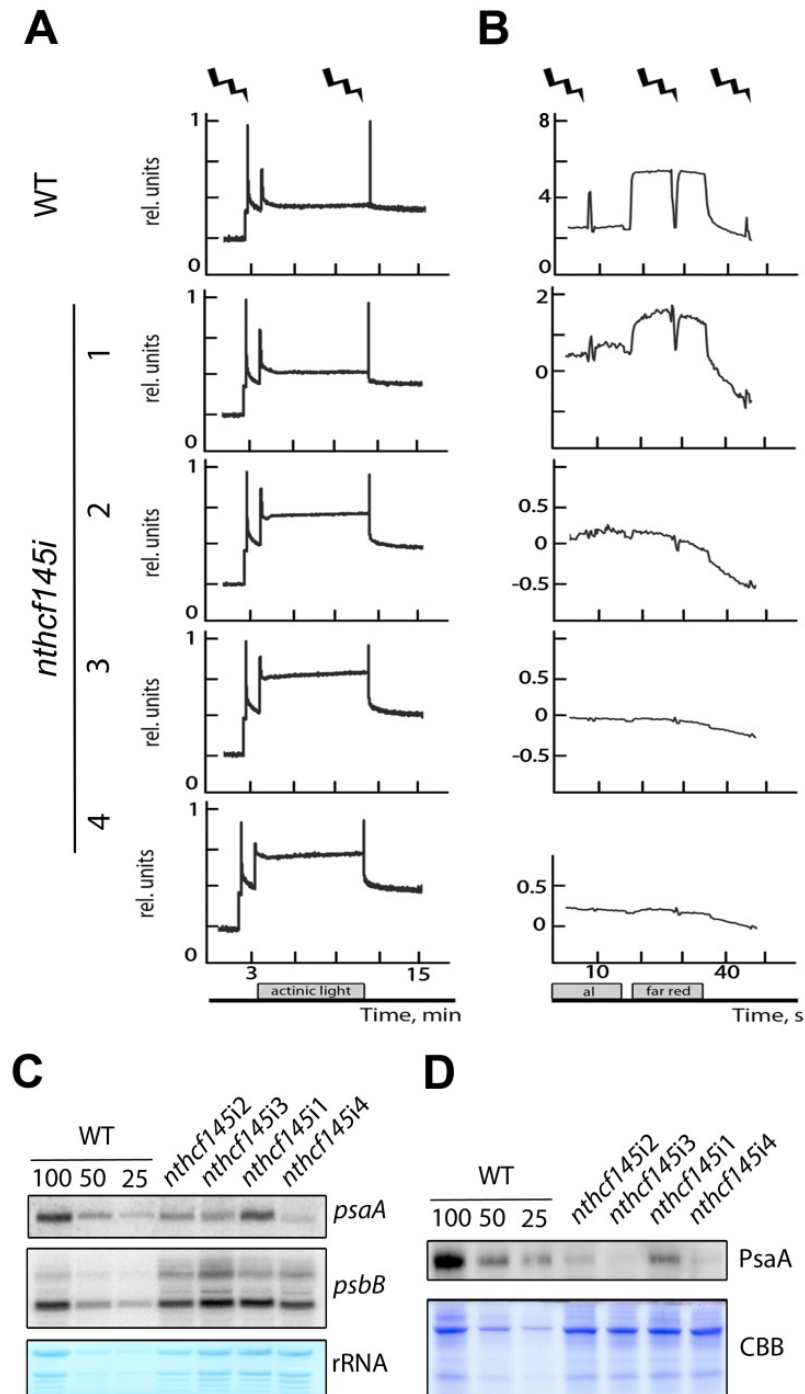


Figure 11. Various degrees of PSI deficiencies among *HCF145* RNAi lines in tobacco. (A) Chlorophyll *a* fluorescence kinetic and (B) P700 redox kinetics in 6-week-old wild type and *nthcf145i* lines grown at $10 \mu\text{mol photons m}^{-2}\text{s}^{-1}$ on sucrose supplemented medium. Strokes indicate saturating light pulses and the bars indicate the duration of actinic light (AL) or far red light (FR) application. (C) RNA gel blot analysis of wild type and *nthcf145i* lines using strand specific 80mer oligonucleotides for *psaA* and *psbB*. Total RNA loading correspond to 8, 4, and 2 μg (100, 50, 25 respectively). Ribosomal RNA (rRNA) was stained with Methylene blue. (D) Immunological analysis of thylakoid membrane proteins isolated from wild type and *nthcf145i* lines using specific antisera for PsaA. Protein loading correspond to 4, 2 and 1 μg of chlorophyll. CBB, Coomassie blue

3.1.8 HCF145 is associated to the 5' UTR of *psaA* transcripts

To prove whether HCF145 is associated with the 5' UTR of *psaA* transcripts *in vivo*, RNA co-immunoprecipitation studies were performed. For this purpose, HCF145-GFP fusions were immunoprecipitated from chloroplast extracts of *hcf145com_{gfp}* and WT control plants using GFP-Trap®. This successfully resulted in an enrichment of the HCF-GFP fusion in the pellet fraction when using *hcf145com_{gfp}* line (Figure 12A). No signal was obtained in the WT sample. Subsequently, co-precipitated RNA was isolated from the supernatants and the pellets and spotted on a nylon membrane using a slot blot apparatus. Hybridization of the slots with radiolabelled probes revealed that HCF145-GFP fusions preferentially precipitated the *psaA* 5' UTR and much less efficiently the *petB* 3' UTR indicating that HCF145 is specifically associated to the *psaA* 5' UTR (Figure 12A).

To narrow down the target site of HCF145 within the *psaA* 5' UTR, the precipitated RNAs were hybridized with probes subdividing the entire UTR into three non-overlapping parts (Figure 12B). It appeared that HCF145-GFP precipitated the very 5' part of the *psaA* 5' UTR with much higher specificity than the middle and the 3' part. Therefore it could be assumed that HCF145-GFP is specifically associated with the 5' region of the *psaA* 5' UTR.

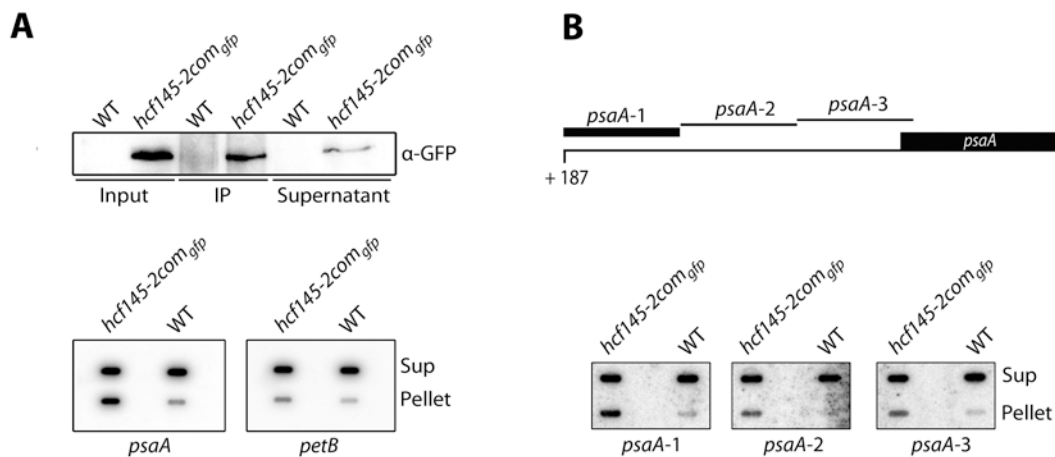


Figure 12. HCF145-GFP fusion is associated with the 5' UTR of *psaA*. (A) Immunoprecipitation (IP) analysis with solubilized chloroplasts of wild type (WT) and *hcf145com_{gfp}* lines. Immunological analysis of IP protein fractions separated by SDS-PAGE with specific antisera against GFP (upper part). Slot blot analysis of RNA isolated from the IP using probes specific for *psaA* and *petB* (lower part). (B) Slot blot analysis using three hybridization probes (*psaA*-1, -2, -3) covering the *psaA* 5' UTR. The analyses were performed by Dr. Nikolay Manavski.

3.2 PsbN is required for the assembly of the PSII RC

3.2.1 Localization and topology of PsbN

For biochemical studies antibodies against the short hydrophilic C-terminal part of PsbN were raised. Washing experiments with different chaotropic and alkaline salt solutions proved the predicted hydrophobic membrane spanning helix in the N-terminal part of PsbN. The periphery thylakoid membrane protein PsbO could be washed off to different extents, while PsbN stayed completely in the thylakoid fraction irrespective of the salt solution used for washing (Figure 13A).

The localization of PsbN within the thylakoid system, was investigated by our collaboration partners in the lab of Prof. Wolfgang P. Schröder. Therefore, thylakoids separated into grana and stroma lamellae were analyzed immunologically. Interestingly, PsbN was highly enriched in the stroma lamellae, showing that this protein is not co-localized with PSII in the grana regions of the thylakoid membranes (Torabi et al., 2014).

To reveal the orientation of PsbN in the membrane, thylakoids were treated with the protease thermolysin followed by immunodecoration (Figure 13B). The luminal PsbO protein was protected inside the thylakoid vesicles whereas PsbN was digested within 60 sec demonstrating that its C-terminus is exposed to the stroma. To strengthen this finding, inside-out vesicles were generated by sonication of the thylakoids prior the protease treatment. This resulted in a partial digestion of PsbO and a partial resistance of PsbN, showing that the C-terminus of PsbN was now to some extent protected inside the vesicles (Figure 13B).

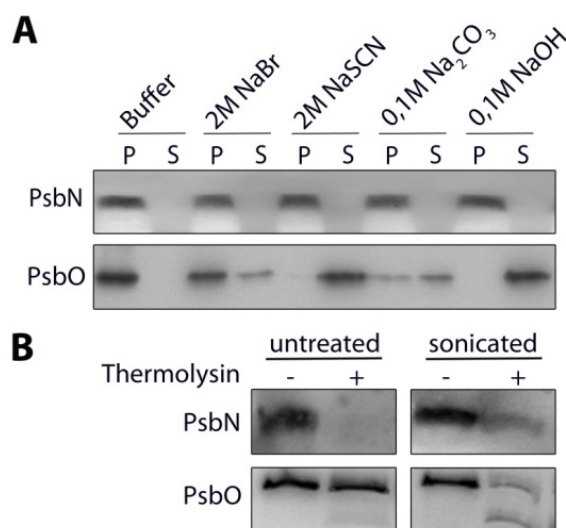


Figure 13. Topology and localization of PsbN in the thylakoid membrane. (A) Thylakoids were fractionated into pellet (P) and supernatant (S) after washing with different salt-containing buffers, and analyzed immunologically with specific antisera against PsbN and the luminal extrinsic PSII protein PsbO. (B) Thylakoids and inside-out vesicles obtained after sonication of thylakoids were incubated with (+) and without (-) thermolysin for 1 min and analyzed using specific antisera for PsbN and PsbO.

3.2.2 Light-induced expression of PsbN

The expression of the PsbN protein was followed in greening experiments with etiolated *Arabidopsis* seedlings and compared with the expression of the light-responsive thylakoid proteins PsaA, HCF136, D1, and PsbH (Figure 14). The plastid-encoded subunits PsaA of PSI, D1 and PsbH of PSII were first detectable after 24 hours of light exposure. The nucleus encoded factor HCF136 required for early PSII assembly (Meurer et al., 1998b), was already detectable in dark grown seedlings and accumulated continuously after light induction. In contrast significant amounts of PsbN were already present in the etiolated seedling and increased rapidly within 4 hours reaching the maximum after 8 hours illumination. Levels of PsbN decreased after 24 hours illumination and remained constant thereafter (Figure 14).

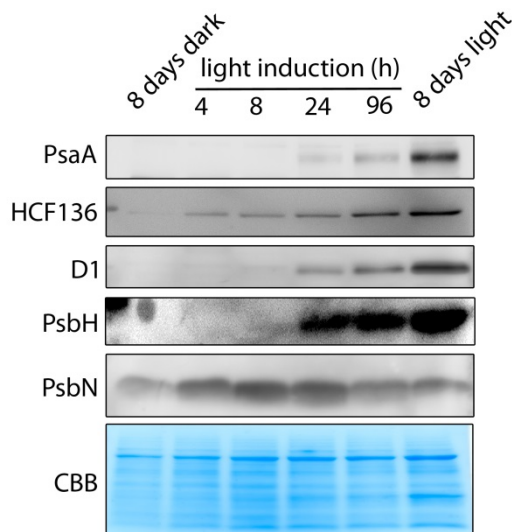


Figure 14. Light dependent expression of PsbN. Eight-day-old etiolated seedlings grown in the dark were illuminated for 4, 8, 24, and 96 h respectively and compared with eight-day-old seedlings grown in the light. Total proteins extracts were analyzed with specific antisera for PsbN, PsaA, HCF136, D1 and PsbH. For loading control the transferred proteins were stained with Coomassie blue (CBB).

3.2.3 Targeted inactivation of the *PsbN* gene

To elucidate the function of PsbN, transplastomic *PsbN* knock-out tobacco plants were generated by Dr. Pavan Umate. Therefore a spectinomycin resistance cassette (*aadA* cassette) was introduced into the 5' region of the *PsbN* gene (Figure 15A). To consider possible effects of the transcription direction on the other genes of the *psbB* operon, the cassette was introduced in forward and reverse direction into *PsbN*.

PCR analysis using the oligonucleotides *psbTc*-for, *psbH*-rev, and *aadA*-for confirmed the homoplastomic state and the orientation of the *aadA* cassette insertion in the transplastomic $\Delta psbN$ -*F* and $\Delta psbN$ -*R* lines (Figure 15B).

The PCR amplified a 569 bp product in the wild type and an *aadA*-containing fragment of 1.504 bp in the $\Delta psbN$ -*F* and $\Delta psbN$ -*R* lines. The *aadA* specific oligonucleotide *aadA*-for amplified only fragments for the $\Delta psbN$ -*F* and $\Delta psbN$ -*R* templates with sizes of 846 bp and 778 bp, respectively. This confirmed the insertion and orientation of the selection cassette in both mutant lines (Figure 15B).

3.2.4 Transcript profile of the *psbB* operon in $\Delta psbN$ -*F* and $\Delta psbN$ -*R*

The transcript accumulation of genes located upstream and downstream of *psbN* within the *psbB* operon was estimated by RNA gel blot analysis using strand-specific probes (Figure 15C).

The prominent 2.0 kb dicistronic *psbB*-*psbTc* transcript is not processed further to monocistronic transcripts in tobacco (Umate et al., 2008; Krech et al., 2013). Expression of this mRNA was not affected in both mutant lines (Figure 15C). As desired, the monocistronic *psbN* transcript could not be detected in both mutant lines, while it was present in the wild type. A strong signal of about 1.5 kb, corresponding to *aadA* transcripts containing truncated *psbN* sequences, was obtained in $\Delta psbN$ -*F* when using *psbN* specific oligonucleotides (Figure 15C).

The *psbH* and *petB* transcript levels were reduced in $\Delta psbN$ -*F* and several fold increased in $\Delta psbN$ -*R* (Figure 15C). This up-regulation of the downstream located gene expression in $\Delta psbN$ -*R*, is likely caused by the introduction of the constitutively strong expressed *aadA* cassette into the *psbB* gene cluster. Probably, the introduction of an additional promoter on the opposite strand to the *psbB* gene cluster in $\Delta psbN$ -*F* might partially inhibit the transcription of the downstream located genes of the insertion site.

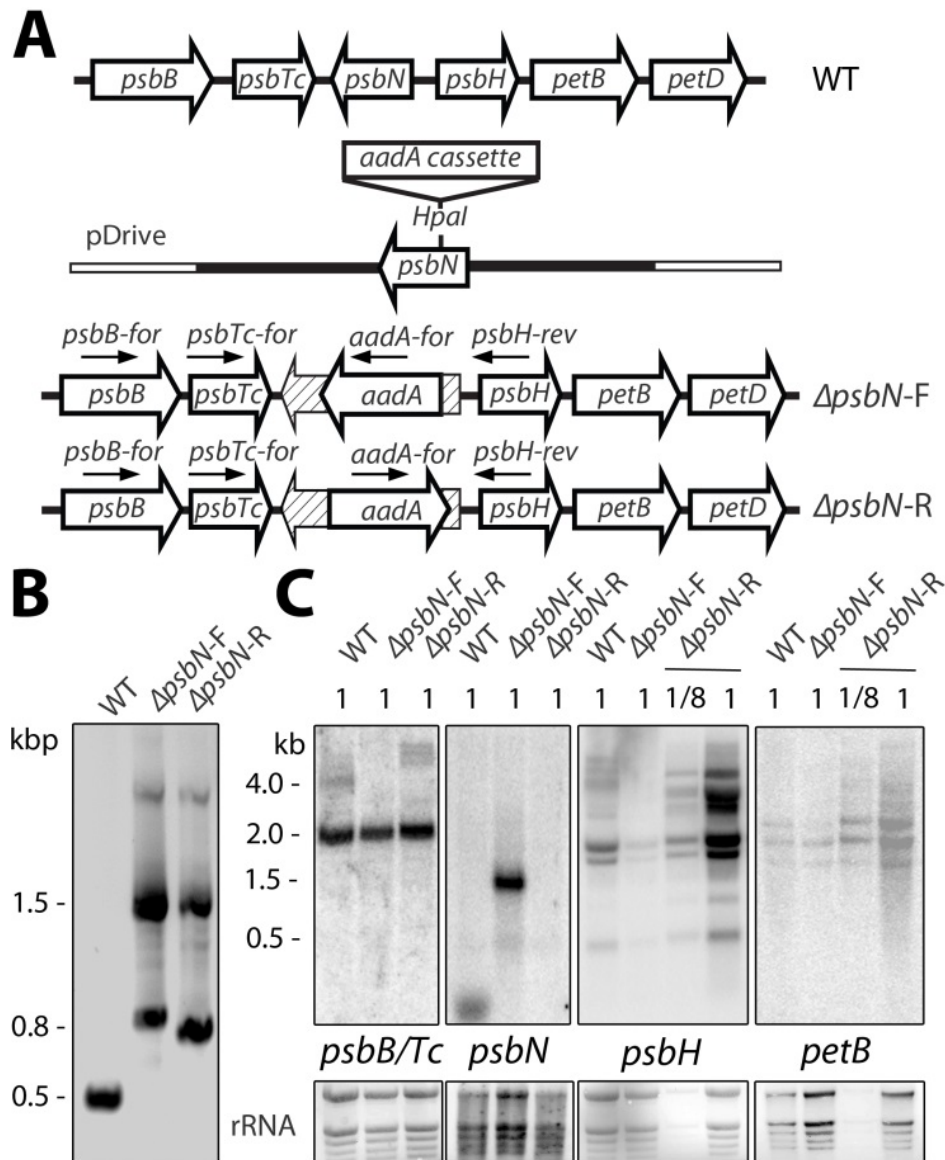


Figure 15. Disruption of the plastid *PsbN* gene. (A) Strategy to insert a spectinomycin resistance marker (*aadA*) cassette into an artificial *HpaI* site into the 5' region of *psbN* within the *psbB* gene cluster. Plasmids (pDrive) carrying the *aadA* cassette in forward (F) or reverse (R) orientation to the *PsbN* coding frame were used for transformation of the wild-type (WT) tobacco plastome resulting in two knockout lines $\Delta psbN-F$ and $\Delta psbN-R$, respectively. Arrows indicate the position of primers used for cloning and PCR analysis. (B) Oligonucleotides *psbTc-for*, *psbH-rev*, and *aadA-for* were used to confirm the homoplasmic state of $\Delta psbN-F$ and $\Delta psbN-R$. (C) RNA gel blot analysis using strand specific oligonucleotides for *psbB*, *psbN*, *psbH* and *petB*. Loading correspond to eight and one microgram of total leaf RNA (1 and 1/8). Ribosomal RNA (rRNA) was stained with methylene blue.

3.2.5 Establishment of a semi-sterile culture technique

Two independently generated transplastomic lines, $\Delta psbN-F$ and $\Delta psbN-R$, were selected and back-crossed three times with the WT for a detailed investigation. Since the *psbN* knock-out lines were extremely light sensitive and their growth was very retarded on soil, a new technique was invented which accelerated growth and flower development under semi-sterile conditions.

Therefore the lower part of the stem and the roots were kept under sterile conditions, in a glass jar with sucrose supplemented medium, while the upper part of the plant could grow outside of the culture vessel in a non-sterile environment (Figure 16). This allowed a fast development of the stem, leaves and fertile flowers of the mutants, thus facilitating the backcrossing experiments with WT pollen in a short period of time.

After transfer to the semi-sterile conditions most $\Delta psbN$ plants began to flower already within 4 weeks compared to several month if at all on soil. The collected seeds germinated efficiently on both medium and soil and all the resultant progeny showed the same phenotype as the parental lines confirming that no background mutation contributed to the observed defects.



Figure 16. Semi-sterile culture of $\Delta psbN$ mutants. Flowering $\Delta psbN-R$ mutant 8 weeks after transfer to semi-sterile culture (left) and $\Delta psbN-F$ mutant one week after transfer to semi-sterile culture (right). For further details, see text. Bar = 5 cm

3.2.6 Growth phenotype of the $\Delta psbN$ plants

PsbN mutant seedlings were solely able to develop to maturity on soil when grown under low light conditions that preferentially favor PSI excitation (state I). However, it took 3 month until they reached a size of about one cm in diameter. Also the wild-type growth, which was several fold faster than the growth of the mutants, was extremely retarded under the state I favored conditions, demonstrating the low excitation energy of this light (Figure 17). This primarily indicates that PSII is prone to photoinhibition even at low light intensities in plants lacking PsbN.

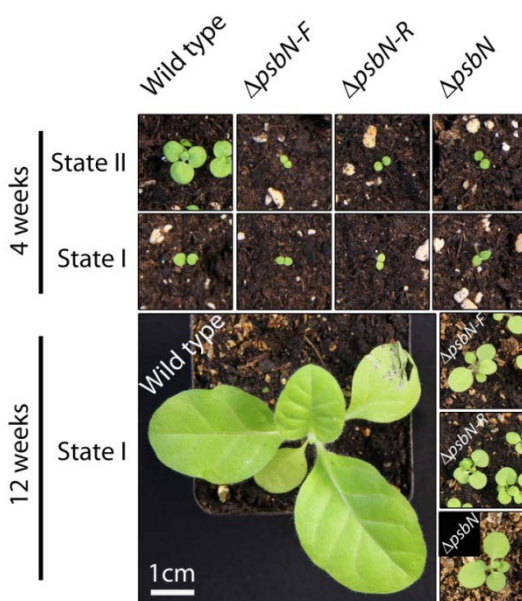


Figure 17. *PsbN* knock-out seedlings could only develop on soil under preferential state I light. Tobacco wild type (WT), $\Delta psbN-F$, $\Delta psbN-R$ and $\Delta psbN$ (Krech et al., 2013) were germinated on soil and grown under low light (State II) and under a dark red filter (State I) with $15 \mu\text{mol photons m}^{-2} \text{s}^{-1}$, respectively.

To demonstrate the light sensitivity of the $\Delta psbN$ mutants, *in vitro* cultured seedlings of $\Delta psbN-F$ and $\Delta psbN-R$ were subjected to different light conditions and compared to the wild type and to the $\Delta psbN$ and *aadA*-control lines recently described (Krech et al., 2013) with respect to their growth phenotype (Figure 18). The $\Delta psbN$ mutants reached maturity only under low light and rapidly bleached when light intensities were increased above $40 \mu\text{mol photons m}^{-2} \text{s}^{-1}$. This agrees with the recently reported findings that the growth of young $\Delta psbN$ seedlings was retarded and seedlings were more sensitive to light than mature plants (Krech et al., 2013).

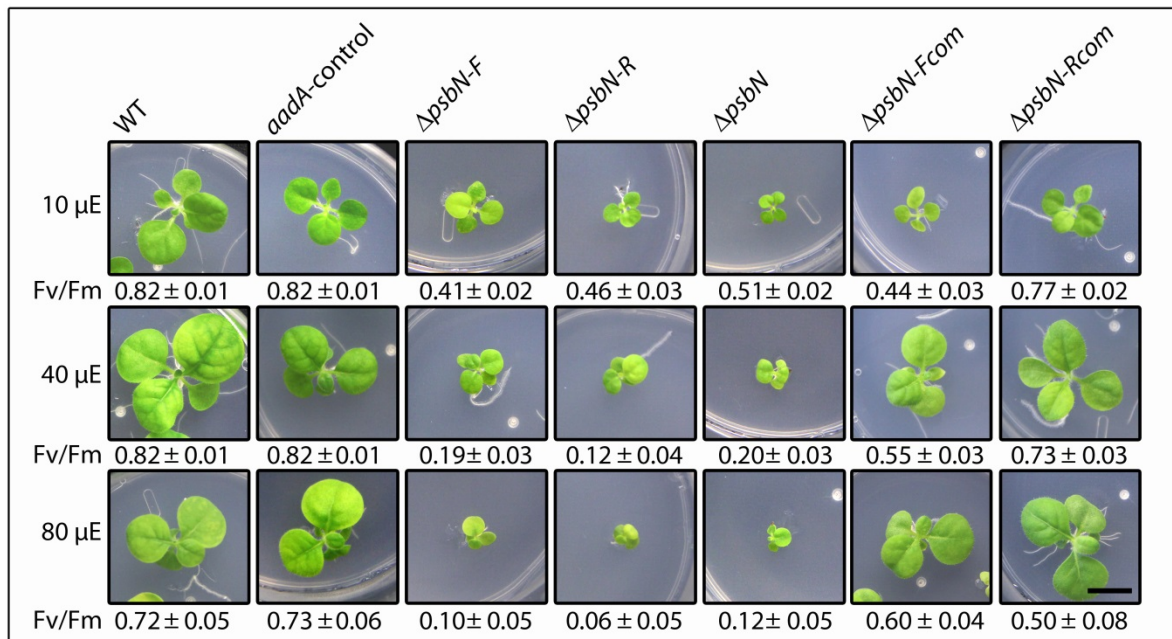


Figure 18. *PsbN* mutant seedlings are extremely light sensitive. *In vitro* culture of tobacco seedlings under continuous light on sucrose supplemented medium. Wild type (WT), *aadA*-control and $\Delta psbN$ plants as described by Krech et al., 2013, $\Delta psbN-F$, $\Delta psbN-R$, $\Delta psbN-Fcom$ and $\Delta psbN-Rcom$ were germinated for 10 days under 10 $\mu mol photons m^{-2} s^{-1}$, piqued and subjected to 10, 40, and 80 $\mu mol photons m^{-2} s^{-1}$ for additional 20 days. The respective maximum quantum yield of PSII (Fv/Fm) and the standard deviation (n=4) are indicated below. Bar=1 cm.

3.2.7 PSII activity is reduced in the $\Delta psbN$ mutants

The maximum quantum yield of PSII (Fv/Fm) was reduced to about 60% in $\Delta psbN-R$ and $\Delta psbN$ and to about 50% in $\Delta psbN-F$ as compared to the WT and the *aadA*-control line when grown at 10 $\mu mol photons m^{-2} s^{-1}$ (Figure 18/Table 1/Appendix). The Fv/Fm of the WT and of the *aadA*-control line remained between 0.82 and 0.72 when 10-day-old seedlings were subjected to 40 and 80 $\mu mol photons m^{-2} s^{-1}$ light intensity during growth for additional 20 days. In contrast, the Fv/Fm of the mutants significantly decreased already at 40 $\mu mol photons m^{-2} s^{-1}$ light intensity and reached almost zero at 80 $\mu mol photons m^{-2} s^{-1}$ growth light (Figure 18/Table 1). This emphasizes that PSII is prone to photoinhibition in the mutants.

In order to minimize secondary effects caused by extensive photodamage of the mutants, the grow light intensities were set to 10 $\mu mol photons m^{-2} s^{-1}$ for all further analyses. Under this condition the chlorophyll content was only slightly decreased in the mutants but the chlorophyll *a/b* ratio was significantly reduced in the mutants (Table 1). This reconfirms that photodamage is diminished and indicates reduced PSII levels in the mutants.

Table 1. Photosynthetic parameters of the wild type, $\Delta psbN$ mutants and complemented lines

	Wild type	$\Delta psbN-F$	$\Delta psbN-R$	$\Delta psbN-Rcom$
Parameter	(n=4) ^a	(n=4)	(n=4)	(n=4)
Chlorophyll a+b	1.32 ± 0.13	1.03 ± 0.19	1.27 ± 0.22	1.22 ± 0.23
Chlorophyll a/b	3.10 ± 0.06	2.41 ± 0.11	2.43 ± 0.12	3.10 ± 0.11
Fv/Fm ^b (10 μ E ^c)	0.81 ± 0.01	0.41 ± 0.02	0.46 ± 0.03	0.77 ± 0.02
Fv/Fm (40 μ E) ^d	0.79 ± 0.02	0.19 ± 0.03	0.12 ± 0.04	0.73 ± 0.03
Φ_{PSII} ^e	0.76 ± 0.01	0.32 ± 0.03	0.35 ± 0.02	0.72 ± 0.02
NPQ ^f	0.03 ± 0.01	0.04 ± 0.01	0.04 ± 0.01	0.03 ± 0.01
Φ_{PSI} ^g	0.78 ± 0.02	0.73 ± 0.06	0.70 ± 0.03	0.73 ± 0.04
$\Phi_{PSI ND}$ ^h	0.02 ± 0.01	0.10 ± 0.04	0.17 ± 0.04	0.03 ± 0.01
^a n, number of plants measured. ^b Fv/Fm, maximum quantum yield of PSII. ^c μ E, μ mol photons $m^{-2}s^{-1}$. ^d After germination for 10 days at 10 μ mol photons $m^{-2}s^{-1}$ seedlings were subjected to 40 μ mol photons $m^{-2}s^{-1}$ for 18 days. ^e Φ_{PSII} , effective quantum yield of PSII. ^f NPQ, non-photochemical quenching. ^g Φ_{PSI} , quantum yield of PSI. ^h $\Phi_{PSI ND}$, quantum yield of non-photochemical energy dissipation due to donor side limitation.				

The minimal fluorescence (F_0) levels were two-fold-increased in $\Delta psbN-R$ and $\Delta psbN$ and threefold-increased in $\Delta psbN-F$ as compared to the wild type and the *aadA*-control line (Appendix). Furthermore the chlorophyll fluorescence level tended to drop below the F_0 level upon induction with actinic light in the mutant lines (Appendix). The strength of this effect appeared to be a function of light intensity and is indicative of a defective photosynthesis (Meurer et al., 1996; Peng et al. 2006; Armbruster et al. 2010). However, non-photochemical quenching (NPQ) appeared not to be altered in the mutants (Table 1/Appendix).

The PSII yield (Φ_{PSII}) was also severely reduced in the $\Delta psbN$ mutants as compared to the WT and the *aadA*-control lines suggesting that the electron flow towards PSI is diminished most likely due to a reduced activity of PSII (Table 1/Appendix). To reinforce this, the yield of PSI (Φ_{PSI}) and the donor side limitation of PSI ($\Phi_{PSI ND}$) were measured in the $\Delta psbN-F$ and $\Delta psbN-R$ mutants (Table 1). The Φ_{PSI} was only slightly reduced but $\Phi_{PSI ND}$ was several fold increased in the mutants as compared to the WT, demonstrating that electron flow towards PSI is affected.

3.2.8 Levels of PSII proteins were reduced in $\Delta psbN-F$ and $\Delta psbN-R$

To determine whether the impaired PSII activity found in the *psbN* mutants also reflects a reduction in the abundance of PSII subunits and to estimate the levels of representative members of other thylakoid membrane complexes, immunoblot analyses were performed (Figure 19). As expected, PsbN could not be detected in $\Delta psbN-F$ and $\Delta psbN-R$. Levels of PSII proteins D1, D2, CP43, CP47, PsbH, and PsbO were reduced to about 25% or below in both mutants (Figure 19A).

Notably, PsbH amounts were reduced irrespective of the difference in *psbH* mRNA levels in both mutants (Figure 19A). This shows that the down regulation of PsbH is independent of the orientation of the *aadA* cassette and that a secondary effect caused by the *aadA* insertion can be excluded. Therefore, it is likely that the observed deficiencies in proteins levels can be attributed solely to the loss of PsbN.

The content of PSI subunits PsaA, PsaC, and PsaF was always around or above 50 % in the mutants as compared to the WT (Figure 19). Levels of outer antenna proteins of both photosystems, LHCa1 and LHCB1, as well as of the AtpC subunit of the ATP synthase were not reduced in both mutants (Figure 19A).

According to the *petB* mRNA levels (Figure 3C), the amounts of Cyt *b*₆ were also reduced in $\Delta psbN-F$ and slightly increased in $\Delta psbN-R$ as compared to the WT (Figure 19B). Taken together, our results imply that disruption of *psbN* specifically affects the accumulation of chlorophyll *a*-containing PSII core proteins irrespective and independent of the orientation of the *aadA* cassette within the *psbB* gene cluster. This is also consistent with a decreased chlorophyll *a/b* ratio in the mutants (Table 1).

3.2.9 Translation of chloroplast encoded proteins in $\Delta psbN$ mutants

In vivo labeling experiments using [³⁵S]-methionine were performed, to uncover alterations in the chloroplast protein translation caused by the insertion of the *aadA* cassette into the *psbB* gene cluster in $\Delta psbN-F$ and $\Delta psbN-R$. The translation rates of the PSI proteins PsaA and PsaB, the α and β subunits of the ATP synthase, and the PSII proteins CP43, CP47, D1 and D2 were comparable to the rates observed in the wild type (Figure 19C).

Corresponding to the changed levels of transcripts, the translation of PsbH and subunit IV of the cytochrome *b*₆*f* complex (PetD) was decreased in $\Delta psbN-F$ and enhanced in $\Delta psbN-R$. In contrast, PsbH levels were reduced to the same extent in both mutants (Figure 19A), indicating that this is a PsbN specific defect, which is independent from the changes observed in the transcript levels and translation rates of the downstream located genes of *psbN*.

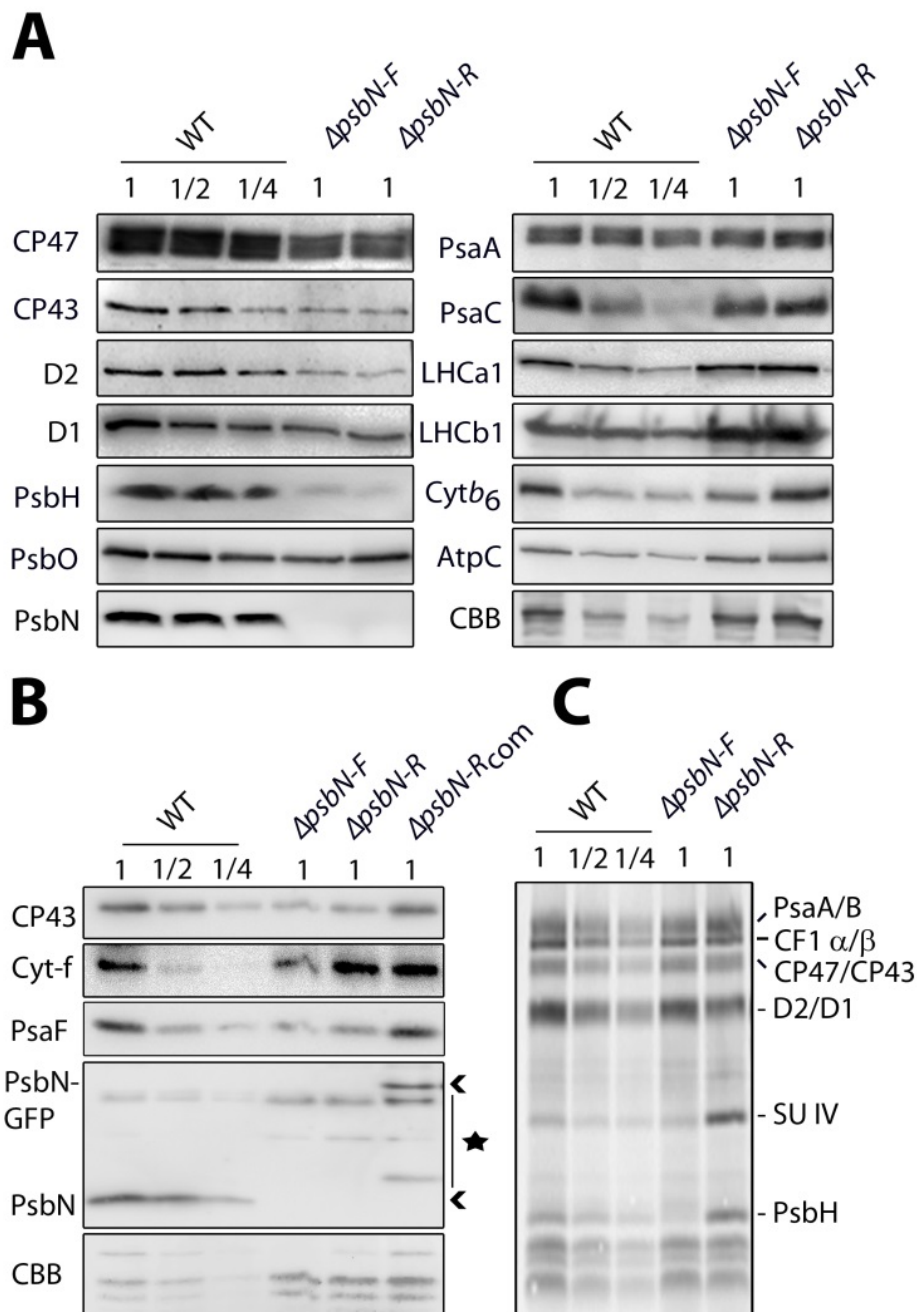


Figure 19. Thylakoid membrane protein levels and translation of chloroplast encoded proteins in $\Delta psbN$. (A) Comparison of wild-type and $\Delta psbN$ thylakoid membrane protein levels by immunoblot analyses using specific antibodies for the PSII core antenna CP47 and CP43, the PSII core subunits D1 and D2, the small subunit of PSII PsbH, the subunit of the OEC PsbO, the low molecular weight protein PsbN, the PSI core subunit PsaA, the small subunit of PSI PsaC, the antenna proteins LHCa1 and LHCb1, the subunit of Cyt $b_{6/f}$ Cyt b_6 , and the ATPase subunit AtpC. CBB, Coomassie blue staining. (B) Immunological analysis of the complemented $\Delta psbN$ -R mutant ($\Delta psbN$ -Rcom). Unspecific cross-reactions of the PsbN antibody and degradations products of the PsbN-GFP fusion are indicated by the star. The native PsbN protein is indicated by the lower arrow, while the upper arrow marks the PsbN-GFP fusion protein. (C) In vivo pulse labeling of chloroplast encoded proteins for 30 min, using [35 S]-methionine in the presence of cycloheximide. Thylakoid membrane proteins were adjusted to incorporated radioactivity of 100.000 cpm, 50.000 cpm and 25.000 cpm (1, 1/2, and 1/4, respectively), separated by SDS-PAGE and transferred to a nitrocellulose membrane. The most prominent appearing bands are indicated.

3.2.10 PSII complex formation is affected in $\Delta psbN$ mutants

Blue-Native PAGE (BN-PAGE) analyses were performed to test, if the reduced stability of PSII proteins is caused by an impaired complex assembly in the *psbN* knock-out lines. In the upper part of the native gel PSII supercomplexes (PSII-SC) were barely detectable in the mutants, while in the WT two distinct and one weak PSII-SC band appeared. This indicates that assembly of higher order PSII complexes is severely abolished in the $\Delta psbN$ mutants (Figure 20A). Furthermore the PSI monomer and PSII dimer band was slightly decreased and an additional band shifted to higher molecular weight appeared in both mutants. To separate the subunits of the thylakoid membrane complexes distributed in the BN-PAGE a second dimension SDS-PAGE was performed. In the colloidal blue staining of the second dimension gel the levels of PSII monomers and dimers were reduced and only minute amounts of proteins assembled to PSII-SC were detectable in both mutants (Figure 20).

The amount of the PSI monomer was also slightly reduced in $\Delta psbN-F$ and $\Delta psbN-R$ and the additional band of higher molecular weight could be identified as PSI complex. Furthermore a small fraction of the PSI antenna proteins was not associated with PSI but accumulated in a subcomplex in both mutants (Figure 20). The appearing spots were identified immunologically and by mass spectrometric analyses as LHCA2 and LHCA3 (data not shown). To proof whether this is caused by the lack of PsbN, the previously described $\Delta psbI$ line, was analyzed by two dimensional BN-/SDS-PAGE (Torabi et al., 2014). The function and accumulation of PSII in the $\Delta psbI$ mutants is less affected than in the $\Delta psbN$ mutants, as they exhibit a higher Fv/Fm ratio of about 0.74 and their PSII subunits are reduced by only 50% (Schwenkert et al., 2006). The analysis showed a similar appearance of smaller LHCA2 and LHCA3 subcomplexes in the plants lacking PsbI, approving that the observed effect can be generally caused by a reduced PSII activity in tobacco (Torabi et al., 2014).

It has to be taken into consideration that the Rubisco, the ATP synthase complexes, and the LHCII assemblies also accumulated to higher amounts in the mutants. This was caused by the adjustment of WT and mutant thylakoid protein amounts to equal chlorophyll contents and the fact, that the chlorophyll levels of both $\Delta psbN$ and $\Delta psbI$ mutants were reduced due to the lack of chlorophyll containing PSII proteins. Furthermore as revealed by western analysis also the chlorophyll containing PSI subunits are slightly decreased in the *psbN* mutants but

compared to that the LHCa2 and LHCa3 protein levels are not reduced (Figure 19). Thus these preassemblies might only reflect the imbalance between the amount of PSI antenna proteins and the PSI monomers in the $\Delta psbN$ mutants.

Additionally immunological analyses of the second dimension were carried out to determine the protein composition of the appearing complexes with a higher sensitivity (Figure 20A). Both mutants had reduced levels of PsbI and PsbH which were found predominantly in PSII monomers and to some extent in RC47, confirming the low abundance of PSII dimers and supercomplexes in $\Delta psbN$ -F and $\Delta psbN$ -R. In addition a part of PsbI could barely be detected in a complex streaking in the low molecular range in both mutants but not in the WT. Notably a part of PsbH was found as a distinct spot in the free fraction of the separated thylakoid membrane proteins in the WT. In both mutants no free PsbH could be found and the detected signal in the LMW range smeared towards higher molecular weight, indicating an impaired assembly of this subunit and a stable association with smaller precomplexes.

PsbN could only be detected in the unassembled fraction of thylakoid proteins in the WT and was absent in the mutants (Figure 20A), confirming previous data based on mass spectrometric analysis (Plöscher et al., 2009). Accordingly it can be expected that PsbN is not or only loosely and/or transiently associated with other proteins or complexes. Additionally the lack of PSII supercomplexes and dimers in $\Delta psbN$ -F and $\Delta psbN$ -R could be confirmed immunologically using antisera for the PSII core antenna proteins CP47 and CP43 and the PSII core protein D2 (Figure 20B). Therefore the ratios of pre-CP43/PSII monomer and RC47/PSII monomer were more pronounced in the mutants than in the WT. The accumulation of pre-CP43 and pre-CP47 in both mutant lines demonstrates the stable assembly of these precomplexes, and suggests a defect in the further efficient assembly and/or stability of PSII complexes.

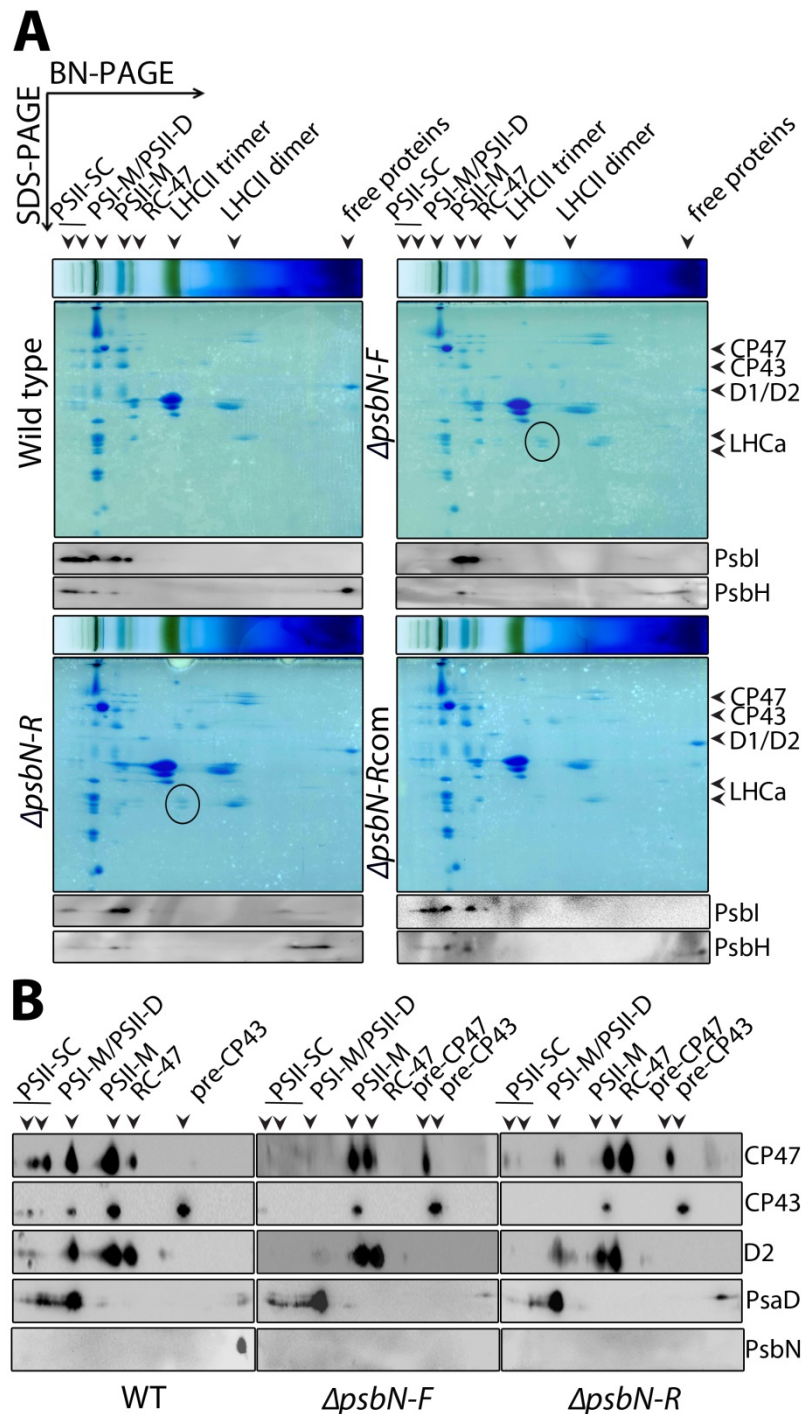


Figure 20. Accumulation of thylakoid membrane complexes in $\Delta psbN$ mutants. (A) Thylakoid membrane complexes were solubilized with 1% n-dodecyl- β -D-maltoside (β -DM), separated by BN-PAGE (top part) and after separation in a second dimension SDS-PAGE, stained with coomassie blue (middle part). The outstanding complexes and proteins are listed on top and on the right, respectively. Circles outline spots of Lhca2 and Lhca3 assemblies in the mutants, verified by mass spectrometry. Replicate gels were used for immunoblot analyses of PsbI and PsbH (bottom part). (B) Immunological analyses of the second dimension BN/SDS-PAGE using specific antisera for CP47, CP43, D2, PsaD, and PsbN.

3.2.11 Time-resolved assembly studies in $\Delta psbN$ mutants

To follow the assembly and the stability of PSII complexes *in vivo* radiolabeling of thylakoid membrane proteins was combined with subsequent two dimensional BN-PAGE analysis (Figure 21). Depending on the incorporation time with [^{35}S]-methionine this method allows the detection of the PSII precomplexes, like pre-D1, pre-D2, pre-CP43, pre-CP47 and PSII RC (D1/D2 heterodimers), as well as their further assembly into the stable accumulating PSII complexes, such as RC47, PSII-M, PSII-D and PSII-SC, in *statu nascendi*. Thus the complexes detected after the radiolabeling represent real assembly intermediates and not solubilized subcomplexes.

After the pulse labeling the [^{35}S]-methionine was mainly incorporated into newly synthesized PSII precomplexes, the lower and higher order PSII complexes and into the nucleus encoded LHCII proteins. Similar as in the BN-PAGE analysis of the stationary protein levels, the radiolabeled RbcL and the ATP synthase complex appeared to be more abundant in the $\Delta psbN$ mutants based on equal loading of chlorophyll. In order to highlight the proteins synthesized in the chloroplast, the cytoplasmic translation was inhibited with cycloheximide. After this treatment a clear discrimination between the PSII RC and the LHCII trimer as well as between the pre-D1 complex and other nuclear encoded proteins could be achieved already in the first dimension of the BN-PAGE (Figure 21A).

In comparison to the wild type, the mutants accumulated considerably less radioactivity in the lower and higher order PSII complexes (PSII RC, RC47, PSII-M, PSII-D and PSII-SC) and more in the PSII precomplexes (pre-D1, pre-D2, pre-CP43 and pre-CP47) (Figure 21A). As pre-D1 and pre-D2 complexes are not detectable in the immunological analysis of stationary protein levels (Figure 20B), it can be concluded that they reflect transient assembly intermediates, which are impaired to assemble into PSII RC if PsbN is absent.

The identities of the protein complexes were confirmed by separating the radiolabeled proteins in a second dimension SDS-PAGE. To get an idea about how fast the assembly process occurs, two different labeling times were chosen (Figure 21B). After a short labeling of 15 min, without inhibition of the cytoplasmic translation, the wild type and the mutant plants incorporated comparable amounts of radiolabel into the PSII precomplexes (pre-CP43 and pre-CP47). Additionally, in the mutants high amounts of pre-D1, pre-D2, free LHCII and LHCII trimer accumulated but barely no radioactivity was detectable in their lower and higher

PSII complexes. In contrast, in the wild type less pre-D1, pre-D2 and unassembled LHCII accumulated and already considerable amounts of radiolabel could be detected in the PSII RC, RC47, PSII-M and PSII-SC (Figure 21B). Even after a longer incubation time of 30 min only minute amounts of radiolabeled PSII complexes could be found in the mutants while they were more pronounced in the wild type. Notably, the assembly of pre-CP43 and pre-CP47 occurred efficiently in the mutants and they accumulated to higher amounts than in the wild type after extensive labeling (Figure 21B). This indicates that their further assembly into PSII complexes is impaired and that the formation of the PSII RC, which is the first outstanding PSII assembly intermediate, is hindered due to the lack of PsbN.

Caused by the lower labeling efficiency of PSI and the noisy background in the higher molecular range, no clear picture about PSI assembly could be drawn (Figure 21B). To reduce the background signals, the cytoplasmic translation was inhibited with cycloheximide and the labeling time was increased from 30 min to 1h for a better labeling of PsaA and PsaB. In the subsequent BN-PAGE analyses, again mainly PSII precomplexes accumulated while barely any lower and higher order PSII complexes could be detected in the mutants. In the area between the pre-D1, pre-D2 and RC the radiolabel appeared smeary indicating an impaired formation of the RC (Figure 22).

The radiolabeled PSI core proteins PsaA and PsaB appeared in five different complexes, the major PSI-M complex, which is attached to the LHCI and four additional PSI precomplexes. Interestingly in the mutants the fully assembled PSI-M and the two next smaller precomplexes were mainly labeled, while in the wild type the two smallest PSI precomplexes showed the highest incorporation of radioactivity (Figure 22). Thus the $\Delta psbN$ mutants assemble the PSI-M faster than the wild type.

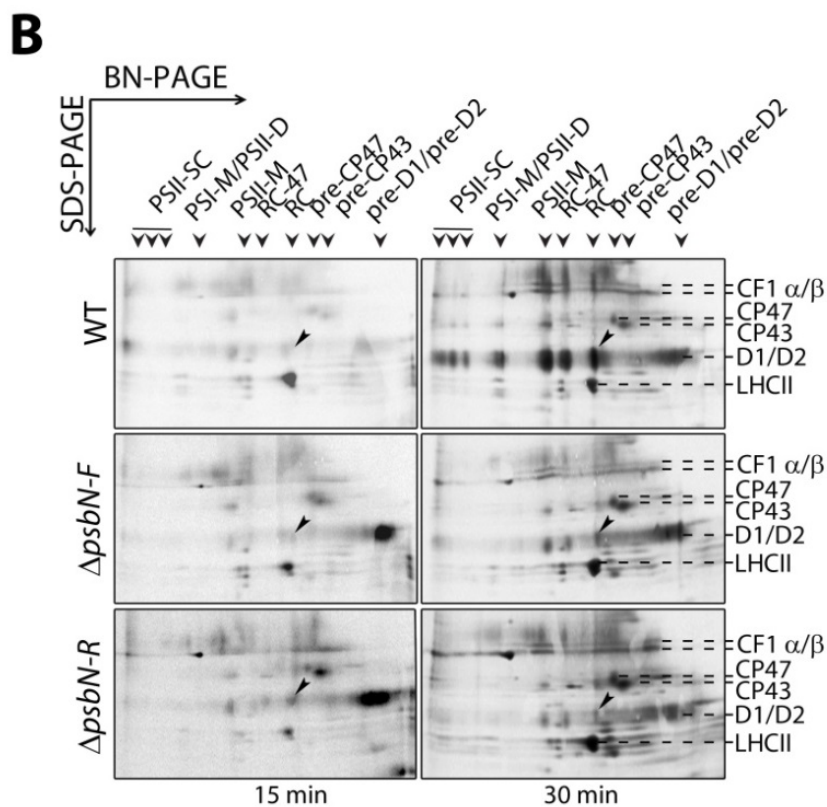
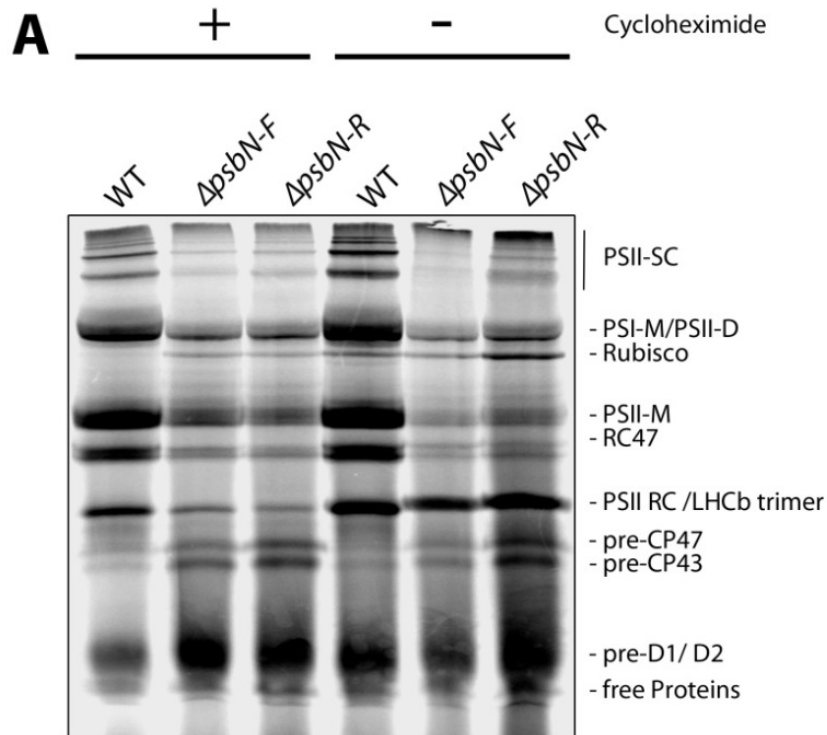


Figure 21. Photosynthetic complex assembly in the Δ psbN mutants. (A) Radiolabeled thylakoid membrane complexes of wild type (WT) and Δ psbN mutants were isolated after a pulse of 15 min, solubilized with 1% β -DM and separated by BN-PAGE. To inhibit the labeling of nuclear encoded proteins the leaves were pretreated with cycloheximide. (B) 2D BN-/SDS-PAGE analysis of radiolabeled thylakoids isolated after a pulse of 15 and 30 min in the absence of cycloheximide. The incorporated [35 S]-methionine was detected by phosphor imaging and the prominent complexes are indicated on the right. The arrow outlines the PSII RC.

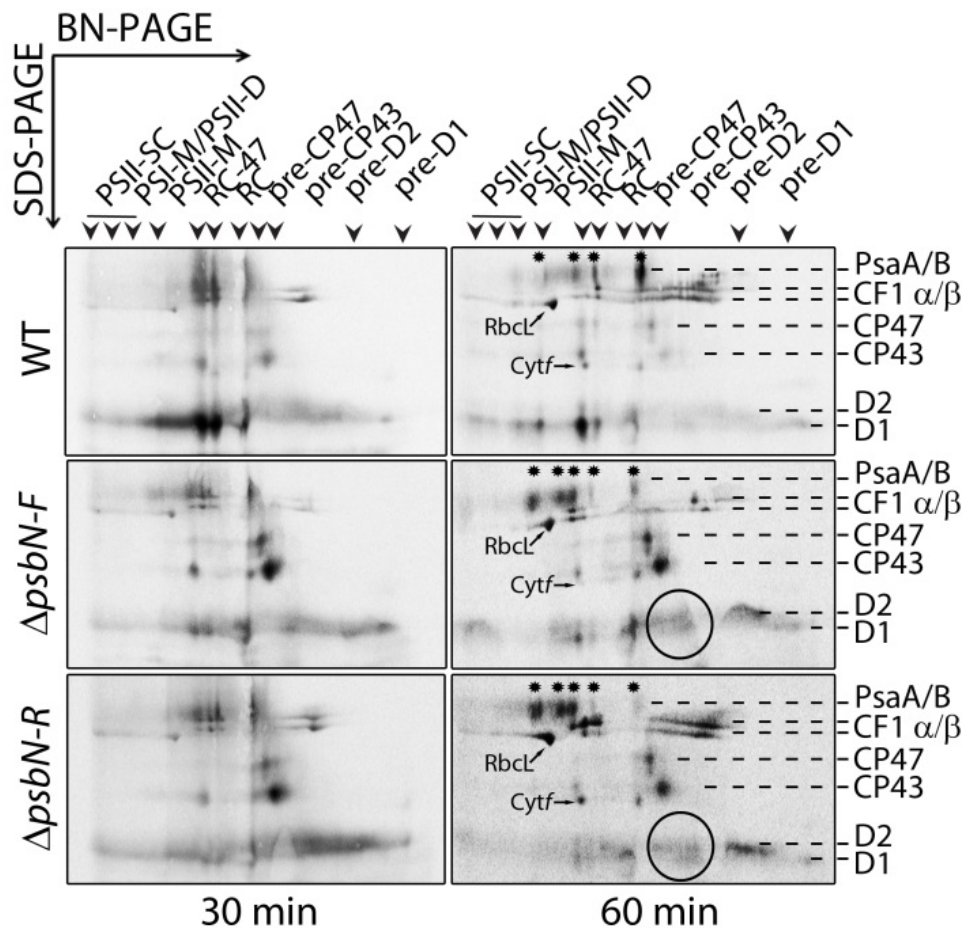


Figure 22. PSI assembly in $\Delta psbN$ mutants. 2D BN-/SDS-Page analysis of radiolabeled chloroplast encoded thylakoid membrane proteins isolated from tobacco wild type (WT) and $\Delta psbN$ mutants after a pulse of 30 and 60 min in the presence of cycloheximide. The incorporated [^{35}S]-methionine was detected by phosphor imaging. The smeary area, caused by the impaired RC formation after 60 min labeling, is encircled in the mutants. Asterisks indicate different PSI complexes. For details, see text.

3.2.12 Low temperature chlorophyll fluorescence analysis

By measuring the low temperature emission spectra (77K measurement) of isolated thylakoids, the energy distribution between the two photosystems gives information about the intactness of the photosystems and the association of the LHC proteins. In both mutants the PSI signal at 735 nm was shifted by maximal 1 nm to shorter wavelengths (Figure 23). The relatively higher abundance of unbound LHCa2 and LHCa3 subcomplexes to the PSI core complex in the mutants might be an explanation for this observation.

As expected the intensity of the PSII emission between 685 and 695 nm was massively reduced in the mutants. Furthermore when the curves were normalized to the PSII peak it became obvious that the emission shoulder of the LHCII at 680 nm is more distinctive in the mutants (Figure 23B). In summary this supports the previous data that both $\Delta psbN$ lines contain less intact PSII and that they accumulate more unassembled LHCII relative to the fully assembled PSII complex as compared to the wild type.

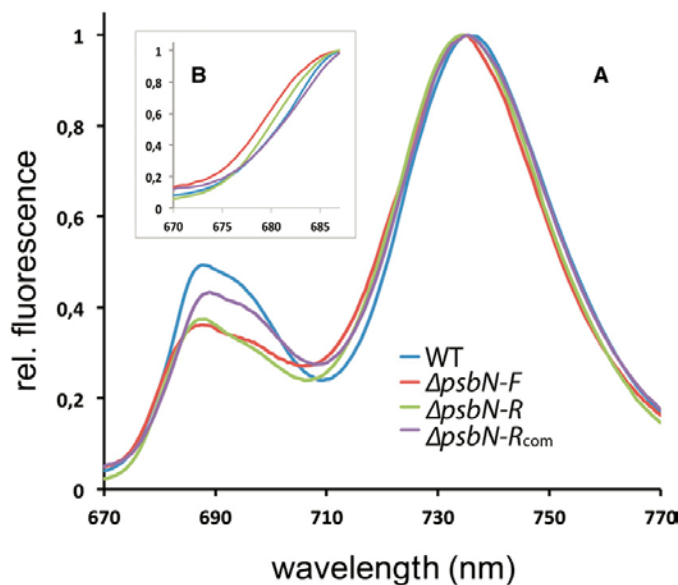


Figure 23. Low temperature (77K) chlorophyll *a* fluorescence spectra. (A) In liquid nitrogen frozen thylakoids of wild type (WT), $\Delta psbN$ mutants, and complemented $\Delta psbN-R$ lines ($\Delta psbN-R_{com}$) were excited at 440 nm and the chlorophyll emission spectra was recorded between 670 and 770 nm. At least four independent measurements were averaged and the fluorescence curves were normalized to the maximum PSI signal at 735 nm. (B) To highlight the LHCII emission shoulder at 680 nm the maximum PSII peak at 685 nm was used for normalization.

3.2.13 The thylakoid ultrastructure is changed in $\Delta psbN$ mutants

To get insights to which extent the absence of PsbN influences the ultrastructure of the chloroplast, electron microscopic pictures were taken (Figure 24). The chloroplasts of the mutant plants were comparable to the WT in size and shape. Interestingly the thylakoid membrane was dominated by the stacked grana regions, which were larger in size and densely packed, while the stroma lamellae was less pronounced in the $\Delta psbN$ -lines.

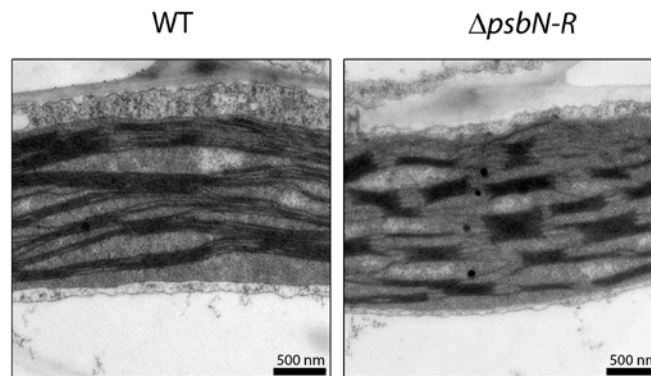


Figure 24. Electron microscope pictures of the thylakoid membranes of wild type and $\Delta psbN-R$. Preparations and pictures were made by the group of Prof. Wanner.

3.2.14 Photosensitivity of $\Delta psbN$ mutants

Inhibition experiments were performed to investigate the photosensitivity of the $\Delta psbN$ mutants, which is presumably a consequence of the affected PSII assembly. Therefore leaves were illuminated with a 5-fold higher light intensity relative to the growth light and the changes in the Fv/Fm were measured during the treatment (Figure 25A). While the Fv/Fm ratio of the WT leaves changed inappreciably within 12 h of light exposure, the Fv/Fm ratio decreased dramatically to about 50% of its initial value in the mutants. This decline could be caused by an increased photosensitivity and/or by a defect of the mutants to recover their damaged photosynthetic apparatus.

To figure out the reason for the observed photosensitivity the recovery process of the leaves was blocked with lincomycin prior the light treatment (Figure 25A). The affected chloroplast protein synthesis resulted in an enhanced photodamage in the lincomycin treated WT leaves. In contrast no significant change in the decline of the Fv/Fm values was observed when the protein synthesis was blocked in the chloroplasts of the mutants. Thus it can be concluded that the recovery process is mainly affected in the mutants.

To investigate the recovery process in more detail, WT and mutant leaves were treated with inhibitory light until the Fv/Fm decreased to about 50% of the original value and the regeneration process under growth light conditions was monitored. Additionally the WT leaves were further treated with high light to reach the same Fv/Fm value than the photodamaged $\Delta psbN$ mutants, which was about 25% of their initial value (Figure 25B).

In comparison to the mutants longer light exposure times and increased light intensities ($500 \mu\text{mol photons m}^{-2} \text{s}^{-1}$) were necessary to reduce the Fv/Fm values in the WT. The recovery rates of the WT leaves were independent of the grade of the light damage and reached about 85% and 65%, respectively, within 14 h. In contrast, both mutants which were very light sensitive even under low light intensity did not show any recovery of the Fv/Fm during the measurements (Figure 25B).

To evaluate whether PSII or PSI is more prone to photoinhibition in $\Delta psbN$ -F and $\Delta psbN$ -R, plants were treated with $100 \mu\text{mol photons m}^{-2} \text{s}^{-1}$ for 3 and 6 h. Subsequent immunoblot analysis revealed just minor decreases of the core subunits PsaA, CP43, and D1 in wild-type plants after the light stress treatment (Figure 25C). In contrast, the levels of PsaA did not change significantly in both mutants, while the amounts of the PSII core proteins D1 and CP43 considerably decreased already after 3 h treatment, indicating that PSII is primarily prone to light damage in the mutants.

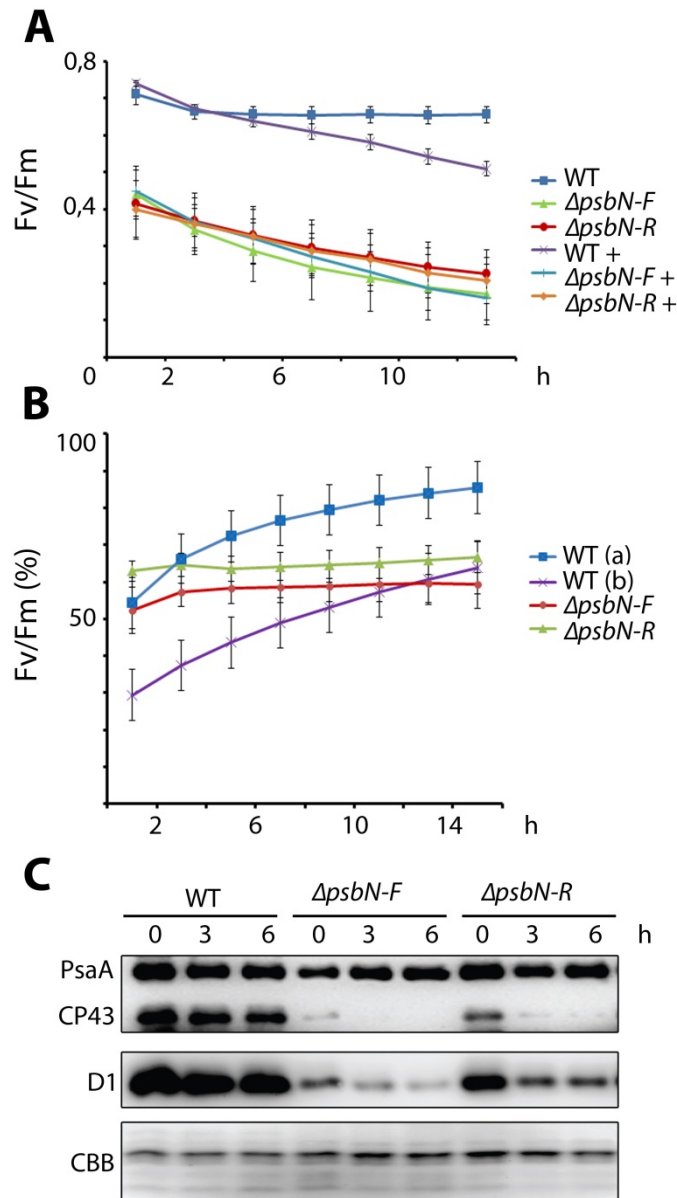


Figure 25. Light sensitivity and recovery of PSII in $\Delta psbN$ mutants. (A) F_v/F_m measurements of untreated and lincomycin treated (+) wild type and mutant leaves during photoinhibition caused by the 6-fold higher intensity of the growth light for 12 h. (B) The recovery process of PSII was measured within 14 h after wild-type (a) and mutant leaves had been treated with photoinhibitory light until the F_v/F_m was reduced to 50% of the original value. In addition the F_v/F_m of the wild type (b) had been reduced to 25%. (A/B) Standard deviations ($n = 12$) are indicated by the error bars. Light treatments and fluorescence measurements were performed using Imaging Pam (Walz). (C) Thylakoid membrane protein levels of wild-type and $\Delta psbN$ mutant leaves before (0) and after photoinhibition for 3 and 6 h using $100 \mu\text{mol photons m}^{-2}\text{s}^{-1}$. Immunological analysis was performed using specific antisera for PsaA, CP43, and D1. Sample amounts correspond to $2.5 \mu\text{g}$ of chlorophyll per lane, and protein loading and transfer was checked by coomassie blue (CBB) staining.

3.2.15 Phosphorylation of the PSII antennae is altered in $\Delta psbN$ mutants

Short-term adaptation of the photosynthetic apparatus to changing environmental conditions is mediated by reversible protein phosphorylation. The main trigger for the phosphorylation cascade is the redox state of the plastoquinone pool. According to the state transition theory, an emerging imbalance in the excitation of the two photosystems is compensated by a mobile part of the LHCII. Its connection to PSII or PSI is regulated by its phosphorylation or dephosphorylation by the STN7 kinase and PPH1/ TAP38 phosphatase, respectively (Pribil et al., 2010; Shapiguzov et al., 2010). Furthermore, changes in the thylakoid folding and the repair cycle of PSII are accompanied by reversible phosphorylation of the RC proteins D1, D2 and CP43 by the STN8 kinase and PBPC phosphatase (Vainonen et al., 2005; Rochaix et al., 2012).

Three different light conditions, dark, red light and far-red light, were chosen to compare the levels of reversible phosphorylation of PSII in the $\Delta psbN$ mutants with the wild type by immunological analyses (Figure 26). In the dark-adapted mutant samples the phosphorylation signal of the LHCII appeared to be higher than in the wild-type sample but this was rather based on the increased outer antenna protein levels as a consequence of equal chlorophyll loading (Figure 26). By increasing the dark-adapted wild type sample to 125% the same amounts of LHCII and same level of phosphorylation were achieved as in the mutant (Figure 26B). In contrast under red light the phosphorylation of the LHCII decreased significantly in the mutants while it increased in the wild type. Due to the exposure to red light the PSII core protein D1 and D2, which accumulate only to about 25% of the wild-type levels in the mutants, were phosphorylated to a comparable extent in the mutant and the wild type (Figure 26). This was reinforced by comparison of the mutant samples with 25% of the wild-type sample (Figure 26B).

The phosphorylation of the PSII core antenna CP43 did not change significantly in both mutants and wild type under all three conditions. Taken together the decrease of LHCII phosphorylation under red light in the mutant can be explained by a higher activity of PSI even under light which preferentially excites PSII. The fact that the plastoquinone pool gets more oxidized under red light supports the previous finding of a severely affected PSII in the mutants. With the application of far red light dephosphorylation of the PSII core proteins D1, D2 and the LHCII was induced in the mutants and in the wild type, indicating a functional redox control in both.

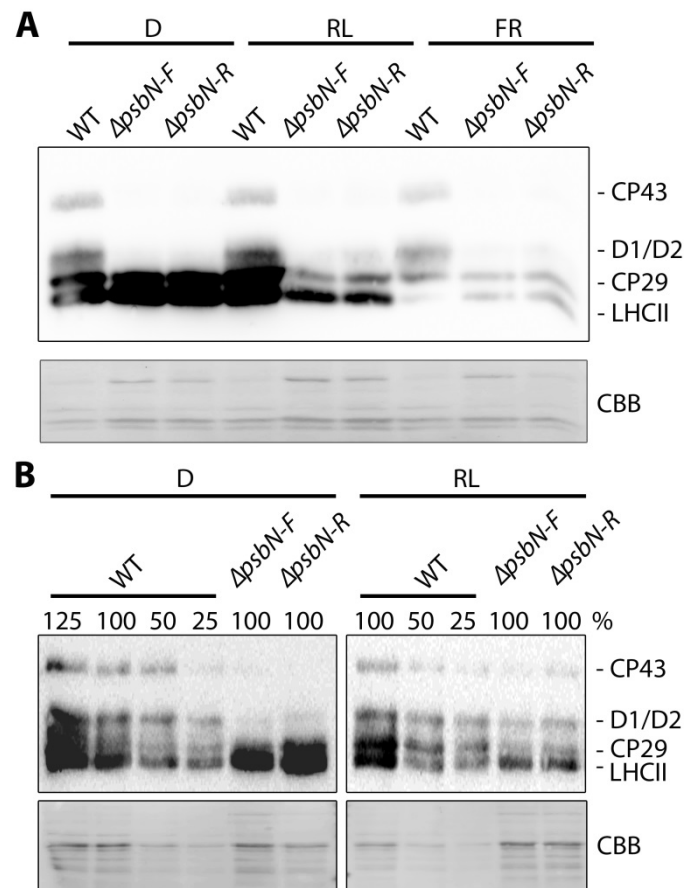


Figure 26. Light induced changes of thylakoid membrane protein phosphorylation. Immunological analyses of thylakoid membrane proteins isolated from 4-week-old tobacco wild-type and $\Delta psbN$ mutant plants using phosphothreonine specific antibodies. (A) Plants were first kept in the dark for 24 h (D) and subsequently illuminated with red (RL) and far-red (FR) light for 2 h. Each lane corresponds to 3 μ g of chlorophyll. (B) To consider increased LHCII and reduced PSII protein levels in the $\Delta psbN$ samples, caused by the adjustment to equal amounts of chlorophyll (100% = 3 μ g) and by the PSII defect, titrations of the D and RL WT samples were compared with the mutant samples. CBB, coomassie blue staining.

3.2.16 Allotopic complementation of $\Delta psbN$ mutants

The characterization of nuclear mutant plants commonly involves a complementation analysis to prove the correlation between the mutated gene and the observed phenotype. Since plastid gene knockouts are produced straightforward by a targeted transformation based on homologous recombination, the complementation of a plastid knockout mutant is usually not necessary. But to consider concerns about to which extent the observed phenotype in the $\Delta psbN$ mutants is caused by the disruption of the *psbB* operon structure, a complementation study was performed with the $\Delta psbN$ mutants. In order to avoid an additional time-consuming plastid transformation, the *PsbN* gene was integrated into the nuclear genome of the mutants using *Agrobacterium tumefaciens*-mediated transformation. To enable the chloroplast import,

the transit peptide of PsbS was fused to the N-terminus of PsbN. Furthermore, a GFP was attached to the C-terminus of PsbN in order to follow its expression and localization within the chloroplast. The PsbN-GFP fusion could be localized in the chloroplast of the transformed plants by confocal laser scanning microscopy (CLSM) (Torabi et al., 2014).

Several independent transformed lines containing either the mutant or wild-type plastome, were regenerated and transferred to semi-sterile culture or to the greenhouse to produce seeds. The transformed lines carrying the wild-type plastome were furthermore used to pollinate flowering $\Delta psbN$ mutants in semi-sterile culture. The transformed mutant lines, were called $\Delta psbN$ -Fcom and $\Delta psbN$ -Rcom as they showed a better growth and a reduced light sensitivity than the mutants under different light intensities (Figure 18).

Fluorescence analysis of $\Delta psbN$ -Fcom revealed a partial complementation of the photosynthetic activity of PSII, reflected by a slight increase of the Fv/Fm and a significant drop of the Fo level (Appendix). In contrast the PSII specific fluorescence signals measured in the $\Delta psbN$ -Rcom line were nearly indiscernible from the wild type, suggesting that the PSII defect is fully complemented (Table 1/Appendix). To confirm the successful PSII reconstitution the nuclear PsbN expression was further investigated in the $\Delta psbN$ -Rcom lines. A recovery could be observed in the chlorophyll *a/b* ratio, the PSII specific fluorescence signals, and all other photosynthetic parameters measured (Table 1/Appendix).

By immunological analysis of thylakoid membrane proteins the expression of the chimeric PsbN-GFP fusion protein was proven. In the thylakoids of $\Delta psbN$ -Rcom plants the PsbN specific antibody detected one band with the expected size of 33 kDa corresponding to the PsbN-GFP fusion and a smaller band which might represent a degradation product. Using specific antibodies for the PSII core antenna CP43 and the PSI subunit PsaF a restoration of the PSII and PSI complex accumulation could be demonstrated in $\Delta psbN$ -Rcom plants. The $\Delta psbN$ -Rcom lines showed the same slight over accumulation of the cytochrome b_6/f complex like the $\Delta psbN$ -R mutants, tested with the specific antibody against the cytochrome *f* subunit (Figure 19B).

Also the assembly of PSII dimers and supercomplexes was recovered in $\Delta psbN$ -Rcom lines as revealed by two-dimensional BN-PAGE analyses (Figures 20A). In summary, this provides evidence that the lack of PsbN is exclusively responsible for the mutant phenotype observed in $\Delta psbN$ -R.

4. Discussion

4.1 HCF145 is a nuclear-encoded factor affecting *psaA*-5' UTR stability

Recently, the nuclear *hcf145* locus was described to encode an unknown trans-acting factor specifically involved in protecting the *psaA-psaB-rps14* mRNA from degradation (Lezhneva and Meurer, 2004). The analysis and complementation studies of two allelic lines *hcf145-1* and *hcf145-2* demonstrated that HCF145 is encoded by the locus AT5G08720. HCF145 is specific for the green lineage and has a modular composition of cyanobacterial origin consisting of tandem repeated SRPBCC and TMR domains.

4.1.1 SRPBCC superfamily domains have diverse functions

Two conserved tandem duplicated domains 145motif-1 and 145motif-2 in the N-terminal part of HCF145 show high homologies to polyketide cyclases. This ubiquitous protein family is a member of the SRPBCC (START/RHO alpha C/PITP/Bet v1/CoxG/CalC) superfamily. The SRPBCC domain consists of a structurally highly conserved versatile hydrophobic scaffold which binds quite diverse ligands such as lipids, polyketides, plant hormones, flavonoids and other metabolites. Members of the SRPBCC superfamily were found in many organisms and many of them were crystallized for structural analyses. The pocket represents a lipid transfer domain of mammalian proteins (Yoder et al., 2001), the catalytic center of aromatic ring-hydroxylating oxygenases (Martins et al., 2005) and is found in phosphatidylinositol transfer proteins (Tsujiyama and Hurley, 2000), polyketide cyclases (Sultana et al., 2004) and many other proteins with still unknown function. A phylogenetic analysis on the major birch pollen allergen Bet v1, classified eleven families with SRPBCC domains and found related proteins among all superkingdoms, suggesting a Bet v1-like protein in the last universal common ancestor (Radauer et al., 2008).

Among the 37 structurally related polyketide cyclases annotated in *Arabidopsis* only 145motif-L (At4g01650) showed sequence similarities to both motifs in HCF145 (Figure 7B/Appendix). Therefore, 145motif-1 and 145motif-2 most probably arose by a duplication of 145motif-L. Homologues of 145motif-L are also found in algae and cyanobacteria. The fact that not all cyanobacteria possess a 145motif-L homolog indicates that the function is dispensable in individuals of this taxon.

4.1.2 The TMR motifs confer RNA binding specificity to HCF145

Many of the SRPBCC superfamily members have a modular composition with multiple domains, which provide them additional features such as enzymatic activity, signaling, protein localization and nucleotide binding affinity (Radauer et al., 2008; Clark, 2012). The same might be true for HCF145 as two unknown tandem repeats motifs could be identified in its C-terminus (Figure 7B/Appendix). *In vitro* RNA binding studies could prove a high affinity of this C-terminal part of HCF145 to the *psaA* 5'UTR, confirming that these motif repeats are truly able to confer specific RNA binding affinity (data not shown). Therefore, the TMR motifs represent a new class of repeated RNA binding domains specific for photosynthetic organisms.

Recently, it could be shown, that degenerated repeats found in the Puf domain and the PPR domain family bind single stranded RNA in a nucleotide specific manner. The Puf domain can bind 8-9 nucleotide sites and it consists of eight 30-40 amino acid repeats of which each forms a triple-helix motif (Lu et al., 2009). The PPR domain, which is the most prominent RNA binding motif found in many proteins of chloroplasts and mitochondria, occurs as 2-30 repeats of about 35 amino acids. Each repeat forms two antiparallel helices, which were shown to bind one nucleotide (Barkan et al., 2012; Yin et al., 2013). Interestingly one TMR motif spans about twice the length of a Puf or a PPR repeat and they most probably form four alpha helices as predicted by the I-Tasser algorithm (data not shown). This raises the interesting question, whether TMR motifs also provide a combinatorial amino acid code for RNA recognition, as it was shown for the Puf and PPR domains (Lu et al., 2009; Barkan et al., 2012).

4.1.3 Phylogenetic conservation of HCF145

In contrast to PPR proteins, which were found only in eukaryotic organisms, TMR proteins are of cyanobacterial origin and seem to be restricted to organisms performing oxygenic photosynthesis. The TMR motifs in HCF145 most likely originate from cyanobacteria, as three C-terminal TMR motif repeats can be found in one protein of *Microcoleus sp.* PCC 7113 (Appendix). The most diverse TMR proteins with up to ten repeated motifs were found in the red algae *Cyannidioschyzon merolae* and *Galdieria sulphuraria* (Appendix). Homologues of the modular HCF145 can only be found in vascular plants and in some green algae. From available sequence data we concluded that HCF145 homologues are restricted to members of viridiplantae, which all encode *PsaA* in a tricistronic operon together with *PsaB*

and *Rsp14*. The high diversity of the chloroplast genome organization found among green algae (Letsch and Lewis, 2012), can explain why HCF145 became dispensable in individual members. A co-evolution of HCF145 with its mRNA target is supported by a conserved *psaA* 5' UTR and highly homologous HCF145 proteins among land plants (Appendix).

Mosses are the oldest clade of land plants and they diverged more than 400 million years ago from the vascular plants (Theißen et al., 2001). Homologous recombination and a dominant haploid gametophyte make the moss *Physcomitrella patens* best suitable for reverse genetic approaches (Schaefer, 2001). Targeted inactivation of *HCF145* in *Physcomitrella patens* resulted in knockout lines, that displayed a similar photosynthetic and molecular phenotype as the *Arabidopsis hcf145* mutants (Figure 8/9). This provides strong evidence, that the function of HCF145 in the stabilization of the *psaA* 5' UTR is highly conserved among all land plants.

It is widely accepted that plants and green algae share a common ancestor (Qiu and Palmer, 1999; Turmel et al., 2006) and that most probably a single green algae-like progenitor gave rise to the monophyletic group of land plants. The most challenging requirement upon the conquest of the land was to cope with dramatically changing environmental conditions (Karol et al., 2001; Waters, 2003). The resulting high evolutionary pressure was proposed to be a bias for the invention of RNA editing (Freyer et al., 1997), the dispersion of an exceptionally high number of PPR proteins (O'Toole et al., 2008), the evolution of a plastidal NEP polymerase (Hedtke et al., 1997; Hedtke et al., 2000), and the recruitment of land plant specific nucleus encoded factors (Meurer et al., 1998a; Stoppel et al., 2011; Stoppel et al., 2012).

One possible explanation for the fast evolving RNA metabolism is that these nuclear factors counteract mutations, which proliferated in the water-to-land transitions (Maier et al., 2008). Contemporary evidences for this hypothesis is the constitutive expression of many PPR proteins (Lurin et al., 2004), the restoration of mitochondrial cytoplasmic male sterility (Wang et al., 2006; Chase, 2007), the secondary loss of organellar RNA editing in the liverwort *Marchantia polymorpha* (Groth-Malonek et al., 2007) and the predominance of posttranscriptional, translational and posttranslational regulation in the chloroplast (Deng and Gruissem, 1987; Marin-Navarro et al., 2007).

Beside the abovementioned debugging hypothesis, it is widely accepted that many species specific regulatory factors evolved in plants to balance the nuclear and organellar gene

expression on the transcriptional and posttranscriptional level (Puthiyaveetil and Allen, 2009; Barkan, 2011; Manavski et al., 2012; Schwarz et al., 2012). The evolution of HCF145 in the ancestor of the green lineage and its high conservation among all photosynthetic land plants might be an indication that it provided an important positive selection to the divergence of land plants. This is supported by the fact that many factors that took over a regulatory function in the chloroplast gene expression on the transcriptional and posttranscriptional level of vascular plants could not be found even in any of the sequenced genomes of green algae (Karcher and Bock, 1998; Emanuel et al., 2004; Liere and Börner, 2007; Stoppel et al., 2011).

4.1.4 The low abundant HCF145 accumulates already in eoplasts

In large-scale expression data only poor information is available about the At5g08720 locus, indicating a low expression and abundance of HCF145. Northern analysis with *Arabidopsis* plants and RT-PCR analyses confirmed that *hcf145* transcripts were barely detectable (Figure 10; data not shown). The protein was found in a proteome analysis of *Arabidopsis* mitochondria (Heazlewood et al., 2004) leading to a miss-assignment in the TAIR and UniProt databases. This finding could be disproven by localization of the HCF145-GFP fusion in the chloroplasts of stomata cells (Figure 7).

In another large-scale proteome approach peptides of HCF145 were found in triton-insoluble extracts, representing mainly the nucleoid fraction of the chloroplast (Phinney and Thelen, 2005). Many proteins involved in posttranscriptional processes were found in the nucleoid fraction (Majeran et al., 2012). The localization of HCF145 in nucleoids might explain the spotted GFP signals observed within the chloroplast of the *hcf145-2com_{gfp}* plants (Figure 7). Since the GFP fluorescence signals were only detectable in stomata cells, which turned out to be inaccessible for DAPI staining in a non-fixed state, this hypothesis has not yet been proven by microscopic imaging in the *hcf145-2com_{gfp}* plants.

Immunological analysis with a peptide specific antibody against HCF145 confirmed a low abundance of HCF145 in light-grown plants. The native HCF145 protein accumulates in etiolated seedlings and the amount declines upon illumination (Figure 11). Studies with germinating *Arabidopsis* seeds showed that the PEP starts to transcribe photosynthesis-related genes during light-induced germination and early seedling out-growth (Demarsy et al., 2012). Thus, the function of HCF145 might be most important before photosynthetic protein synthesis takes place during illumination.

4.1.5 HCF145 protects the *psaA-psaB-rps14* transcripts at the 5' UTR

Nucleus-encoded factors involved in the posttranscriptional regulation of plastids mainly interact with cis-regulatory elements (Stern et al., 2010). Co-immunoprecipitation analysis of the HCF145-GFP fusion confirmed the very 5' UTR of *psaA* as the putative target of HCF145 (Figure 12). A destabilization of mRNA at the 5' UTR is often accompanied by an impaired translation (Barkan, 1993; Meurer et al., 2002). Northern analysis with inhibitors of protein synthesis, *in vivo* labeling studies of chloroplast encoded proteins and ribosomal loading of *psaA* mRNA gave no hints about a primary defect of PsaA synthesis in *hcf145* mutants (Lezhneva and Meurer, 2004; data not shown). As revealed by primer extension analysis the mature 5' end of *psaA* appeared shorter and much less abundant in *hcf145* mutants than in the wild type (data not shown). Since the transcription rate of *psaA* was not significantly altered in the *hcf145* mutants, it can be expected that this 5' end represents a meta-stable degradation product.

In vitro experiments with PPR proteins showed that site specific binding to 5' and 3' UTRs can protect mRNAs from 5'→3' and 3'→5' exonucleases (Pfalz et al., 2009; Prikryl et al., 2011; Hammani et al., 2012; Zhelyazkova et al., 2012). The same might be true for HCF145 as the recombinant protein showed a high affinity to the *psaA* 5' UTR and protected the *psaA* 5' UTR from an exonucleolytic attack *in vitro* (data not shown). Some chloroplast specific RNases were shown to be activated in the dark (Baginsky and Gruissem, 2002; Qi et al., 2012). Taken into account that HCF145 could only be detected in etiolated seedlings (Figure 10A), it might be possible that HCF145 accumulates in the dark or is already present at the onset of germination, to protect the *psaA* 5' UTR against unspecific nucleolytic degradation.

4.1.6 PSI biogenesis highly depends on HCF145

Interestingly, the half-life of *psaA* mRNA appeared to be much shorter than that of other chloroplast mRNAs after illumination of etiolated barley seedlings, suggesting a coregulation of transcription activity and stability of *psaA* mRNA (Klein and Mullet, 1987; Mullet and Klein, 1987). *HCF145* RNAi lines in tobacco showed gradual variations of the *hcf* phenotypes (Figure 11), implying that the repression of HCF145 directly limits the accumulation of PSI.

Treatment with different light conditions and stressors showed that the *hcf145* transcript accumulation is responsive to the redox state of the chloroplast within several

hours. After 24 h of darkness, red light and far-red light treatment the levels of *hcf145* transcripts decreased while the *psaA* mRNA levels increased only in the dark and remained stable under the other light conditions (Figure 10B). It can be assumed that the levels of *hcf145* mRNA change in response to light quality and stress faster than those of the *psaA* mRNA. The *hcf145* and *psaA* mRNA levels rapidly increased and decreased after induction of massive stress conditions by DCMU and Paraquat, respectively (Figure 10B). This demonstrates that the regulation of *hcf145* and *psaA* mRNA accumulation respond to the status of the chloroplast in a concerted manner.

4.1.7 HCF145 might be linked to a metabolic pathway

The modular nature of HCF145 with its hydrophobic ligand binding domains homologous to polyketide cyclases makes a metabolic control of *psaA* mRNA accumulation very likely. The previous findings that DPT1, which is related to prokaryotic UMP-kinases, is involved in the stabilization of *psaA-psaB-rps14* transcripts supports this suggestion (Hein et al., 2009). UMP-kinases are involved in the pyrimidine metabolism, which is linked to the citric acid cycle. The citric acid cycle can be seen as a metabolic hub to regulate energy homeostasis and overall cell metabolism (Krebs, 1970). The biosynthesis of polyketides initiates with acetyl-CoA or malonyl-CoA. The citric acid cycle as well as the fatty acid synthesis also begins with acetyl-CoA and malonyl-CoA is the first product in the fatty acid synthesis. In terms of their phylogenetic background, HCF145 and DPT1 are obviously related to enzymes of eubacterial origin, which catalyze primary or secondary metabolites.

Different developmental stages of plants produce various metabolic cell environments, which have to be connected to the expected photosynthesis activity in the chloroplast. To link the cell homeostasis with the accumulation of PSI at the level of mRNA stability makes economically sense. In comparison to PSII the PSI is much more stable and additionally it is protected by PSII from excess light (Tikkanen et al., 2014). Therefore, it seems obvious that plants need to regenerate a vast number of PSII complexes to cope with harmful light intensities, which can change within seconds under natural conditions. This is reflected by the high accumulation and stability of the *psbA* mRNA encoding for D1, the chloroplast protein with the highest turnover in the light (Mattoo et al., 1984; Bate et al., 1991). In contrast, the synthesis of the iron sulfur (Fe-S) clusters within PSI needs high reducing power and is limited by the iron availability. Furthermore, the number of newly synthesized PSI complexes has to be adapted to the amounts of PSII complexes for balancing the light reactions and avoiding photoprotection.

4.1.8 HCF145 might be integrated into a signal transduction pathway

Future studies will address the question, whether the SRPBCC domains of HCF145 confer an authentic metabolic control for binding to and stabilization of the *psaA* mRNA and, hence, adaptation of PSI levels. One recent study might have answered already part of this question. In a larger scale split ubiquitin analysis, with the purpose to create an interaction map of the two-component signaling (TCS) pathway, HCF145 showed interaction to several *Arabidopsis* response regulators (ARR) (Dortay et al., 2008). All these regulators are thought to be involved in the cytokinin response.

HCF145 showed interactions with ARR15 using cDNA libraries isolated from flowers, 5-7-day-old hormone treated seedlings and 5-day-old seedlings. ARR5, ARR9 and ARR16 showed interactions with HCF145 using cDNA libraries isolated from roots, and ARR7 interacted with HCF145 using cDNA libraries isolated from flowers (Dortay et al., 2008). Interestingly, the interaction with the ARR15 response regulator showed only three other interactions, each in a different tissue: (1) with Lhcb1 in 5-7-day-old seedlings; (2) with zinc finger protein 3 (ZFP 3), a stress responding DNA binding protein in flowers; (3) with an unknown zinc ion-binding protein containing an ubiquitin-associated domain, which might be involved in protein targeting to the vacuole, in 5-7-day-old hormone treated seedlings (Dortay et al., 2008).

If these interactions were true, the accumulation of HCF145 in the chloroplast could be regulated by the secondary metabolite cytokinin in the cytosol. Furthermore, the stabilization of the *psaA* mRNA via HCF145 and the import of the outer PSII antenna protein Lhcb1 could be regulated at the same branch point. The cytokinin signaling pathway was recently shown to be dependent on proteasome-mediated degradation (Kurepa et al., 2013). The unknown protein, with the ubiquitin-associated domain, could therefore be involved in the degradation pathway of ARR15, HCF145 and/or Lhcb1.

If we further speculate an interesting phylogenetic aspect could be found between ARR15 and the TMR domain of HCF145. ARR15 belongs to the CheY-like superfamily of two component response regulators of bacteria. Interestingly one of the three different TMR domain proteins, found in the red algae *Cyanidoschyzon merolae* shows homology to a CheY-like response regulator receiver domain. This raises the questions whether all TMR domain proteins connect mRNA stability to a specific signal transduction pathways. Dramatic changes in the signal transduction pathways of plants (Pils and Heyl, 2009) could explain why only

HCF145 remained in land plants and why the TMR domain did not spread as a general nucleotide binding domain like the PPR domain.

4.1.9 Outlook of the HCF145 project

Further *in vivo* and *in vitro* studies will be performed to narrow down the RNA binding site of HCF145 in the 5' UTR of *psaA* and to clarify if HCF145 has additional RNA target sites. For this purpose, RNA immunoprecipitation sequencing, using the complemented *hcf145-2com_{gfp}* plants, and Electrophoretic Mobility Shift Assay (EMSA) analyses are in progress. In addition, these analyses could be used to elucidate the general function of the TMR domain in RNA binding. Therefore, further TMR domain proteins of algae and cyanobacteria have to be investigated.

To find a possible interaction partner and/or ligand of HCF145 further co-immunoprecipitation analyses with mature plants as well as etiolated seedlings, roots and 5-7 day old seedlings could be performed, followed by mass spectrometric analyses.

To test if HCF145 is integrated into a signaling pathway, the molecular and biochemical analyses could be extended by treatments with cytokinines or other phytohormones. Furthermore ubiquitin pathway inhibitors could be used to investigate, if the observed light induced decrease of HCF145 levels is mediated by degradation in the cytosol.

4.2 PsbN is required for the assembly of PSII

4.2.1 PsbN is not a constituent subunit of PSII

The assembly of PSII is widely accepted to occur in a stepwise manner. First cofactor-containing intermediate precomplexes are formed which sequentially assemble forming higher order PSII complexes together with the outer antenna system. In the last years many factors were identified to be involved in the PSII assembly, like HCF136, LPA1, LPA2, LPA3, PAM68, HCF243, Psb27, Psb28, CYP38, and RBD1 (Calderon et al., 2013; Nickelsen and Rengstl, 2013). Due to the highly conserved function, structure and composition of PSII most of the assembly factors are highly conserved in structure and function from cyanobacteria to plants. Many of these proteins were first described in cyanobacteria and all of them found in plants so far are encoded in the nuclear genome.

In this work the first plastid encoded factor necessary for the accumulation of PSII was described. To decipher the function of PsbN, its gene was knocked out in tobacco by plastid transformation and antibodies were raised against its C-terminal part. The antibody production was proven to be successful as it detected a protein of the right size which was lacking in both generated knock out lines $\Delta psbN-F$ and $\Delta psbN-R$ (Figure 19A/B). Unlike as in the case of most mutants specifically affected in the accumulation of PSII, the $\Delta psbN$ mutants showed no significant defect in the translation of PSII core subunits.

PsbN was found to mainly reside in the stroma lamellae, the place where PSI resides and where PSII assembly and repair occurs. Furthermore it turned out, that PsbN is not or only loosely associated with other proteins and or complexes. As it could be proven that PsbN is not a constituent subunit of PSII, the involvement of PsbN in the PSII accumulation could be restricted to the subunit and or precomplex assembly. The functional part of PsbN is most likely its highly conserved C-terminus, which was shown to be exposed to the stromal face of the thylakoids, while the N-terminal hydrophobic part function as an integral membrane anchor. A 3D model predicted by the I-Tasser algorithm showed a flexible spacer between the longer N-terminal hydrophobic helix and the shorter C-terminal hydrophilic helix, which might enable a dynamic transaction of the PsbN C-terminus (Torabi et al., 2014).

Most cyanobacteria and plastids of plants express *psbN* next to *psbH* from the opposite strand. The transcription of *psbN* in the *psbB* gene cluster of chloroplasts was shown to be mainly regulated by a single transcription factor, SIG3 (Zghidi et al., 2007). The *psbN* transcripts are supposed to function as a natural occurring antisense RNA to the *psbTc* transcripts, as they influence the PsbT accumulation in *SIG3* mutants (Zghidi-Abouzid et al., 2011). Due to the high complexity of the posttranscriptional processes found within the *psbB* gene cluster (Stoppel and Meurer, 2013), it can be expected that additional factors are required for fine-tuning and adjusting the expression of PsbN. Upon light induction hundreds of coregulated nuclear and plastid encoded genes were found in tight transcriptional clusters (Cho et al., 2009). In contrast PsbN was found to accumulate already in dark grown seedlings uncoupled from the general expression network of photosynthetic genes.

To consider possible effects of the *psbN* transcription on the other genes in the *psbB* gene cluster two orientations of the *aadA* cassette insertion were chosen to knockout *psbN*, resulting in the two lines $\Delta psbN-F$ and $\Delta psbN-R$. The fact that *PsbN* is one of the few plastid genes that has never been transferred successfully to the nucleus or was lost during the

evolution, suggests that its expression in the plastid is necessary for efficient early PSII assembly. Remarkably it was possible to substitute the lack of PsbN in the mutants by the import of a nuclear encoded form equipped with a transit peptide. Under controlled conditions the ectopic PsbN expression partially restored the PSII defect in $\Delta psbN-F$ and completely recovered the wild-type phenotype in $\Delta psbN-R$.

The *Arabidopsis* mutant *hcf107*, which is impaired in the accumulation of translation-competent *psbH* transcripts, is severely affected in PSII accumulation (Felder et al., 2001; Meierhoff et al., 2003b; Sane et al., 2005; Hammani et al., 2012). Therefore the still observed PSII deficiency in $\Delta psbN-F$ com might be a consequence of the *aadA* cassette insertion, which caused reduced *psbH* transcript levels (Figure 19C).

Recently this problem was completely avoided by a co-transformation approach, in which the PsbN translation was cut-off by the insertion of a premature stop codon, without disturbing the transcription of the *psbB* gene cluster (Krech et al., 2013). A preliminary comparison of this $\Delta psbN$ mutant with the $\Delta psbN-F$ and $\Delta psbN-R$ lines showed a similar growth and fluorescence phenotype (Appendix). Thus the disordered *psbB* gene cluster in $\Delta psbN-F$ and $\Delta psbN-R$ caused only minor effects compared to the primary role of PsbN in the PSII assembly.

Nevertheless a regulatory reason of the opposite transcription of *psbN* should not be disregarded, since all experiments were performed under controlled conditions. Using complemented versions of all three $\Delta psbN$ mutants one could compare the impact of the over expressed *psbB/psbTc* antisense transcription in $\Delta psbN-F$ com, the absent *psbB/psbTc* antisense transcription in $\Delta psbN-R$ com, and the unchanged transcription of the *psbB* gene cluster in a complemented version of the $\Delta psbN$, under various growth and stress conditions and at different developmental stages.

4.2.2 PsbN is specifically required for PSII RC formation

In *Synechocystis* sp PCC6803, no obvious additional phenotypic effects were observed under controlled conditions when deleting *psbN* alongside *psbH* (Mayers et al., 1993). This is in accordance with the only slightly increased PSII defect observed in the $\Delta psbN-F$ line, although the synthesis of PsbH was additionally affected (Figure 18). The lack of PsbN could therefore be contributed to an inefficient assembly of the dimeric co-factor-containing PSII RC, but had no influence on the synthesis of PSII proteins and the assembly of the

intermediate precomplexes pre-D1, pre-D2, pre-CP43, and pre-CP47 under low light intensities (Figure 18-21). This was reflected by a transient accumulation of all PSII precomplexes while the assembly of the higher PSII complexes was retarded.

On the stationary protein levels less higher order PSII complexes were found in the mutants compared to the wild type, and only the PSII core antenna precomplexes stably accumulated. Furthermore streaking signals of the small PSII subunits PsbI and PsbH could be found in the low molecular weight range. The instability of the pre-D1 and pre-D2 complexes in the mutant might be caused by impaired folding, membrane integration, association of small subunits, cofactors or lipids. Although the formation of the PSII RC appeared to be the first step affected due to the lack of PsbN, it could not be excluded that PsbN guides the whole PSII formation process as well as taking part in the PSII repair cycle after photoinhibition.

4.2.3 PsbN shares functional characteristics with HCF136

The functional characterization of PsbN revealed several similarities with the nuclear encoded protein HCF136, which was shown to be required for PSII formation (Meurer et al., 1998b). Both proteins are conserved from cyanobacteria to higher plants, mainly reside in the stromal lamellae and are required for the formation of the dimeric PSII RC. In comparison to most known PSII assembly/repair factors, the loss of PsbN as well as of HCF136 showed more dramatic effects on plant growth and photosynthetic performance, suggesting their role in the early stages of PSII assembly.

Interestingly also the thylakoid ultrastructure with more pronounced stacked grana regions was similar in both mutants (Meurer et al., 1998b; Figure 23). Both mutants assembled pre-D1 and pre-D2 at wild-type comparable rates but were impaired in the efficient formation of the RC (Plücker et al., 2002; Figure 20/21). Also the PSI-M formation which appeared to be enhanced in $\Delta psbN$ mutants compared to the wild type (Figure 21), showed similar characteristics in the analysis of thylakoid membrane complex assembly in *hcf136* mutants (Plücker et al., 2002). Therefore it can be expected that the observed higher assembly efficiency of PSI in both mutants, might be a secondary effect caused by the impaired PSII RC formation.

Of course it could not be excluded that HCF136 and PsbN directly influence PSI assembly, but at least it could clearly be shown that this must be of less importance for the PSI

biogenesis and functionality. Neither PSI precomplexes stably accumulate nor the formation of the PSI-M is hindered in the mutants. Furthermore in contrast to the PSII proteins, the PSI core subunit PsaA is stable upon light stress in the $\Delta psbN$ mutants (Figure 24). The assumption that both PsbN and HCF136 mainly function in the early PSII biogenesis is supported by their similar expression pattern. While the expression of most thylakoid membrane proteins was highly light dependent, PsbN and HCF136 were already found in dark-grown seedlings (Meurer et al., 1998b; Figure 14). The early expression of PsbN could also explain why older plants transferred from in vitro culture to soil were able to survive under low and even moderate light, while mutant seedlings could only develop under low light in state I favored conditions (Figure 17).

The membrane integral protein PsbN and the membrane associated HCF136 protein might therefore function in parallel to assemble the PSII RC. As the highly conserved part of PsbN was found to be exposed to the stromal face of the thylakoids (Figure 13) and as HCF136 was shown to be a luminal membrane associated protein, a direct interaction of both is unlikely. Furthermore the PsbN protein showed to reach maximum levels between 8 and 24 h of illumination, while HCF136 protein levels were further increasing, suggesting that they do not form a complex together (Figure 14). Therefore it can be expected that the formation of the PSII RC is guided on both sides of the stroma lamellae without direct physical contact of PsbN and HCF136.

If PsbN is associated to any protein or complex stays an open question, as PsbN was always found in the unassembled state even under very mild detergent concentrations or when using cross-linkers. This might imply a transient and/or very loose association of PsbN to its interaction partners. In contrast, all other PSII assembly factors investigated were found to form stable complexes, indicating a tight interaction with PSII subunits and/or other chaperones (Nickelsen and Rengstl, 2013). Because of the small size of PsbN and the only 17 amino acid long conserved C-terminal part, which is most probably the transacting domain it is no wonder that associated proteins could get easily lost during preparation. Furthermore the small amount of crosslinkable amino acid residues in the functional part of PsbN could get inaccessible upon protein binding.

Apparently, it could not be solved how exactly PsbN acts as a low molecular weight chaperone in the efficient assembly of the PSII RC. It could either interact with its own or in transient association with other factors and/or PSII subunits. The formation of the complexes

and the surrounding lipid composition within the thylakoids was shown to be very flexible upon different light and stress conditions, to enable proper photosynthesis and repair mechanisms (Kirchhoff, 2014). Therefore the changed ultrastructure and the impaired PSII RC formation observed in $\Delta psbN$ mutants, might also be caused by a direct influence of PsbN on the thylakoid membrane properties and/or lipid composition.

4.2.4 The $\Delta psbN$ mutants are extremely light sensitive

PsbN was found to mainly reside in the stroma lamellae, the place where the PSII RC formation and the PSII repair cycle occurs. It can be assumed that both the RC formation and the PSII repair cycle share identical steps in which PsbN is involved. This became obvious because the inhibition of the chloroplast protein synthesis showed no additional effect on the light sensitivity of PSII in the mutants. Furthermore the $\Delta psbN$ mutants failed to recover from photoinhibition and D1 was very prone to degradation upon treatment with moderate light.

To avoid secondary effects caused by excess light, the mutants were cultivated under low light intensities of $10 \mu\text{mol photons m}^{-2} \text{s}^{-1}$. Due to that it was possible to define the primary function of PsbN, which appeared to be involved in the assembly and function of PSII while the other thylakoid membrane complexes were unaffected. This could be proven by measurements of chlorophyll fluorescence induction, PSI yield, fluorescence emission at 77K, assembly studies, and by immunological analysis of various thylakoid membrane proteins.

Recently it was concluded, that the lack of PsbN affects PSII as well as PSI accumulation (Krech et al., 2013). This preliminary analysis showed a about 5 times lower Fv/Fm, a lower chlorophyll content and a several fold larger shift of the PSI peak at 77K to shorter wavelength and stronger reduced levels of PSII and PSI proteins compared to this analysis. These results can be explained by the 5 times higher growth light intensities used in this analysis (Krech et al., 2013). An identical growth and fluorescence phenotype could be observed in a preliminary comparison of the $\Delta psbN$ line with the $\Delta psbN-F$ and $\Delta psbN-R$ lines (Figure 18/Appendix).

For several reasons it is likely that the PSI defect observed in $\Delta psbN$ mutants grown under higher light intensities is mainly of secondary nature. The influence on PSI was compared with a *psbD* knockdown mutant, which is much milder affected in PSII accumulation than the $\Delta psbN$ mutants (Krech et al., 2013). Several studies showed that

already moderate light intensities are harmful to PSI when PSII assembly is affected (Meurer et al., 1998b; Plücker et al., 2002; Swiatek et al., 2003). Furthermore the treatment with inhibitory light for six hours affected PSII but not PSI accumulation in the $\Delta psbN$ mutants (Figure 24). Moreover the accumulation of unassociated PSI antenna subcomplexes found in the $\Delta psbN$ mutants was most likely caused for secondary reasons. This was revealed by comparison with $\Delta psbI$, which shows a milder PSII defect compared to the $psbN$ knockouts.

But, as already mentioned, a minor role of PsbN in the PSI assembly cannot be excluded completely. This could also be taken into consideration for *hcf136* mutants, which showed a strong PSI deficiency when grown at 50 - 70 $\mu\text{mol photons m}^{-2} \text{s}^{-1}$ (Plücker et al., 2002). The localization of PsbN and HCF136 in the stroma lamellae and the effects seen on the thylakoid ultrastructure could of course directly or indirectly influence PSI formation. Although it is hard to draw a line between direct and indirect effects on the two photosystems, it was finally proven that PsbN is an essential factor for an efficient PSII RC formation already in early stages of thylakoid membrane formation.

4.2.5 Outlook of the PsbN project

Further studies which are already in progress, will address possible interactions of PsbN with other proteins and/ or specific classes of lipids. The complemented $\Delta psbN$ lines, which express a functional chimeric PsbN-GFP fusion will be best suitable for this aim. For successful immunoprecipitation and/or crosslinking experiments, the short C-terminal functional domain of PsbN should not be targeted by the antibodies and/or crosslinkers. This will make the capture of a possible interaction partner more likely. Furthermore, recombinant PsbN can be used for pull down, overlay assays and lipid binding assays. The *PsbN* gene was cloned into prey and bait vectors for split ubiquitin analyses, which are already in progress in the cooperation with Prof. Danja Schünemann (Ruhr-University Bochum).

4.2.6 Establishment of a semi-sterile culture system

Due to the extreme light sensitivity of the $\Delta psbN-F$ and $\Delta psbN-R$ mutants, their propagation on soil turned out to be difficult and time consuming. The same was reported for the $\Delta psbN$ mutants, which took 9 month to flower (Krech et al., 2013). To overcome this problem a new technique was developed, which allowed a semi-sterile culture on sucrose supplemented medium. This allowed a rapid growth and flower development and enabled several crossing experiments with sufficient quantity of viable seeds (Figure 16).

A similar culture technique was developed for the sterile co-cultivation of potato plantlets and mycorrhiza without addition of a carbon source (Voets et al., 2005). The application of sucrose in a semi-sterile manner might enable also many other photosynthetic vascular plant mutants to develop flowers and to set seeds. Additionally, this cultivation technique allows to generate more biomass, with a greater age gradient between and within leaves from a photosynthetic mutant plant. It also enables the measurements of photosynthetic parameters, removal of leaf probes, and the application of different substrates to the culture medium. All these actions can be performed with plants grown on a carbon source without opening or exchanging the culture vessel. Further improvements could therefore help researchers to use this technique for a wide range of plants and purposes by having less effort and tissue culture work.

Summary

The biogenesis of photosynthetic complexes in plants depends on the gene expression in two genetic compartments, the nucleus and the plastid. To maintain photosynthesis in the plastid, nuclear encoded proteins have to be imported into the plastid where they act in transcriptional and posttranscriptional processes or are directly involved in complex assembly or photosynthesis.

Due to changes in the organization and the divergence of sequences in the untranslated regions of the plastid genome, especially the RNA metabolism turned out to be a fast evolving process. HCF145 is a nuclear encoded factor which was proven to specifically affect the stability of the tricistronic *psaA-psaB-rps14* transcripts. HCF145 most probably evolved in green algae and consists of two duplicated domains of bacterial origin. Two homologous domains of the polyketide cyclase family, a ubiquitous motif found in all superkingdoms, comprising 37 annotated *Arabidopsis* proteins of unknown function.

Two further unknown tandem repeated motifs at the C-terminus confer RNA binding capability to HCF145. These motifs were therefore designated as transcript binding motif repeat (TMR). TMR motifs are mainly found as multiple repeats and seem to be specific for photosynthetic organisms. In higher plants HCF145 represents the only TMR protein. The analysis of *hcf145* mutants in *Arabidopsis thaliana* and *Physcomitrella patens* and knock downs in *Nicotiana tabacum* indicate that HCF145 has been recruited to protect the *psaA-psaB-rps14* mRNA by binding to the 5' UTR. The Photosystem I biogenesis highly depends on HCF145, which is regulated in a developmental, light, temperature, stress, and photosynthesis dependent manner.

In contrast to the fast evolving RNA metabolism the assembly and the function of photosynthetic complexes remained highly conserved from cyanobacteria to higher plants. Mainly proteins of high demand like the core subunits of the photosynthetic complexes and ribosomal proteins are still encoded in the plastid, while many genes encoding for accessory subunits and assembly factors were transferred to the nucleus.

Plastid transformation in tobacco helped to study the function of most genes that remained in the chloroplast of higher plants. The chloroplast-encoded low molecular weight protein PsbN was misleadingly annotated as a photosystem II (PSII) subunit, although its function, localization and topology remained elusive. The gene which is encoded on the

opposite strand of the *psbB* gene cluster was deleted in *Nicotiana tabacum* by insertion of a spectinomycin resistance cassette into *PsbN* in both directions. The resulting homoplasmic mutants $\Delta psbN-F$ and $\Delta psbN-R$ showed essentially the same PSII deficiencies as revealed by spectroscopic and biochemical analysis.

Immunological analyses with a peptide specific antisera against the C-terminal part of PsbN, confirmed a transmembrane helix in the N terminus of PsbN and the localization of the highly conserved C-terminus in the stroma. PsbN was mainly found in the stroma lamellae not associated to any complex, approving that PsbN represent not a constituent subunit of PSII. In vivo labeling experiments combined with native PAGE analyses helped to follow the synthesis and assembly of photosynthetic complexes in *statu nascendi*, uncovering a specific defect in the formation of the PSII RC in the both $\Delta psbN$ mutants. PsbN that accumulated to high amounts already in dark grown seedlings, showed many phenotypic similarities to the PSII assembly factor HCF136, which is also important for efficient PSII RC assembly.

To consider concerns about the disruption of the *psbB* gene cluster induced by the insertion of the spectinomycin resistance marker, the mutant plants were complemented by allotopic expression of the *PsbN* gene fused to the sequence of a chloroplast transit peptide in the nuclear genome. This resulted in a full complementation of the $\Delta psbN-R$ and a partial complementation of the $\Delta psbN-F$ line. A preliminary comparison of the $\Delta psbN$ mutants with the translational incompetent $\Delta psbN$ lines described by Krech et al. (2013), showed a similar phenotype. For backcrossing experiments of the severely light sensitive and photosynthetic impaired $\Delta psbN$ mutants, a semi-sterile culture technique was developed. This allowed the supply of sucrose under sterile conditions and a rapid plant and flower development outside the culture vessel.

Zusammenfassung

Die Entstehung von Photosynthese-Komplexen in Pflanzen hängt von zwei genetischen Kompartimenten, dem Zellkern und den Plastiden ab. Um Photosynthese im Plastiden zu betreiben, müssen im Zellkern kodierte Proteine importiert werden, welche an der Transkription, an posttranskriptionellen Prozessen, der Komplexassemblierung oder direkt an der Photosynthese beteiligt sind. Aufgrund der variablen Genanordnung und den divergenten nicht kodierenden Sequenzbereichen (UTR) in pflanzlichen Plastidengenomen, erweist sich besonders der RNA Metabolismus als ein schnell evolvierender Prozess. HCF145 ist ein im Kern kodierter Stabilitätsfaktor für die tricistronischen *psaA-psaB-rps14* Transkripte. HCF145 besteht aus zwei duplizierten Domänen bakteriellen Ursprungs und entstand höchstwahrscheinlich in Grünalgen. Zwei homologe Domänen gehören zu der Polyketide Zyklase Familie, dessen ubiquitäres Motiv in allen Artenreichen einschließlich 37 annotierten *Arabidopsis* Proteinen mit unbekannter Funktion zu finden ist.

Zwei weitere unbekannte aufeinanderfolgend wiederholte Motive am C-terminus verleihen HCF145 RNA-Bindekapazität. Daher wurden diese Motive als „transcript binding motif repeat“ (TMR) bezeichnet. Die TMR Motive werden meist als multiple Wiederholungen gefunden und scheinen spezifisch für photosynthetische Organismen zu sein. In höheren Pflanzen repräsentiert HCF145 das einzige TMR Protein. Die Analysen der *hcf145* Mutanten in *Arabidopsis thaliana* und *Physcomitrella patens* sowie die Analyse von RNA-Interferenz Linien in *Nicotiana tabacum* zeigen, dass HCF145 entstanden ist, um die *psaA-psaB-rps14* mRNA zu schützen, indem sie deren 5'-UTR bindet. Die Photosystem I Biogenese hängt stark von HCF145 ab, dessen Expression Entwicklungs-, Licht-, Temperatur-, Stress- und Photosyntheseabhängig reguliert wird.

Im Gegensatz zu dem schnell evolvierenden RNA Metabolismus blieben die Assemblierung und die Funktion der Photosynthese-Komplexe von Cyanobakterien bis zu den höheren Pflanzen stark konserviert. Hauptsächlich Proteine von hohem Bedarf wie die Kernuntereinheiten der Photosynthese-Komplexe und Ribosomale Proteine sind noch im Plastiden kodiert, während die Gene von vielen angrenzenden Untereinheiten und Assemblierungsfaktoren in den Kern transferiert wurden.

Die Plastiden Transformation in Tabak ermöglichte es die Funktion der meisten im Chloroplasten verbliebenen Gene in höheren Pflanzen zu studieren. Das im Chloroplast

kodierte Protein PsbN, mit geringem Molekulargewicht, wurde fälschlicherweise als kleine Untereinheit von PSII annotiert, obwohl seine Funktion, Lokalisation und Topologie unbekannt blieben. *PsbN* befindet sich auf dem gegenüber liegenden Strang im *psbB* Genecluster und wurde in *Nicotiana tabacum* ausgeschaltet. Dafür wurde eine Spectinomycin-Resistenz-Kassette in das *PsbN* Gen in beiden Orientierungen inseriert. Die daraus resultierenden homoplastomischen Mutanten $\Delta psbN-F$ und $\Delta psbN-R$ zeigten in den spektrometrischen und biochemischen Analysen einen vergleichbaren PSII Defekt.

Immunologische Analysen mit einem peptidspezifischen Antikörper gegen den C-terminalen Teil von PsbN bestätigte eine Transmembranhelix im N-Terminus und lokalisierte den C-terminalen Teil von PsbN im Stroma. PsbN wurde hauptsächlich in der Stromalamelle gefunden und war nicht an einem Komplex assoziiert. Dies zeigte, dass PsbN keine wesentliche Untereinheit von PSII ist. Radioaktive Markierungsexperimente in Kombination mit nativen Gelanalysen ermöglichte es die Synthese und Assemblierung von Photosyntesekomplexen während ihrer Entstehung zu verfolgen und zeigte bei beiden $\Delta psbN$ Mutanten einen Defekt in der Formation des PSII RC. PsbN welches schon in hohen Mengen in etiolierten Keimlingen angereichert war, zeigte viele phänotypische Ähnlichkeiten zu dem PSII Assemblierungsfaktor HCF136, welcher auch wichtig für eine effiziente Assemblierung des PSII RC ist.

Um Bedenken wegen der Unterbrechung des *psbB* Geneclusters durch die Insertion der Spectinomycin-Resistenzkassette zu berücksichtigen, wurden die Mutanten komplementiert. Dazu wurde das *PsbN* Gene mit der Sequenz von einem Transitpeptid für den Chloroplastenimport fusioniert und allotopisch im Zellkern exprimiert. Damit konnte eine vollständige Komplementierung von $\Delta psbN-R$ und eine teilweise Komplementierung von $\Delta psbN-F$ erzielt werden. Ein vorläufiger Vergleich der $\Delta psbN$ Mutanten mit der Translationsinkompetenten $\Delta psbN$ Line, welche von Krech et al. (2013) beschrieben wurde, zeigte einen vergleichbaren Phänotyp. Für Rückkreuzungsexperimente der extrem lichtsensitiven und photosynthetisch defekten $\Delta psbN$ Mutanten wurde eine semi-sterile Kultivierungstechnik entwickelt. Diese ermöglichte die Verabreichung von Zucker unter sterilen Bedingungen und eine schnelle Wachstums- und Blütenentwicklung der Pflanzen außerhalb der Kulturgefäße.

Abbreviations

μg	microgramm
μl	microliter
Å	Ångstroem (10^{-10} m)
aadA	aminoglycoside 3'-adenylyl-transferase
ATP	adenosine triphosphate
BN-PAGE	blue native polyacrylamide gel electrophoresis
bp	base pairs
CBB	Coomassie Brilliant Blue
cDNA	complementary DNA
Cyt <i>b₆f</i>	cytochrome <i>b₆f</i> complex
DAPI	4',6-Diamidin-2-phenylindol,
ddH ₂ O	double distilled water
DNA	deoxyribonucleic acid
EDTA	ethylenediaminetetraacetic acid
EST	expressed sequence tag
FNR	ferredoxin (NADP ⁺) reductase
F _o	minimal fluorescence
FR	far red
F _v /F _m	maximum quantum yield of PSII
<i>g</i>	gravitational acceleration
GFP	green fluorescent protein
GL	growth light

h	hour
<i>hcf</i>	high chlorophyll fluorescence
HEPES	N-(2-hydroxyethyl)-piperazine-N'-(2-ethanesulfonic-acid)
Hz	Hertz
kb	kilobases
LHC	light harvesting complex
LMW	low molecular weight
MB	methylene blue
mol	amount of substance (SI base unit)
mRNA	messenger ribonucleic acid
NADP ⁺	nicotinic adenine dinucleotide phosphate
NEP	nuclear encoded RNA-polymerase
nm	nanometer
NPQ	non-photochemical chlorophyll <i>a</i> fluorescence quenching
OEC	oxygen evolving complex
OPR	octotricopeptide
ORF	open reading frame
Φ_{PSI}	quantum yield of PSI
$\Phi_{\text{PSI ND}}$	quantum yield of nonphotochemical energy dissipation due to donor side limitation
Φ_{PSII}	quantum yield of PSII
P680	PSII primary electron donor (chlorophyll dimer)
P700	PSI primary electron donor (chlorophyll dimer)
PC	plastocyan

pD1	precursor D1
PEP	plastid encoded RNA-polymerase
Pet	cytochrome complex subunit
PFD	photon flux density
PPR	pentatricopeptide repeat
<i>psa</i>	gene coding for a photosystem I subunit
<i>psb</i>	gene coding for a photosystem II subunit
PSI	photosystem I
PSII	photosystem II
PSII-D	photosystem II dimer
PSII-M	photosystem II monomer
PSII-RC	photosystem II reaction center
PSII-SC	photosystem II supercomplexes
PVDF	polyvinylidenfluorid
Q	plastoquinone pool
RL	red light
RMOP	plant regeneration medium
RNA	ribonucleic acid
ROS	reactive oxygen species
rRNA	ribosomal ribonucleic acid
RT	room temperature
SC	supercomplexes
SDS	sodium dodecyl sulfate

SRPBCC	(START/RHO alpha C/PITP/Bet v1/CoxG/CalC) superfamily
T-DNA	transfer deoxyribonucleic acid
TMR	transcript binding motif repeat
TPR	tetratricopeptide repeat
Tricine	N-(Tri-(hydroxymethyl)-methyl)glycine
Tris	tris-(hydroxymethyl)-aminomethane
Tween	polyoxyethylenesorbitan monolaurate
UTR	untranslated region
w/v	weight per volume
WT	wild type
β -DM	<i>n</i> -doceyl- β -d-maltoside

Literature

- Adam, Z., Charuvi, D., Tsabari, O., Knopf, R., and Reich, Z.** (2011). Biogenesis of thylakoid networks in angiosperms: knowns and unknowns. *Plant molecular biology* **76**, 221-234.
- Allen, J.F.** (2003). Cyclic, pseudocyclic and noncyclic photophosphorylation: new links in the chain. *Trends in Plant Science* **8**, 15-19.
- Amann, K., Lezhneva, L., Wanner, G., Herrmann, R.G., and Meurer, J.** (2004). ACCUMULATION OF PHOTOSYSTEM ONE1, a member of a novel gene family, is required for accumulation of [4Fe-4S] cluster-containing chloroplast complexes and antenna proteins. *The Plant cell* **16**, 3084-3097.
- Armbruster, U., Zühlke, J., Rengstl, B., Kreller, R., Makarenko, E., Rühle, T., Schunemann, D., Jahns, P., Weisshaar, B., Nickelsen, J., and Leister, D.** (2010). The Arabidopsis thylakoid protein PAM68 is required for efficient D1 biogenesis and photosystem II assembly. *The Plant cell* **22**, 3439-3460.
- Baginsky, S., and Gruissem, W.** (2002). Endonucleolytic activation directs dark-induced chloroplast mRNA degradation. *Nucleic acids research* **30**, 4527-4533.
- Baginsky, S., Grossmann, J., and Gruissem, W.** (2007). Proteome analysis of chloroplast mRNA processing and degradation. *Journal of proteome research* **6**, 809-820.
- Barkan, A.** (1988). Proteins encoded by a complex chloroplast transcription unit are each translated from both monocistronic and polycistronic mRNAs. *The EMBO journal* **7**, 2637-2644.
- Barkan, A.** (1993). Nuclear Mutants of Maize with Defects in Chloroplast Polysome Assembly Have Altered Chloroplast RNA Metabolism. *The Plant cell* **5**, 389-402.
- Barkan, A.** (2011). Expression of Plastid Genes: Organelle-Specific Elaborations on a Prokaryotic Scaffold. *Plant physiology* **155**, 1520-1532.
- Barkan, A., Walker, M., Nolasco, M., and Johnson, D.** (1994). A nuclear mutation in maize blocks the processing and translation of several chloroplast mRNAs and provides evidence for the differential translation of alternative mRNA forms. *The EMBO journal* **13**, 3170-3181.
- Barkan, A., Klipcan, L., Ostersetzer, O., Kawamura, T., Asakura, Y., and Watkins, K.P.** (2007). The CRM domain: an RNA binding module derived from an ancient ribosome-associated protein. *RNA (New York, N.Y.)* **13**, 55-64.
- Barkan, A., Rojas, M., Fujii, S., Yap, A., Chong, Y.S., Bond, C.S., and Small, I.** (2012). A combinatorial amino acid code for RNA recognition by pentatricopeptide repeat proteins. *PLoS genetics* **8**, e1002910.
- Bate, N.J., Rothstein, S.J., and Thompson, J.E.** (1991). Expression of Nuclear and Chloroplast Photosynthesis-Specific Genes During Leaf Senescence. *Journal of Experimental Botany* **42**, 801-811.
- Bock, R.** (2007). Structure, function, and inheritance of plastid genomes. In *Cell and Molecular Biology of Plastids*, R. Bock, ed (Springer Berlin Heidelberg), pp. 29-63.
- Bruce, B.D.** (2000). Chloroplast transit peptides: structure, function and evolution. *Trends in cell biology* **10**, 440-447.
- Cai, W., Ma, J., Chi, W., Zou, M., Guo, J., Lu, C., and Zhang, L.** (2010). Cooperation of LPA3 and LPA2 is essential for photosystem II assembly in Arabidopsis. *Plant physiology* **154**, 109-120.
- Calderon, R.H., Garcia-Cerdan, J.G., Malnoe, A., Cook, R., Russell, J.J., Gaw, C., Dent, R.M., de Vitry, C., and Niyogi, K.K.** (2013). A conserved rubredoxin is necessary

- for photosystem II accumulation in diverse oxygenic photoautotrophs. *The Journal of biological chemistry* **288**, 26688-26696.
- Chase, C.D.** (2007). Cytoplasmic male sterility: a window to the world of plant mitochondrial-nuclear interactions. *Trends Genet* **23**, 81-90.
- Chi, W., Sun, X., and Zhang, L.** (2012). The roles of chloroplast proteases in the biogenesis and maintenance of photosystem II. *Biochimica et biophysica acta* **1817**, 239-246.
- Cho, W.K., Geimer, S., and Meurer, J.** (2009). Cluster Analysis and Comparison of Various Chloroplast Transcriptomes and Genes in *Arabidopsis thaliana*. *DNA Research* **16**, 31-44.
- Clark, B.J.** (2012). The mammalian START domain protein family in lipid transport in health and disease. *Journal of Endocrinology* **212**, 257-275.
- Clough, S.J., and Bent, A.F.** (1998). Floral dip: a simplified method for *Agrobacterium*-mediated transformation of *Arabidopsis thaliana*. *Plant J* **16**, 735-743.
- Corpet, F.** (1988). Multiple sequence alignment with hierarchical clustering. *Nucleic acids research* **16**, 10881-10890.
- Demarsy, E., Buhr, F., Lambert, E., and Lerbs-Mache, S.** (2012). Characterization of the plastid-specific germination and seedling establishment transcriptional programme. *J Exp Bot* **63**, 925-939.
- Deng, X.W., and Gruissem, W.** (1987). Control of plastid gene expression during development: the limited role of transcriptional regulation. *Cell* **49**, 379-387.
- Dobakova, M., Sobotka, R., Tichy, M., and Komenda, J.** (2009). Psb28 protein is involved in the biogenesis of the photosystem II inner antenna CP47 (PsbB) in the cyanobacterium *Synechocystis* sp. PCC 6803. *Plant physiology* **149**, 1076-1086.
- Dortay, H., Gruhn, N., Pfeifer, A., Schwerdtner, M., Schmülling, T., and Heyl, A.** (2008). Toward an Interaction Map of the Two-Component Signaling Pathway of *Arabidopsis thaliana*. *Journal of proteome research* **7**, 3649-3660.
- Drager, R.G., Higgs, D.C., Kindle, K.L., and Stern, D.B.** (1999). 5' to 3' exoribonucleolytic activity is a normal component of chloroplast mRNA decay pathways. *Plant J* **19**, 521-531.
- Emanuel, C., Weihe, A., Graner, A., Hess, W.R., and Borner, T.** (2004). Chloroplast development affects expression of phage-type RNA polymerases in barley leaves. *Plant J* **38**, 460-472.
- Felder, S., Meierhoff, K., Sane, A.P., Meurer, J., Driemel, C., Plücken, H., Klaff, P., Stein, B., Bechtold, N., and Westhoff, P.** (2001). The nucleus-encoded HCF107 gene of *Arabidopsis* provides a link between intercistronic RNA processing and the accumulation of translation-competent psbH transcripts in chloroplasts. *The Plant cell* **13**, 2127-2141.
- Feldmann, K.A.** (1991). T-DNA insertion mutagenesis in *Arabidopsis*: mutational spectrum. *The Plant Journal* **1**, 71-82.
- Fisk, D.G., Walker, M.B., and Barkan, A.** (1999). Molecular cloning of the maize gene *crp1* reveals similarity between regulators of mitochondrial and chloroplast gene expression. *The EMBO journal* **18**, 2621-2630.
- Freyer, R., Kiefer-Meyer, M.-C., and Kössel, H.** (1997). Occurrence of plastid RNA editing in all major lineages of land plants. *Proceedings of the National Academy of Sciences* **94**, 6285-6290.
- Fristedt, R., Willig, A., Granath, P., Crevecoeur, M., Rochaix, J.D., and Vener, A.V.** (2009). Phosphorylation of photosystem II controls functional macroscopic folding of photosynthetic membranes in *Arabidopsis*. *The Plant cell* **21**, 3950-3964.
- Fu, A., He, Z., Cho, H.S., Lima, A., Buchanan, B.B., and Luan, S.** (2007). A chloroplast cyclophilin functions in the assembly and maintenance of photosystem II in

- Arabidopsis thaliana*. Proceedings of the National Academy of Sciences of the United States of America **104**, 15947-15952.
- Garcia-Cerdan, J.G., Kovacs, L., Toth, T., Kereiche, S., Aseeva, E., Boekema, E.J., Mamedov, F., Funk, C., and Schröder, W.P.** (2011). The PsbW protein stabilizes the supramolecular organization of photosystem II in higher plants. *Plant J* **65**, 368-381.
- Groth-Malonek, M., Wahrmund, U., Polsakiewicz, M., and Knoop, V.** (2007). Evolution of a pseudogene: exclusive survival of a functional mitochondrial *nad7* gene supports Haplomitrium as the earliest liverwort lineage and proposes a secondary loss of RNA editing in Marchantiidae. *Molecular biology and evolution* **24**, 1068-1074.
- Hager, M., Biehler, K., Illerhaus, J., Ruf, S., and Bock, R.** (1999). Targeted inactivation of the smallest plastid genome-encoded open reading frame reveals a novel and essential subunit of the cytochrome b(6)f complex. *The EMBO journal* **18**, 5834-5842.
- Hammani, K., Cook, W.B., and Barkan, A.** (2012). RNA binding and RNA remodeling activities of the half- α -tetratricopeptide (HAT) protein HCF107 underlie its effects on gene expression. Proceedings of the National Academy of Sciences of the United States of America **109**, 5651-5656.
- Hausuhl, K., Andersson, B., and Adamska, I.** (2001). A chloroplast DegP2 protease performs the primary cleavage of the photodamaged D1 protein in plant photosystem II. *The EMBO journal* **20**, 713-722.
- Heazlewood, J.L., Tonti-Filippini, J.S., Gout, A.M., Day, D.A., Whelan, J., and Millar, A.H.** (2004). Experimental Analysis of the Arabidopsis Mitochondrial Proteome Highlights Signaling and Regulatory Components, Provides Assessment of Targeting Prediction Programs, and Indicates Plant-Specific Mitochondrial Proteins. *The Plant Cell Online* **16**, 241-256.
- Heckman, D.S., Geiser, D.M., Eidell, B.R., Stauffer, R.L., Kardos, N.L., and Hedges, S.B.** (2001). Molecular Evidence for the Early Colonization of Land by Fungi and Plants. *Science* **293**, 1129-1133.
- Hedtke, B., Börner, T., and Weihe, A.** (1997). Mitochondrial and chloroplast phage-type RNA polymerases in Arabidopsis. *Science* **277**, 809-811.
- Hedtke, B., Börner, T., and Weihe, A.** (2000). One RNA polymerase serving two genomes. *EMBO Rep* **1**, 435-440.
- Hein, P., Stockel, J., Bennewitz, S., and Oelmüller, R.** (2009). A protein related to prokaryotic UMP kinases is involved in *psaA/B* transcript accumulation in Arabidopsis. *Plant molecular biology* **69**, 517-528.
- Hicks, A., Drager, R.G., Higgs, D.C., and Stern, D.B.** (2002). An mRNA 3' Processing Site Targets Downstream Sequences for Rapid Degradation in Chlamydomonas Chloroplasts. *Journal of Biological Chemistry* **277**, 3325-3333.
- Holland, H.D.** (2002). Volcanic gases, black smokers, and the great oxidation event. *Geochimica et Cosmochimica Acta* **66**, 3811-3826.
- Hsu, B.D., Lee, J.Y., and Pan, R.L.** (1986). The two binding sites for DCMU in Photosystem II. *Biochemical and biophysical research communications* **141**, 682-688.
- Ikeuchi, M., Koike, H., and Inoue, Y.** (1989). N-terminal sequencing of low-molecular-mass components in cyanobacterial photosystem II core complex. Two components correspond to unidentified open reading frames of plant chloroplast DNA. *FEBS letters* **253**, 178-182.
- Joliot, P., and Joliot, A.** (2006). Cyclic electron flow in C3 plants. *Biochimica et Biophysica Acta (BBA) - Bioenergetics* **1757**, 362-368.
- Karcher, D., and Bock, R.** (1998). Site-selective inhibition of plastid RNA editing by heat shock and antibiotics: a role for plastid translation in RNA editing. *Nucleic acids research* **26**, 1185-1190.

- Karnauchov, I., Herrmann, R.G., and Klösgen, R.B.** (1997). Transmembrane topology of the Rieske Fe/S protein of the cytochrome b6/f complex from spinach chloroplasts. *FEBS letters* **408**, 206-210.
- Karol, K.G., McCourt, R.M., Cimino, M.T., and Delwiche, C.F.** (2001). The closest living relatives of land plants. *Science* **294**, 2351-2353.
- Kashino, Y., Koike, H., Yoshio, M., Egashira, H., Ikeuchi, M., Pakrasi, H.B., and Satoh, K.** (2002). Low-molecular-mass polypeptide components of a photosystem II preparation from the thermophilic cyanobacterium *Thermosynechococcus vulcanus*. *Plant & cell physiology* **43**, 1366-1373.
- Keren, N., Ohkawa, H., Welsh, E.A., Liberton, M., and Pakrasi, H.B.** (2005). Psb29, a conserved 22-kD protein, functions in the biogenesis of Photosystem II complexes in *Synechocystis* and *Arabidopsis*. *The Plant cell* **17**, 2768-2781.
- Kirchhoff, H.** (2014). Structural changes of the thylakoid membrane network induced by high light stress in plant chloroplasts. *Philosophical transactions of the Royal Society of London. Series B, Biological sciences* **369**, 20130225.
- Klein, R.R., and Mullet, J.E.** (1987). Control of gene expression during higher plant chloroplast biogenesis. Protein synthesis and transcript levels of psbA, psaA-psaB, and rbcL in dark-grown and illuminated barley seedlings. *The Journal of biological chemistry* **262**, 4341-4348.
- Klughammer, C., and Schreiber, U.** (1994). An improved method, using saturating light pulses, for the determination of photosystem I quantum yield via P700 absorbance changes at 830 nm. *Planta* **192**, 261-268.
- Kofer, W., Koop, H.U., Wanner, G., and Steinmüller, K.** (1998). Mutagenesis of the genes encoding subunits A, C, H, I, J and K of the plastid NAD(P)H-plastoquinone-oxidoreductase in tobacco by polyethylene glycol-mediated plastome transformation. *Molecular & general genetics : MGG* **258**, 166-173.
- Kohchi, T., Yoshida, T., Komano, T., and Ohyama, K.** (1988). Divergent mRNA transcription in the chloroplast psbB operon. *The EMBO journal* **7**, 885-891.
- Komenda, J., Sobotka, R., and Nixon, P.J.** (2012). Assembling and maintaining the Photosystem II complex in chloroplasts and cyanobacteria. *Current opinion in plant biology* **15**, 245-251.
- Koncz, C., Martini, N., Szabados, L., Hroudá, M., Bachmair, A., and Schell, J.** (1994). Specialized vectors for gene tagging and expression studies. In *Plant Molecular Biology Manual*, S. Gelvin and R. Schilperoort, eds (Springer Netherlands), pp. 53-74.
- Krebs, H.A.** (1970). The history of the tricarboxylic acid cycle. *Perspectives in biology and medicine* **14**, 154-170.
- Krech, K., Fu, H.Y., Thiele, W., Ruf, S., Schöttler, M.A., and Bock, R.** (2013). Reverse genetics in complex multigene operons by co-transformation of the plastid genome and its application to the open reading frame previously designated psbN. *Plant J* **75**, 1062-1074.
- Kroeger, T.S., Watkins, K.P., Friso, G., van Wijk, K.J., and Barkan, A.** (2009). A plant-specific RNA-binding domain revealed through analysis of chloroplast group II intron splicing. *Proceedings of the National Academy of Sciences of the United States of America* **106**, 4537-4542.
- Kupsch, C., Ruwe, H., Gusewski, S., Tillich, M., Small, I., and Schmitz-Linneweber, C.** (2012). *Arabidopsis* chloroplast RNA binding proteins CP31A and CP29A associate with large transcript pools and confer cold stress tolerance by influencing multiple chloroplast RNA processing steps. *The Plant Cell Online* **24**, 4266-4280.
- Kurepa, J., Li, Y., and Smalle, J.A.** (2013). Proteasome-dependent proteolysis has a critical role in fine-tuning the feedback inhibition of cytokinin signaling. *Plant Signaling & Behavior* **8**, e23474.

- Laemmli, U.K.** (1970). Cleavage of Structural Proteins during the Assembly of the Head of Bacteriophage T4. *Nature* **227**, 680-685.
- Laloi, C., Stachowiak, M., Pers-Kamczyc, E., Warzych, E., Murgia, I., and Apel, K.** (2007). Cross-talk between singlet oxygen- and hydrogen peroxide-dependent signaling of stress responses in *Arabidopsis thaliana*. *Proceedings of the National Academy of Sciences of the United States of America* **104**, 672-677.
- Lawrence, J.G.** (2002). Shared Strategies in Gene Organization among Prokaryotes and Eukaryotes. *Cell* **110**, 407-413.
- Letsch, M.R., and Lewis, L.A.** (2012). Chloroplast gene arrangement variation within a closely related group of green algae (Trebouxiophyceae, Chlorophyta). *Molecular Phylogenetics and Evolution* **64**, 524-532.
- Levin-Karp, A., Barenholz, U., Bareia, T., Dayagi, M., Zelcbuch, L., Antonovsky, N., Noor, E., and Milo, R.** (2013). Quantifying Translational Coupling in *E. coli* Synthetic Operons Using RBS Modulation and Fluorescent Reporters. *ACS Synthetic Biology* **2**, 327-336.
- Lezhneva, L., and Meurer, J.** (2004). The nuclear factor HCF145 affects chloroplast *psaA-psaB-rps14* transcript abundance in *Arabidopsis thaliana*. *Plant J* **38**, 740 - 753.
- Li de la Sierra-Gallay, I., Zig, L., Jamalli, A., and Putzer, H.** (2008). Structural insights into the dual activity of RNase J. *Nature structural & molecular biology* **15**, 206-212.
- Liere, K., and Börner, T.** (2007). Transcription and transcriptional regulation in plastids. In *Cell and Molecular Biology of Plastids*, R. Bock, ed (Springer Berlin Heidelberg), pp. 121-174.
- Lima, A., Lima, S., Wong, J.H., Phillips, R.S., Buchanan, B.B., and Luan, S.** (2006). A redox-active FKBP-type immunophilin functions in accumulation of the photosystem II supercomplex in *Arabidopsis thaliana*. *Proceedings of the National Academy of Sciences of the United States of America* **103**, 12631-12636.
- Lu, G., Dolgner, S.J., and Hall, T.M.** (2009). Understanding and engineering RNA sequence specificity of PUF proteins. *Curr Opin Struct Biol* **19**, 110-115.
- Lurin, C., Andres, C., Aubourg, S., Bellaoui, M., Bitton, F., Bruyere, C., Caboche, M., Debast, C., Gualberto, J., Hoffmann, B., Lecharny, A., Le Ret, M., Martin-Magniette, M.L., Mireau, H., Peeters, N., Renou, J.P., Szurek, B., Taconnat, L., and Small, I.** (2004). Genome-wide analysis of *Arabidopsis* pentatricopeptide repeat proteins reveals their essential role in organelle biogenesis. *The Plant cell* **16**, 2089-2103.
- Mabbitt, P.D., Wilbanks, S.M., and Eaton-Rye, J.J.** (2014). Duplication and divergence of the Psb27 subunit of Photosystem II in the green algal lineage. *New Zealand Journal of Botany* **52**, 74-83.
- Maier, U., Bozarth, A., Funk, H., Zauner, S., Rensing, S., Schmitz-Linneweber, C., Börner, T., and Tillich, M.** (2008). Complex chloroplast RNA metabolism: just debugging the genetic programme? *BMC Biology* **6**, 36.
- Majeran, W., Friso, G., Asakura, Y., Qu, X., Huang, M., Ponnala, L., Watkins, K.P., Barkan, A., and van Wijk, K.J.** (2012). Nucleoid-Enriched Proteomes in Developing Plastids and Chloroplasts from Maize Leaves: A New Conceptual Framework for Nucleoid Functions. *Plant physiology* **158**, 156-189.
- Manavski, N., Torabi, S., Stoppel, R., Meurer, J.** (2012). Phylogenetic and ontogenetic integration of organelles into the compartmentalized genome of the eukaryotic cell. *Journal of Endocytobiosis and Cell Research* **23**, 25-31.
- Marin-Navarro, J., Manuell, A.L., Wu, J., and S, P.M.** (2007). Chloroplast translation regulation. *Photosynthesis research* **94**, 359-374.
- Martin, W., and Müller, M.** (1998). The hydrogen hypothesis for the first eukaryote. *Nature* **392**, 37-41.

- Martins, B.M., Svetlitchnaia, T., and Dobbek, H.** (2005). 2-Oxoquinoline 8-monoxygenase oxygenase component: active site modulation by Rieske-[2Fe-2S] center oxidation/reduction. *Structure* (London, England : 1993) **13**, 817-824.
- Mathy, N., Benard, L., Pellegrini, O., Daou, R., Wen, T., and Condon, C.** (2007). 5'-to-3' exoribonuclease activity in bacteria: role of RNase J1 in rRNA maturation and 5' stability of mRNA. *Cell* **129**, 681-692.
- Mattoo, A.K., Hoffman-Falk, H., Marder, J.B., and Edelman, M.** (1984). Regulation of protein metabolism: Coupling of photosynthetic electron transport to in vivo degradation of the rapidly metabolized 32-kilodalton protein of the chloroplast membranes. *Proceedings of the National Academy of Sciences of the United States of America* **81**, 1380-1384.
- Mayers, S.R., Dubbs, J.M., Vass, I., Hideg, E., Nagy, L., and Barber, J.** (1993). Further characterization of the psbH locus of *Synechocystis* sp. PCC 6803: inactivation of psbH impairs QA to QB electron transport in photosystem 2. *Biochemistry* **32**, 1454-1465.
- Meierhoff, K., Felder, S., Nakamura, T., Bechtold, N., and Schuster, G.** (2003a). HCF152, an Arabidopsis RNA binding pentatricopeptide repeat protein involved in the processing of chloroplast psbB-psbT-psbH-petB-petD RNAs. *The Plant cell* **15**, 1480-1495.
- Meierhoff, K., Felder, S., Nakamura, T., Bechtold, N., and Schuster, G.** (2003b). HCF152, an Arabidopsis RNA Binding Pentatricopeptide Repeat Protein Involved in the Processing of Chloroplast psbB-psbT-psbH-petB-petD RNAs. *The Plant Cell Online* **15**, 1480-1495.
- Meurer, J., Berger, A., and Westhoff, P.** (1996). A nuclear mutant of Arabidopsis with impaired stability on distinct transcripts of the plastid psbB, psbD/C, ndhH, and ndhC operons. *The Plant cell* **8**, 1193-1207.
- Meurer, J., Meierhoff, K., and Westhoff, P.** (1996). Isolation of high-chlorophyll-fluorescence mutants of Arabidopsis thaliana and their characterisation by spectroscopy, immunoblotting and northern hybridisation. *Planta* **198**, 385-396.
- Meurer, J., Grevelding, C., Westhoff, P., and Reiss, B.** (1998a). The PAC protein affects the maturation of specific chloroplast mRNAs in Arabidopsis thaliana. *Molecular & general genetics : MGG* **258**, 342-351.
- Meurer, J., Plücker, H., Kowallik, K.V., and Westhoff, P.** (1998b). A nuclear-encoded protein of prokaryotic origin is essential for the stability of photosystem II in Arabidopsis thaliana. *The EMBO journal* **17**, 5286-5297.
- Meurer, J., Lezhneva, L., Amann, K., Godel, M., Bezhani, S., Sherameti, I., and Oelmüller, R.** (2002). A peptide chain release factor 2 affects the stability of UGA-containing transcripts in Arabidopsis chloroplasts. *The Plant cell* **14**, 3255-3269.
- Millen, R.S., Olmstead, R.G., Adams, K.L., Palmer, J.D., Lao, N.T., Heggie, L., Kavanagh, T.A., Hibberd, J.M., Gray, J.C., Morden, C.W., Calie, P.J., Jermin, L.S., and Wolfe, K.H.** (2001). Many parallel losses of infA from chloroplast DNA during angiosperm evolution with multiple independent transfers to the nucleus. *The Plant cell* **13**, 645-658.
- Mullet, J.E., and Klein, R.R.** (1987). Transcription and RNA stability are important determinants of higher plant chloroplast RNA levels. *The EMBO journal* **6**, 1571-1579.
- Mulo, P., Sirpio, S., Suorsa, M., and Aro, E.M.** (2008). Auxiliary proteins involved in the assembly and sustenance of photosystem II. *Photosynthesis research* **98**, 489-501.
- Nakamura, T., Meierhoff, K., Westhoff, P., and Schuster, G.** (2003). RNA-binding properties of HCF152, an Arabidopsis PPR protein involved in the processing of chloroplast RNA. *European journal of biochemistry / FEBS* **270**, 4070-4081.

- Nakamura, T., Schuster, G., Sugiura, M., and Sugita, M.** (2004). Chloroplast RNA-binding and pentatricopeptide repeat proteins. *Biochemical Society transactions* **32**, 571-574.
- Nelson, N., and Ben-Shem, A.** (2004). The complex architecture of oxygenic photosynthesis. *Nat Rev Mol Cell Biol* **5**, 971-982.
- Newman, J.A., Hewitt, L., Rodrigues, C., Solovyova, A., Harwood, C.R., and Lewis, R.J.** (2011). Unusual, dual endo- and exonuclease activity in the degradosome explained by crystal structure analysis of RNase J1. *Structure (London, England : 1993)* **19**, 1241-1251.
- Nickelsen, J., and Rengstl, B.** (2013). Photosystem II assembly: from cyanobacteria to plants. *Annual review of plant biology* **64**, 609-635.
- Nixon, P.J., Michoux, F., Yu, J., Boehm, M., and Komenda, J.** (2010). Recent advances in understanding the assembly and repair of photosystem II. *Annals of botany* **106**, 1-16.
- O'Toole, N., Hattori, M., Andres, C., Iida, K., Lurin, C., Schmitz-Linneweber, C., Sugita, M., and Small, I.** (2008). On the expansion of the pentatricopeptide repeat gene family in plants. *Molecular biology and evolution* **25**, 1120-1128.
- Ohad, I., Adir, N., Koike, H., Kyle, D.J., and Inoue, Y.** (1990). Mechanism of photoinhibition in vivo. A reversible light-induced conformational change of reaction center II is related to an irreversible modification of the D1 protein. *The Journal of biological chemistry* **265**, 1972-1979.
- Ossenbühl, F., Gohre, V., Meurer, J., Krieger-Liszkay, A., Rochaix, J.D., and Eichacker, L.A.** (2004). Efficient assembly of photosystem II in *Chlamydomonas reinhardtii* requires Alb3.1p, a homolog of Arabidopsis ALBINO3. *The Plant cell* **16**, 1790-1800.
- Peng, L., Ma, J., Chi, W., Guo, J., Zhu, S., Lu, Q., Lu, C., and Zhang, L.** (2006). LOW PSII ACCUMULATION1 is involved in efficient assembly of photosystem II in *Arabidopsis thaliana*. *The Plant cell* **18**, 955-969.
- Pfalz, J., Bayraktar, O.A., Prikryl, J., and Barkan, A.** (2009). Site-specific binding of a PPR protein defines and stabilizes 5' and 3' mRNA termini in chloroplasts. *The EMBO journal* **28**, 2042-2052.
- Phinney, B.S., and Thelen, J.J.** (2005). Proteomic characterization of a triton-insoluble fraction from chloroplasts defines a novel group of proteins associated with macromolecular structures. *Journal of proteome research* **4**, 497-506.
- Puthiyaveetil, S., and Allen, J.F.** (2009). Chloroplast two-component systems: evolution of the link between photosynthesis and gene expression. *Proceedings. Biological sciences / The Royal Society* **276**, 2133-2145.
- Pils, B., and Heyl, A.** (2009). Unraveling the evolution of cytokinin signaling. *Plant physiology* **151**, 782-791.
- Planavsky, N.J., Asael, D., Hofmann, A., Reinhard, C.T., Lalonde, S.V., Knudsen, A., Wang, X., Ossa Ossa, F., Pecoits, E., Smith, A.J.B., Beukes, N.J., Bekker, A., Johnson, T.M., Konhauser, K.O., Lyons, T.W., and Rouxel, O.J.** (2014). Evidence for oxygenic photosynthesis half a billion years before the Great Oxidation Event. *Nature Geosci* **7**, 283-286.
- Plösch, M., Granvogl, B., Reisinger, V., Masanek, A., and Eichacker, L.A.** (2009). Organelle proteomics. *Methods in molecular biology (Clifton, N.J.)* **519**, 65-82.
- Plücken, H., Müller, B., Grohmann, D., Westhoff, P., and Eichacker, L.A.** (2002). The HCF136 protein is essential for assembly of the photosystem II reaction center in *Arabidopsis thaliana*. *FEBS letters* **532**, 85-90.
- Pribil, M., Pesaresi, P., Hertle, A., Barbato, R., and Leister, D.** (2010). Role of plastid protein phosphatase TAP38 in LHCII dephosphorylation and thylakoid electron flow. *PLoS biology* **8**, e1000288.

- Prikryl, J., Rojas, M., Schuster, G., and Barkan, A.** (2011). Mechanism of RNA stabilization and translational activation by a pentatricopeptide repeat protein. *Proceedings of the National Academy of Sciences of the United States of America* **108**, 415-420.
- Qi, Y., Armbruster, U., Schmitz-Linneweber, C., Delannoy, E., de Longevialle, A.F., Rühle, T., Small, I., Jahns, P., and Leister, D.** (2012). Arabidopsis CSP41 proteins form multimeric complexes that bind and stabilize distinct plastid transcripts. *J Exp Bot* **63**, 1251-1270.
- Qiu, Y.L., and Palmer, J.D.** (1999). Phylogeny of early land plants: insights from genes and genomes. *Trends Plant Sci* **4**, 26-30.
- Radauer, C., Lackner, P., and Breiteneder, H.** (2008). The Bet v 1 fold: an ancient, versatile scaffold for binding of large, hydrophobic ligands. *BMC evolutionary biology* **8**, 286.
- Rasmussen, B., Fletcher, I.R., Brocks, J.J., and Kilburn, M.R.** (2008). Reassessing the first appearance of eukaryotes and cyanobacteria. *Nature* **455**, 1101-1104.
- Raven, J.A.** (2009). Contributions of anoxygenic and oxygenic phototrophy and chemolithotrophy to carbon and oxygen fluxes in aquatic environments. *Aquatic Microbial Ecology* **56**, 177-192.
- Raven, J.A., Beardall, J., Larkum, A.W., and Sanchez-Baracaldo, P.** (2013). Interactions of photosynthesis with genome size and function. *Philosophical transactions of the Royal Society of London. Series B, Biological sciences* **368**, 20120264.
- Reiss, B., Schubert, I., Kopchen, K., Wendeler, E., Schell, J., and Puchta, H.** (2000). RecA stimulates sister chromatid exchange and the fidelity of double-strand break repair, but not gene targeting, in plants transformed by *Agrobacterium*. *Proceedings of the National Academy of Sciences of the United States of America* **97**, 3358-3363.
- Rochaix, J.D.** (2011). Reprint of: Regulation of photosynthetic electron transport. *Biochimica et biophysica acta* **1807**, 878-886.
- Rochaix, J.D., Lemeille, S., Shapiguzov, A., Samol, I., Fucile, G., Willig, A., and Goldschmidt-Clermont, M.** (2012). Protein kinases and phosphatases involved in the acclimation of the photosynthetic apparatus to a changing light environment. *Philosophical transactions of the Royal Society of London. Series B, Biological sciences* **367**, 3466-3474.
- Ruf, S., Kössel, H., and Bock, R.** (1997). Targeted inactivation of a tobacco intron-containing open reading frame reveals a novel chloroplast-encoded photosystem I-related gene. *The Journal of cell biology* **139**, 95-102.
- Saito, K., Rutherford, A.W., and Ishikita, H.** (2013). Mechanism of proton-coupled quinone reduction in Photosystem II. *Proceedings of the National Academy of Sciences* **110**, 954-959.
- Sambrook, J., and Russell, D.W.** (2001). *Molecular Cloning: A Laboratory Manual*. (Cold Spring Harbor Laboratory Press).
- Sane, A.P., Stein, B., and Westhoff, P.** (2005). The nuclear gene HCF107 encodes a membrane-associated R-TPR (RNA tetratricopeptide repeat)-containing protein involved in expression of the plastidial psbH gene in *Arabidopsis*. *Plant J* **42**, 720-730.
- Schaefer, D.G.** (2001). Gene targeting in *Physcomitrella patens*. *Current opinion in plant biology* **4**, 143-150.
- Schein, A., Sheffy-Levin, S., Glaser, F., and Schuster, G.** (2008). The RNase E/G-type endoribonuclease of higher plants is located in the chloroplast and cleaves RNA similarly to the *E. coli* enzyme. *RNA (New York, N.Y.)* **14**, 1057-1068.
- Schmitz-Linneweber, C., and Small, I.** (2008). Pentatricopeptide repeat proteins: a socket set for organelle gene expression. *Trends Plant Sci* **13**, 663-670.

- Schneider, A., Steinberger, I., Strissel, H., Kunz, H.H., Manavski, N., Meurer, J., Burkhard, G., Jarzombski, S., Schünemann, D., Geimer, S., Flugge, U.I., and Leister, D.** (2014). The Arabidopsis Tellurite resistance C protein together with ALB3 is involved in photosystem II protein synthesis. *Plant J* **78**, 344-356.
- Schwarz, C., Bohne, A.V., Wang, F., Cejudo, F.J., and Nickelsen, J.** (2012). An intermolecular disulfide-based light switch for chloroplast psbD gene expression in *Chlamydomonas reinhardtii*. *Plant J* **72**, 378-389.
- Schwenkert, S., Umate, P., Dal Bosco, C., Volz, S., Mlcochova, L., Zoryan, M., Eichacker, L.A., Ohad, I., Herrmann, R.G., and Meurer, J.** (2006). PsbI affects the stability, function, and phosphorylation patterns of photosystem II assemblies in tobacco. *The Journal of biological chemistry* **281**, 34227-34238.
- Seki, M., Narusaka, M., Kamiya, A., Ishida, J., Satou, M., Sakurai, T., Nakajima, M., Enju, A., Akiyama, K., Oono, Y., Muramatsu, M., Hayashizaki, Y., Kawai, J., Carninci, P., Itoh, M., Ishii, Y., Arakawa, T., Shibata, K., Shinagawa, A., and Shinozaki, K.** (2002). Functional annotation of a full-length Arabidopsis cDNA collection. *Science* **296**, 141-145.
- Shapiguzov, A., Ingelsson, B., Samol, I., Andres, C., Kessler, F., Rochaix, J.D., Vener, A.V., and Goldschmidt-Clermont, M.** (2010). The PPH1 phosphatase is specifically involved in LHClI dephosphorylation and state transitions in Arabidopsis. *Proceedings of the National Academy of Sciences of the United States of America* **107**, 4782-4787.
- Shi, L.X., and Schröder, W.P.** (2004). The low molecular mass subunits of the photosynthetic supracomplex, photosystem II. *Biochimica et biophysica acta* **1608**, 75-96.
- Sirpio, S., Khrouchtchova, A., Allahverdiyeva, Y., Hansson, M., Fristedt, R., Vener, A.V., Scheller, H.V., Jensen, P.E., Haldrup, A., and Aro, E.M.** (2008). AtCYP38 ensures early biogenesis, correct assembly and sustenance of photosystem II. *Plant J* **55**, 639-651.
- Stegemann, S., and Bock, R.** (2006). Experimental reconstruction of functional gene transfer from the tobacco plastid genome to the nucleus. *The Plant cell* **18**, 2869-2878.
- Stern, D.B., Goldschmidt-Clermont, M., and Hanson, M.R.** (2010). Chloroplast RNA metabolism. *Annual review of plant biology* **61**, 125-155.
- Stoppel, R., and Meurer, J.** (2012). The cutting crew – ribonucleases are key players in the control of plastid gene expression. *Journal of Experimental Botany* **63**, 1663-1673.
- Stoppel, R., and Meurer, J.** (2013). Complex RNA metabolism in the chloroplast: an update on the psbB operon. *Planta* **237**, 441-449.
- Stoppel, R., Manavski, N., Schein, A., Schuster, G., Teubner, M., Schmitz-Linneweber, C., and Meurer, J.** (2012). RHON1 is a novel ribonucleic acid-binding protein that supports RNase E function in the Arabidopsis chloroplast. *Nucleic acids research* **40**, 8593-8606.
- Stoppel, R., Lezhneva, L., Schwenkert, S., Torabi, S., Felder, S., Meierhoff, K., Westhoff, P., and Meurer, J.** (2011). Recruitment of a ribosomal release factor for light- and stress-dependent regulation of petB transcript stability in Arabidopsis chloroplasts. *The Plant cell* **23**, 2680-2695.
- Sultana, A., Kallio, P., Jansson, A., Wang, J.S., Niemi, J., Mantsala, P., and Schneider, G.** (2004). Structure of the polyketide cyclase SnaoL reveals a novel mechanism for enzymatic aldol condensation. *The EMBO journal* **23**, 1911-1921.
- Svab, Z., Hajdukiewicz, P., and Maliga, P.** (1990). Stable transformation of plastids in higher plants. *Proceedings of the National Academy of Sciences of the United States of America* **87**, 8526-8530.

- Swiatek, M., Regel, R.E., Meurer, J., Wanner, G., Pakrasi, H.B., Ohad, I., and Herrmann, R.G.** (2003). Effects of selective inactivation of individual genes for low-molecular-mass subunits on the assembly of photosystem II, as revealed by chloroplast transformation: the *psbEFLJ* operon in *Nicotiana tabacum*. *Molecular genetics and genomics* : MGG **268**, 699-710.
- Theißen, G., Münster, T., and Henschel, K.** (2001). Why don't mosses flower? *New Phytologist* **150**, 1-5.
- Tikkanen, M., and Aro, E.M.** (2012). Thylakoid protein phosphorylation in dynamic regulation of photosystem II in higher plants. *Biochimica et biophysica acta* **1817**, 232-238.
- Tikkanen, M., Mekala, N.R., and Aro, E.M.** (2014). Photosystem II photoinhibition-repair cycle protects Photosystem I from irreversible damage. *Biochimica et biophysica acta* **1837**, 210-215.
- Tomitani, A., Knoll, A.H., Cavanaugh, C.M., and Ohno, T.** (2006). The evolutionary diversification of cyanobacteria: Molecular-phylogenetic and paleontological perspectives. *Proceedings of the National Academy of Sciences* **103**, 5442-5447.
- Torabi, S., Umate, P., Manavski, N., Plöckinger, M., Kleinknecht, L., Bogireddi, H., Herrmann, R.G., Wanner, G., Schröder, W.P., and Meurer, J.** (2014). *PsbN* Is Required for Assembly of the Photosystem II Reaction Center in *Nicotiana tabacum*. *The Plant Cell Online* **26**, 1183-1199.
- Tsujishita, Y., and Hurley, J.H.** (2000). Structure and lipid transport mechanism of a StAR-related domain. *Nature structural biology* **7**, 408-414.
- Turmel, M., Otis, C., and Lemieux, C.** (2006). The chloroplast genome sequence of *Chara vulgaris* sheds new light into the closest green algal relatives of land plants. *Molecular biology and evolution* **23**, 1324-1338.
- Umate, P., Fellerer, C., Schwenkert, S., Zoryan, M., Eichacker, L.A., Sadanandam, A., Ohad, I., Herrmann, R.G., and Meurer, J.** (2008). Impact of *PsbTc* on forward and back electron flow, assembly, and phosphorylation patterns of photosystem II in tobacco. *Plant physiology* **148**, 1342-1353.
- Umena, Y., Kawakami, K., Shen, J.R., and Kamiya, N.** (2011). Crystal structure of oxygen-evolving photosystem II at a resolution of 1.9 Å. *Nature* **473**, 55-60.
- Vainonen, J.P., Hansson, M., and Vener, A.V.** (2005). STN8 protein kinase in *Arabidopsis thaliana* is specific in phosphorylation of photosystem II core proteins. *The Journal of biological chemistry* **280**, 33679-33686.
- Voets, L., Dupré de Boulois, H., Renard, L., Strullu, D.-G., and Declerck, S.** (2005). Development of an autotrophic culture system for the in vitro mycorrhization of potato plantlets. *FEMS Microbiology Letters* **248**, 111-118.
- von Heijne, G., Steppuhn, J., and Herrmann, R.G.** (1989). Domain structure of mitochondrial and chloroplast targeting peptides. *European journal of biochemistry / FEBS* **180**, 535-545.
- Wang, Z., Zou, Y., Li, X., Zhang, Q., Chen, L., Wu, H., Su, D., Chen, Y., Guo, J., Luo, D., Long, Y., Zhong, Y., and Liu, Y.G.** (2006). Cytoplasmic male sterility of rice with boro II cytoplasm is caused by a cytotoxic peptide and is restored by two related PPR motif genes via distinct modes of mRNA silencing. *The Plant cell* **18**, 676-687.
- Waters, E.R.** (2003). Molecular adaptation and the origin of land plants. *Mol Phylogenet Evol* **29**, 456-463.
- Watkins, K.P., Rojas, M., Friso, G., van Wijk, K.J., Meurer, J., and Barkan, A.** (2011). APO1 promotes the splicing of chloroplast group II introns and harbors a plant-specific zinc-dependent RNA binding domain. *The Plant cell* **23**, 1082-1092.
- Wei, L., Guo, J., Ouyang, M., Sun, X., Ma, J., Chi, W., Lu, C., and Zhang, L.** (2010). LPA19, a *Psb27* homolog in *Arabidopsis thaliana*, facilitates D1 protein precursor

- processing during PSII biogenesis. *The Journal of biological chemistry* **285**, 21391-21398.
- Westhoff, P., and Herrmann, R.G.** (1988). Complex RNA maturation in chloroplasts. The psbB operon from spinach. *European journal of biochemistry / FEBS* **171**, 551-564.
- Wicke, S., Schneeweiss, G., dePamphilis, C., Müller, K., and Quandt, D.** (2011). The evolution of the plastid chromosome in land plants: gene content, gene order, gene function. *Plant molecular biology* **76**, 273-297.
- Williams-Carrier, R., Kroeger, T., and Barkan, A.** (2008). Sequence-specific binding of a chloroplast pentatricopeptide repeat protein to its native group II intron ligand. *RNA (New York, N.Y.)* **14**, 1930-1941.
- Yamamoto, T., Burke, J., Autz, G., and Jagendorf, A.T.** (1981). Bound Ribosomes of Pea Chloroplast Thylakoid Membranes: Location and Release in Vitro by High Salt, Puromycin, and RNase. *Plant physiology* **67**, 940-949.
- Yin, P., Li, Q., Yan, C., Liu, Y., Liu, J., Yu, F., Wang, Z., Long, J., He, J., Wang, H.-W., Wang, J., Zhu, J.-K., Shi, Y., and Yan, N.** (2013). Structural basis for the modular recognition of single-stranded RNA by PPR proteins. *Nature* **504**, 168-171.
- Yoder, M.D., Thomas, L.M., Tremblay, J.M., Oliver, R.L., Yarbrough, L.R., and Helmkamp, G.M.** (2001). Structure of a Multifunctional Protein: MAMMALIAN PHOSPHATIDYLINOSITOL TRANSFER PROTEIN COMPLEXED WITH PHOSPHATIDYLCHOLINE. *Journal of Biological Chemistry* **276**, 9246-9252.
- Zghidi-Abouid, O., Merendino, L., Buhr, F., Malik Ghulam, M., and Lerbs-Mache, S.** (2011). Characterization of plastid psbT sense and antisense RNAs. *Nucleic acids research* **39**, 5379-5387.
- Zghidi, W., Merendino, L., Cottet, A., Mache, R., and Lerbs-Mache, S.** (2007). Nucleus-encoded plastid sigma factor SIG3 transcribes specifically the psbN gene in plastids. *Nucleic acids research* **35**, 455-464.
- Zhang, L., Paakkarinen, V., van Wijk, K.J., and Aro, E.M.** (1999). Co-translational assembly of the D1 protein into photosystem II. *The Journal of biological chemistry* **274**, 16062-16067.
- Zhelyazkova, P., Hammani, K., Rojas, M., Voelker, R., Vargas-Suarez, M., Borner, T., and Barkan, A.** (2012). Protein-mediated protection as the predominant mechanism for defining processed mRNA termini in land plant chloroplasts. *Nucleic acids research* **40**, 3092-3105.

Transcript Binding Motif Repeat (TMR) Proteins

Consensus sequence:

MP-x4-L-x3-GR-x-DL-x2-AI-x(2-4)-HGG-x3-VA-x4-L-x(5-27)-GYW

Plants*Arabidopsis thaliana* HCF145 At5g08720

1. FMPMRKQLRLHGRVDIEKAIT--RMGGFRRIALMMNL-SLAYKHRKPKGYWD
 2. FMPSRKSFERAGRYDIARALE--KWGGLHEVSRLAL-LNVRHPNRLQNSRKD

Green algae*Chlorella variabilis* XM_005846292 Chlorellales

1. TMPTSAQLEAAGRRDLVAAVRA--AGGFLEVAQALGLR----SQRKPAYGYWE
 2. VMPRSALQAAGRYDLHHAVML--HGGYTVASQSLDR-----RPAWP
 3. CLPTASQLLEAGRGDLYQASRW--GGGAIVRRGGFCA-----AGQALGWE
 4. RMPHTLQLASAGRHDLKYALQL--HGSASIAAM-LGLQ-----GNTQGAHN

Bathycoccus prasinos CC017813 Mamiellales

1. GMPSKRSLKRNKDLIKRVEK--LFGYDWLTMAVLLDF--EPFRKPFYYWD
 2. VMPTRDLIDARRWDLHHAVVL--HGGYGAVAKTLKWPR--ARWAEDRHLLN
 3. RLPSALELRNVGRDDLARHMVE--HGGPVTVAKRMRMKP-----GKGAWI
 4. YMPDEELINAGRHDLYRVKE--IGSATVAKYAKLQNRTEKMSLAEARAFL

Coccomyxa subellipsoidea C-169 XP_005645828 Coccomyxaceae

1. RMPSCTELEAGAFLLYSISK--HGGVGAFARQLGLDP----KRRDSGYWE
 2. GMPTIQDLQRSGHNSLIKAINH--WGGRSAVARRLGLACSPTRRLMTLGDLS
 3. VMPSTRQLLEAGRPDLLQAVKR--MGGFKRVAALLELAF----LPARRGRSA

Ostreococcus lucimarinus XM_001415510 Mamiellophyceae

1. CMPTRQLR-GGRHWDAIQQIE-SLGGFVKVAQLLDWSG---AKTRPRGYWT

Red algae*Cyanidioschyzon merolae* XM_005538035 Cyanidiales

1. TMPTAGQLAAHRSDLIRAIR-KHGGFP-KVAEQLGLK----AHRRPNGYWN

Cyanidioschyzon merolae XM_005538687 Cyanidiales

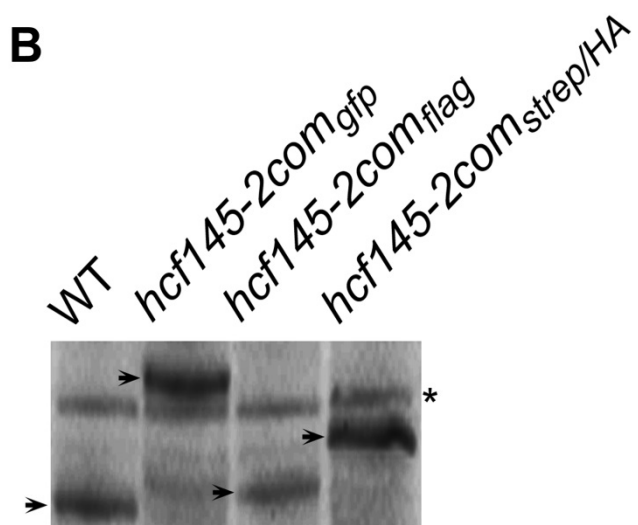
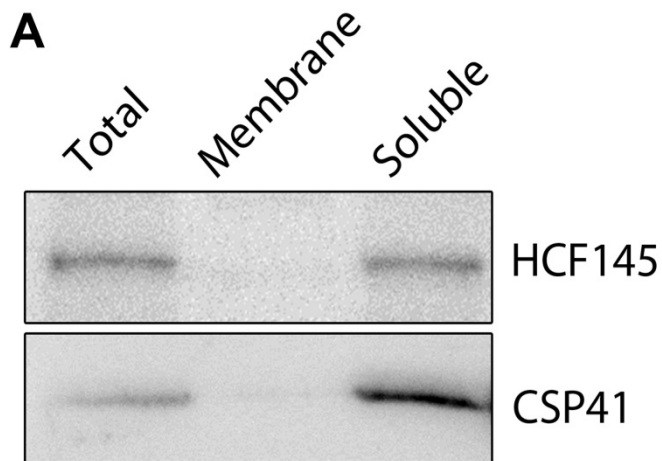
1. YMPTSNELEAKRSDLVRAIV--HGGYAKVAERCGL--QPHR--RSFGYWR
 2. RMPTYNELVAAKKRILAYAIAE--NGGFLEVARMMNLQLSSDE-----TPWR
 3. RFPRQQDLVRLGRYDLDWAIHRW--HGGYTRLAAELGYLRSRLPC-KPRNFWS
 4. RMPNRKELEALDRHDLIYAIRK--FGGFLTVAATKGLSRDALHTTRPRGYWS
 5. IMPRLEQLRMYNREDLINAIHR--HGGANVARRLHLFWY----GPKTFWR
 6. KMPTQQELISAGRVDVAYGVHL--HGGVYEVARRLRLQVLDPP--RAPFYWN
 7. VMPTSMTIVRSRRDLAAAIR--HGGWDAFARRLNLRLPAAPK--RPKGYWN
 8. FVRNYAADFVRRPGDDEDDPDAAGKIAYSDVSEILAGNVGNKRCRTVVGAIR
 9. VMPTAEELRLDGRADLVFACERI-HGGLATVARGLGWPLLAER--LPPESLK
 10. EMPTAEADLLRTGGIDIHEAIVC--HGGYVEVARSLNLRHPEDP---EWTDWS

Galdieria sulphuraria XM_005705295 Cyanidiales

1. SVHLLQVKKSGGECPLPRSSTKCYGGGTPSFELLVP-20aa-VRDVRGYWK
 2. RMPSANELRKSGRYALALAISSH-HGGFHAVAREIGLQPNHHS----SGYWD
 3. YMPYHQLLKARRLDLAKAIHK--YGGFPVAEKLGR---IPN--KRRKYWH
 4. QLPTMTLLSTCKRWDLMGAIRL--HGGLYEVSRKTQIPLSKSTR-QPRGYWS
 5. IVPTLSNLKRNQRQDLVEAIRK--HGGVQTVAAKLYMLRQSKR--KAKGYWN
 6. VMPLGHELRRHQRRDLCYAIQL--HGGFSVAVAGKLHL---NWI--GPI SFWR
 7. RMPTLNDLVIRGRVDLAFGIRL--HHGFPAVAKAFGLEWTIPS--RPRMYWN
 8. YMPSNETLYQLGRGDLADAIRD--TKGWVYAKRLGLVPHYRCI-SSHKLWK
 9. AVASVEELYRDGRGDIAFAIMKY-HQGATQLAHLRLKWKAPHMRP-LPPAYYR
 10. LMPSKKELFQTYGRDLVFIYR--HGGFQKVA CRMGWTIHEDNP-HWLTQWL

Cyanobacteria*Microcoleus* sp. PCC 7113 CP003634.1 Oscillatoriales

1. VMPKAAQLRQLGRYDLA-MAISKYHGGYRSVASRLGLTYT----GQRFYGYWH
 2. VMPSRQQLAQAGEKPLAAAIIG-LHGGVL-AVARRLGFKLP--YGRKPRGYWK
 3. VMPTRQLVQIQRAELISAIA-TNGGWP-SVARRFGL-----ANPNKGYT

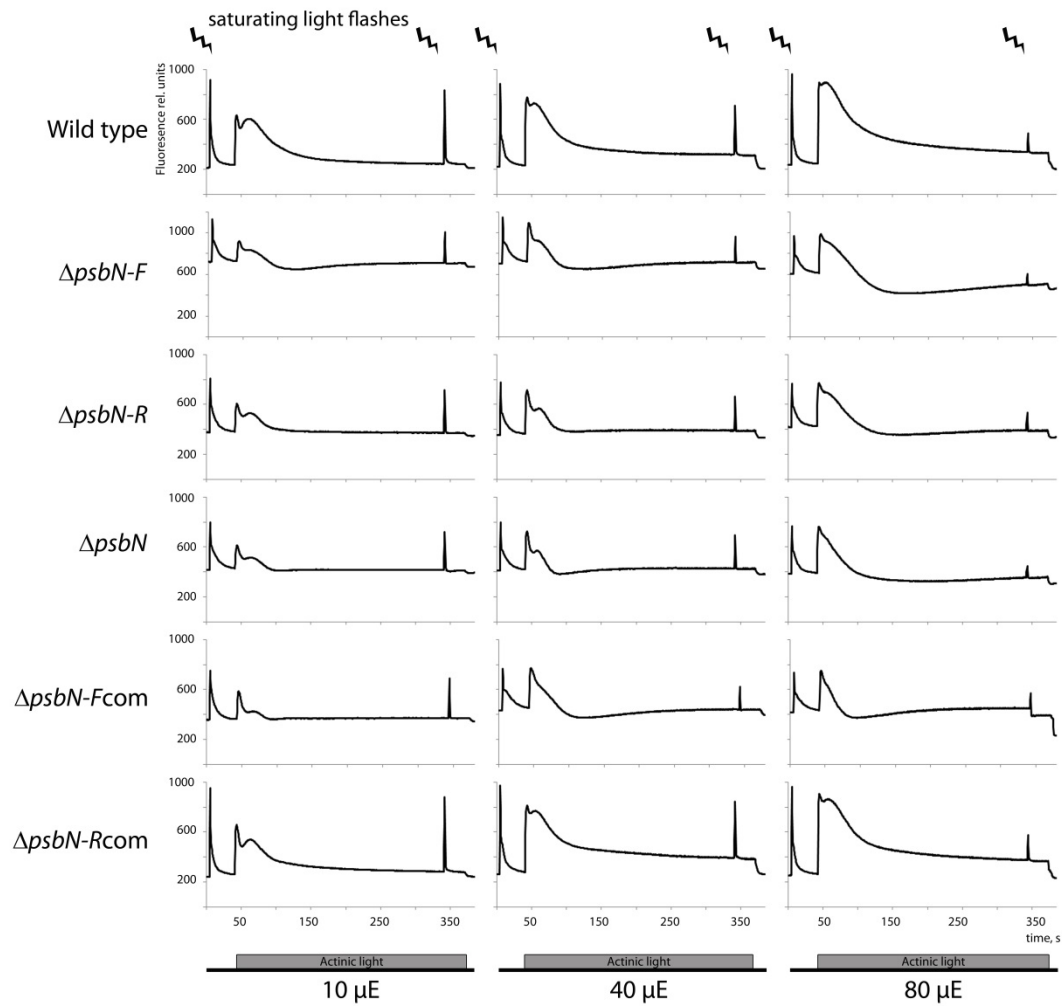


Appendix 5. HCF145 is a soluble protein. (A). Immunological analysis of fractionated protein extracts of 8 h illuminated dark grown seedlings using specific antisera against HCF145 and CSP41. (B) Specificity test of the HCF145 antisera by the comparison of various tagged version of HCF145 in the mutant background. Asterisk indicate unspecific cross reaction of the antibody.

	Fv/Fm ^b	$\Phi_{\text{PSII}}^{\text{c}}$
WT	0,82 ± 0,01	0,70 ± 0,02
<i>nthcf145i-1</i>	0,75 ± 0,02	0,63 ± 0,02
<i>nthcf145i-2</i>	0,70 ± 0,02	0,37 ± 0,03
<i>nthcf145i-3</i>	0,68 ± 0,03	0,26 ± 0,04
<i>nthcf145i-4</i>	0,67 ± 0,03	0,31 ± 0,02

^an, number of plants measured.
^bFv/Fm, maximum quantum yield of PSII.
^c Φ_{PSII} , effective quantum yield of PSII

Appendix 6. Maximum and steady state quantum yield of PSII of HCF145 RNAi lines in *N. tabacum*.



Appendix 7. Chlorophyll *a* fluorescence kinetic of wild type, $\Delta psbN$ mutants and complemented lines. Tobacco plants grown for 6-8 weeks on sucrose supplemented medium in continues light of 10 $\mu mol photons m^{-2} s^{-1}$ were measured with Imaging PAM (Walz). Grey bars indicate 5 min application of actinic light with intensities of 10, 40 and 80 $\mu mol photons m^{-2} s^{-1}$, respectively.

Application	Parameter	WT (n=4) ^a	$\Delta psbN-F$ (n=4)	$\Delta psbN-R$ (n=4)	$\Delta psbN$ (n=4)	$\Delta psbN-Fcom$ (n=4)	$\Delta psbN-Rcom$ (n=4)
	Fv/Fm ^b	0,81 ± 0,01	0,41 ± 0,02	0,46 ± 0,03	0,51 ± 0,02	0,48 ± 0,02	0,77 ± 0,02
AL ^c 10 μ E ^d	ϕ_{PSII} ^e	0,76 ± 0,01	0,32 ± 0,03	0,35 ± 0,02	0,42 ± 0,02	0,41 ± 0,05	0,72 ± 0,02
AL 40 μ E	ϕ_{PSII}	0,60 ± 0,02	0,28 ± 0,03	0,30 ± 0,02	0,39 ± 0,03	0,30 ± 0,03	0,56 ± 0,03
AL 80 μ E	ϕ_{PSII}	0,33 ± 0,02	0,18 ± 0,03	0,28 ± 0,06	0,31 ± 0,03	0,21 ± 0,03	0,34 ± 0,06
AL 10 μ E	NPQ ^f	0,03 ± 0,01	0,04 ± 0,01	0,04 ± 0,01	0,04 ± 0,01	0,04 ± 0,01	0,03 ± 0,01
AL 40 μ E	NPQ	0,07 ± 0,02	0,06 ± 0,02	0,05 ± 0,01	0,05 ± 0,01	0,07 ± 0,01	0,05 ± 0,01
AL 80 μ E	NPQ	0,25 ± 0,03	0,16 ± 0,02	0,12 ± 0,03	0,19 ± 0,01	0,08 ± 0,01	0,17 ± 0,03
^a n, number of plant measured. ^b Fv/Fm, maximum quantum yield of PSII. ^c AL, actinic light. ^d μ E, μ mol photons $m^{-2}s^{-1}$. ^e ϕ_{PSII} , effective quantum yield of PSII after application of 5 min actinic light (AL). ^f NPQ, nonphotochemical quenching.							

Appendix 8. Chlorophyll *a* fluorescence kinetic measurements of wild type (WT), $\Delta psbN$ mutants, and complemented lines. Tobacco plants grown for 6-8 weeks on sucrose supplemented medium in continues light of 10 μ mol photons $m^{-2} s^{-1}$ were measured with Imaging PAM (Walz).

720-ATG-f	atgtcagtgagcaagttccacatctc
720-3UTR-r	tatctttgagttacaagactacac
Cacc-145-for	caccatgtcagtgagcaagttccacatctc
145-rev	atattgaaccaattgatatcaagatc
145ex7-for	ctgaagcaatcatggaagagg
145ex8-for	agctttgatgatgaatcttcacttgc
145ex10.2-rev	ggatgtctcacgttcaatgc
145ex10.1-rev	aagacgagatacttcgtgtaatcctc
LBb1	gcgtggaccgttgcgcaact
A1-for	cacctgaagtggaagtgggtg
A1-rev	gtacaacgcgagcttctatgt
psbB-for	ttctacggcgggtaactcaacg
psbTc-for	cacgatcgaatctatggaag
psbH-rev	gacacccatcaaggagtagttc
aadA-for	gttgtgcacgacacatcattccgtg
psbS-for	caccatggctcaaacatgctgcttactcagg
psbS-rev	aataaaaagcttcttttggtttgggttgaagagcgcgagag
psbN-for	taattaagcttatgaaacagcaaccctagtcgc
psbN-rev	gtctccatgtcctcgaatgg
PsaA-Probe	ccacatctccattcaggatttttggcccactattggccaaaccctgagcactaggtccaatgtgagtaggatactc
PsbN-Probe	ctagtctccatgttctcgaatggatctcttagttgtgagaaggtgccccaaaagcggatataaggcgtaccagtaa
PsbB-Probe	gccatcgaaccggcccaaccagcaaccagagctgtatgcattatgaacagaagcaaccgacgggatcattca
PsbH-Probe	caggagctactttaccatattccgaatcaatggttttaataaatctcctaccgagtcgtcttgaccagatctagaa
PetB-Probe	gagatacacagaaatacatgcaggatcatcattaggaccatcacttgcggaccatcgatgaactgatcggattaac

Appendix 9. Oligonucleotide list

Acknowledgements

First I would like to thank my supervisor PD Dr. Jörg Meurer for the opportunity to work on several interesting projects, for his support, his confidence and the interesting scientific discussions. Furthermore for the great time with his whole group, for the funny barbecues, conferences, and skiing trips that created a wonderful and motivating atmosphere to accomplish all barriers, that I was confronted during my PhD.

I would like to thank Prof. Wolfgang Frank for being my second reviewer and I like to thank his whole group, especially Asif for the great cooperation on the HCF145 project.

I also want to thank Prof. Dario Leister for his support and for providing the lab space.

I would like to thank Prof. Wolfgang Schröder for the cooperation on the PsbN project.

I would like to thank Prof. Ralph Bock for providing *psbN* mutant and control seeds.

Next I would like to express my gratitude to my colleagues:

I want to thank Rhea Stoppel for the familiarization into the lab and to the whole AG Leister group. I want to thank Laura Kleinknecht and Magdalena Plöchinger, who helped a lot in the PsbN project and for keeping my company to lunch and coffee. And I want to thank Kayo (Dr. Nikolay Manavski), who did an essential contribution to the HCF145 project.

I want to thank all the other past and present people of the institute who helped me or just had a good time with me.

Special thanks to Stefan Kirchner for the coffee meetings in the morning, the fishing trips, and his support in all questions I had about plastid transformation and tissue culture.

Special thanks also to the Abstäuber and all the other guys playing football with us!

And also to all the gardeners for taking care of my plants, especially to Ulli looking after my tobacco jungle and to Basti for providing me tobacco.

Finally, I would like to thank my family and my friends for their constant encouragement.

Especially my mom, who helped me a lot in all IT and Word problems,

and my girlfriend Paula Kern, who always had to wait for me and had to soften my bad mood when things went wrong.

Publications

Parts of this work have already been published or will be submitted for publication

- Torabi, S., Umate, P., Manavski, N., Plöchinger, M., Kleinknecht, L., Bogireddi, H., Herrmann, R.G., Wanner, G., Schröder, W.P., and Meurer, J.** (2014). PsbN Is Required for Assembly of the Photosystem II Reaction Center in *Nicotiana tabacum*. *The Plant Cell Online* **26**, 1183-1199.
- Stoppel, R., Lezhneva, L., Schwenkert, S., Torabi, S., Felder, S., Meierhoff, K., Westhoff, P., and Meurer, J.** (2011). Recruitment of a ribosomal release factor for light- and stress-dependent regulation of petB transcript stability in *Arabidopsis* chloroplasts. *The Plant Cell* **23**, 2680-2695.
- Wittek, F., Torabi, S., Kolb, M., and Walther, U.I.** (2014). Pro-oxidative toxicity of cells in suspension does not point to a cell cultural artefact as an explanation of the increased susceptibility of alveolar epithelial-like cells after glucocorticoid pretreatment. *Toxicology in Vitro* **28**, 1089-1096.
- Manavski, N., Torabi, S., Stoppel, R., Meurer, J.** (2012). Phylogenetic and ontogenetic integration of organelles into the compartmentalized genome of the eukaryotic cell. *Journal of Endocytobiosis and Cell Research* **23**, 25-31.

Curriculum vitae

Personal Profile

Salar Abu-Torab Torabi

Born 17th of June 1981 in Berlin (Germany)

Citizenship: German

Research Experience

11/2009 – 08/2014 Ludwig-Maximilians-Universität München (Germany)
Department Biology I, Botany
-PhD Supervisor PD Dr. Jörg Meurer

09/2008 – 06/2009 Ludwig-Maximilians-Universität München (Germany)
Department Biology I, Botany
-Diploma thesis Supervisor Prof. Dr. H. U. Koop

Education

11/2009 – 08/2014 PhD at the Ludwig-Maximilians-Universität München
(Germany)

Topic of the thesis:

Establishment of photosynthetic complexes in the chloroplast

10/2003 – 06/2009 Studies of Biology at the Ludwig-Maximilians-Universität
München (Germany)

Topic of the thesis:

Plastidtransformation in *Brassica napus*

10/2001 – 07/2003 Vocational High School Altötting (Germany)

09/1997 – 09/2001 Industrial Mechanic at the Wacker Siltronic AG

Craft certificate (01/2001)

Eidesstattliche Versicherung

Ich versichere hiermit an Eides statt, dass die vorgelegte Dissertation von mir selbstständig und ohne unerlaubte Hilfe angefertigt ist.

München, den

Salar Torabi

Erklärung

Hiermit erkläre ich, dass die Dissertation nicht ganz oder in wesentlichen Teilen einer anderen Prüfungskommission vorgelegt worden ist und dass ich zuvor nicht versucht habe, anderweitig eine Dissertation einzureichen oder mich einer Doktorprüfung zu unterziehen.

München, den

Salar Torabi